UNIVERSIDADE DE SÃO PAULO
INSTITUTO DE QUÍMICA

Programa de Pós-Graduação em Ciências Biológicas (Bioquímica)

ADRIANO DE BRITTO CHAVES FILHO

Redox-triggered events in lipid biology: thiol modification and lipidome alteration in ALS

Versão corrigida da Tese conforme Resolução CoPGr 5890
O original se encontra disponível na Secretaria de Pós-Graduação do IQ-USP

São Paulo

Data do Depósito na SPG:
16/07/2018

ADRIANO DE BRITTO CHAVES FILHO

Eventos redox na biologia dos lipídios: modificação de tióis e alterações do lipidoma em ELA

Tese apresentada ao Instituto de Química da Universidade de São Paulo para obtenção do Título de Doutor em Ciências Biológicas (Bioquímica)

Orientador (a): Profa. Dra. Sayuri Miyamoto

São Paulo
2018

Ficha Catalográfica elaborada eletronicamente pelo autor, utilizando o programa desenvolvido pela Seção Técnica de Informática do ICMC/USP e adaptado para a Divisão de Biblioteca e Documentação do Conjunto das Químicas da USP

Bibliotecária responsável pela orientação de catalogação da publicação:
Marlene Aparecida Vieira - CRB - 8/5562

C512e

Chaves-Filho, Adriano
Eventos redox na biologia dos lipídios: modificação de tióis e alterações do lipidoma em ELA / Adriano Chaves-Filho. - São Paulo, 2018.
117 p.

Tese (doutorado) - Instituto de Química da Universidade de São Paulo. Departamento de Bioquímica.
Orientador: Miyamoto, Sayuri

1. Lipídios. 2. Tióis. 3. Estresse oxidativo. 4. Doenças neurodegenerativas. 5. Espectrometria de massas. I. T. II. Miyamoto, Sayuri, orientador.

UNIVERSIDADE DE SÃO PAULO
INSTITUTO DE QUÍMICA

"Eventos redox na biologia dos lipídios: modificação de tióis e alterações do lipidoma em ELA"

ADRIANO DE BRITTO CHAVES FILHO

Tese de Doutorado submetida ao Instituto de Química da Universidade de São Paulo como parte dos requisitos necessários à obtenção do grau de Doutor em Ciências - Área: Bioquímica.

Profa. Dra. Sayuri Miyamoto
(Orientadora e Presidente)

Aprovado (a) por:

Profa. Dra. Ohara Augusto
IQ - USP

Prof. Dr. Oswaldo Keith Okamoto
IB - USP

Prof. Dr. José Pedro Friedmann Angeli
UW-ALEMANHA

SÃO PAULO
18 de maio de 2018

À minha família e amigos

“Life is not easy for any of us. But what of that? We must have perseverance and above all confidence in ourselves. We must believe that we are gifted for something and that this thing must be attained.”

Marie Curie

AGRADECIMENTOS

Chegando ao final deste longo período de doutorado, pude confirmar ainda mais que não conseguimos fazer nada sozinhos e que devemos agradecer sempre por tudo e a todos que nos apoiam. A todos vocês, familiares, amigos, professores e colegas, a minha eterna gratidão.

A Deus por sempre me guiar e me dar determinação para superar todas as dificuldades enfrentadas no dia a dia e a nunca desistir.

À Professora Sayuri Miyamoto por ser uma orientadora presente nos momentos mais difíceis, pela confiança, incentivo, pela oportunidade de crescer tanto profissional como pessoalmente, meus sinceros agradecimentos.

Aos professores Humberto Matos, Ohara Augusto, Paolo Di Mascio, Graziella Ronsein, Marisa Medeiros, Isaias Glezer, William Festuccia, Flávia Meotti, Miriam Uemi, Yoshito Kumagai, Yumi Abiko e aos demais professores do USP e de outras universidades pelas colaborações e/ou contribuições para o meu aprendizado durante esse período.

Aos meus amigos e companheiros de laboratório Patrícia Appolinário, Nicole Noda, Beatriz Gasques, Alex Inague, Rodrigo de Faria, Karen campos, Fernanda Junqueira, Silvio Oliveira, Daniela Cunha, Camila Roubik, Albert Peixoto, Angélica Sanchez, Adriana Domarques, Florêncio Freitas, Marcela Mineiro, Felipe Akihiro, Nho Luong, Thiago Belchior, Maynara Andrade, Tiago Eugênio, Kátia Prieto, Bruno Chausse e Bárbara Freitas.

Aos técnicos de laboratório Izaura Toma, Adriana Wendel, Sirley Mendes, Zilda Izzo, Fernando Coelho, Fernanda Manso, Emerson Marques, Edlaine Linares e Janaina Nicanuzia por todo suporte durante o meu doutorado. Ao pessoal do biotério IQ-FCF, em especial à Renata Fontes e Flávia Ong que nos auxiliaram em todos os momentos durante a experimentação com os animais. Muito obrigado a todos vocês!

A todos os órgãos de apoio à pesquisa tornam possível o trabalho dentro da universidade: Conselho Nacional de Desenvolvimento Científico e tecnológico (CNPq),

Fundação de Amparo à Pesquisa do Estado de São Paulo (FAPESP), Coordenação de Aperfeiçoamento de Pessoa de Nível Superior (CAPES), INCT de Processos redox em Biomedicina-Redoxoma e Pró-Reitoria-USP.

Aos meus amigos Isabella Dantas, Lucas Souza e Railmara Pereira pelos anos de convivência juntos, risadas, amizade verdadeira e pela parceria de sempre. Vocês também são minha família! Muito obrigado por tudo! Ao meu amigo Marcos Yoshinaga pela força dada nos momentos mais difíceis, pela parceria nos experimentos e discussões científicas e por sempre nos motivar a dar o nosso melhor. Muito obrigado! Aos meus amigos Priscilla Derogis e Vanderson Bispo pela amizade e por fazerem minha adaptação no IQ muito mais fácil. Muito obrigado! Aos meus amigos Juliana Gouveia, Gabriela Gomes, Christiano Dantas, Hercílio Rezende, Vitor Dias e Douglas Baracho, que mesmo apesar da distância física nunca deixaram de estar ao meu lado sempre que precisei. Por sempre me apoiarem e acreditarem em mim. A todos vocês meu muito obrigado! Nossa amizade é eterna!

A meus familiares, especialmente a minha irmã Lísia Britto, irmão Alexandre Britto, pai Adriano Britto, avós Maria Lísia e Pedro Chaves, a Ana Santos, a meus primos Matheus Unger, Juliano Unger, Cláudia Unger, Vitória Unger, a tia Elza Unger, tios Pedrinho e Tércia Chaves, Hortência e William Britto. A todos vocês o meu muito obrigado! Sem vocês eu não teria chegado até aqui.

Em especial, gostaria de agradecer à minha avó Maria dos Prazeres e à minha mãe Aline Chaves por sempre me darem todo o apoio que precisei desde sempre. Por toda ajuda e compreensão nos momentos mais difíceis. Sem vocês eu não teria chegado até aqui. Eu amo muito vocês.

Muito obrigado a todos!

RESUMO

Chaves-Filho, A.B. **Redox-triggered events in lipid biology: thiol modification and lipidome alteration in ALS**. 2018. 117p. Tese - Programa de Pós-Graduação em Ciências Biológicas (Bioquímica). Instituto de Química - Universidade de São Paulo - São Paulo.

Os lipídeos abrangem uma ampla gama de moléculas hidrofóbicas presentes nas células. As características moleculares dos lipídios determinam sua localização celular e função biológica. Em geral, os lipídios são considerados componentes essenciais de membranas, reservatórios de energia e moduladores de vias de sinalização ligadas ao metabolismo celular, sobrevivência, entre outros. Em mamíferos, grande parte dos lipídios é esterificada em ácidos graxos poli-insaturados (PUFAs), especialmente os ácidos docosahexaenóico (DHA) e araquidônico (ARA), essenciais para vários processos fisiológicos, incluindo o desenvolvimento normal do cérebro. No entanto, os PUFAs são muito suscetíveis à oxidação por espécies reativas de oxigênio (ROS) geradas endogenamente. Uma vez oxidados, lipídios são capazes de modificar grupos tióis de peptídeos e proteínas, levando à modulação das vias de sinalização e alterando o balanço redox celular. No capítulo 1, foram investigados os mecanismos envolvidos na modificação de grupos tióis de peptídeos e proteínas por produtos de auto-oxidação de PUFAs. Com as análises realizadas foi possível identificar vários adutos de glutationa (GSH) covalentemente modificados por endoperóxidos cíclicos derivados de DHA e ARA. Uma análise detalhada dos espectros de MS/MS dos adutos de GSH revelou que GSH e endoperóxidos cíclicos são provavelmente ligados através de uma ligação química de enxofre-oxigênio, em uma reação que envolve um ataque nucleofílico do ânion tiolato. Além disso, sugerimos que a eficiência da modificação do tiol por endoperóxidos cíclicos também é dependente da reatividade do tiol, como demonstrado pela modificação covalente do resíduo de cisteína mais reativo (Cys111) da enzima antioxidante superóxido dismutase 1

(SOD1). Modificações químicas de tióis por endoperóxidos cíclicos podem modular a agregação proteica e o status redox celular, produzindo adutos de GSH capazes de modular a inflamação, como relatado para os conjugados de GSH gerados enzimaticamente. No capítulo 2, nós investigamos o papel dos lipídios na esclerose lateral amiotrófica (ALS), uma vez que a inflamação e o estresse oxidativo nos neurônios motores contribuem para o desenvolvimento desta doença neurodegenerativa. Usando uma abordagem lipidômica não direcionada baseada em espectrometria de massa acoplada à cromatografia líquida (UHPLC-MS/MS), nós investigamos o metabolismo lipídico no córtex motor e na medula espinhal de um modelo de ratos com ALS. A análise do córtex motor mostrou que as principais alterações lipídicas foram dependentes da idade e ligadas ao metabolismo dos esfingolipídios. Em contraste, as principais alterações lipídicas na medula espinhal foram encontradas no grupo sintomático da ALS, sendo o metabolismo de ceramidas, ésteres de colesterol e cardiolipinas os mais afetados. De acordo com os resultados obtidos e dados relatados na literatura, propusemos um mecanismo baseado em neuroproteção que envolve o acúmulo de ésteres de colesterol esterificados em PUFAs em astrócitos. Coletivamente, nossos achados sugerem que os lipídios desempenham um papel crucial na modulação de processos celulares ligado à oxidação de tióis e à neurodegeneração.

Palavras-chave: Lipídios, peroxidação lipídica, tióis, estresse oxidativo, esclerose lateral amiotrófica, espectrometria de massas.

ABSTRACT

Chaves-Filho, A.B. **Redox-triggered events in lipid biology: thiol modification and lipidome alteration in ALS.** 2018. 117p. PhD Thesis - Graduate Program in Biochemistry. Instituto de Química - Universidade de São Paulo - São Paulo.

Lipids encompass a wide range of hydrophobic molecules present in cells. The molecular characteristics of lipids determine their cellular localization and biological function. In general, lipids are regarded as essential components of membranes, as energy reservoir and modulators of signaling pathways linked to cellular metabolism and survival, among others. In mammals, a large part of the lipids are esterified to polyunsaturated fatty acids (PUFAs), especially docosahexaenoic (DHA) and arachidonic (ARA) acids, essential for several physiological processes, including normal brain development. However, PUFAs are very susceptible to oxidation by reactive oxygen species (ROS) generated endogenously. Once oxidized, lipids are able to modify thiol groups of peptides and proteins leading to modulation of signaling pathways and cellular redox balance. In the chapter 1, we investigated the mechanisms involved in modification of thiol groups of peptides and protein by autoxidation products derived from PUFAs. Here, we identified several glutathione (GSH) adducts covalently modified by hydroxy-endoperoxides derived from both DHA and ARA. Detailed inspection of MS/MS spectra of GSH-adducts revealed that GSH and hydroxy-endoperoxides are likely bonded through a sulfur-oxygen chemical bond in a reaction which involves a nucleophilic attack by the thiolate anion. Also, we suggest that the efficiency of modification of thiol by hydroxy-endoperoxides are also dependent of the thiol reactivity, as demonstrated by covalent modification of the most reactive cysteine residue (Cys111) of the antioxidant enzyme Cu,Zn-superoxide dismutase (SOD1). Chemical modifications of thiol groups by hydroxy-endoperoxides may modulate protein aggregation and cellular redox status, yielding

GSH adducts capable to modulate inflammation, as reported for the enzymatically generated counterparts. In the chapter 2, we investigated the role of lipids in amyotrophic lateral sclerosis (ALS), since inflammation and oxidative stress in motor neurons are hallmarks of this neurodegenerative disease. Using an untargeted lipidomics approach based on mass spectrometry coupled to liquid chromatography (UHPLC-MS/MS), we investigated the lipid metabolism in motor cortex and spinal cord tissues of a rodent model of ALS. Analysis of the motor cortex showed that the main lipid alterations were age-dependent and linked to metabolism of sphingolipids. In contrast, the major lipid alterations in the spinal cord were found in ALS symptomatic group, being the metabolism of ceramides, cholesteryl esters and cardiolipin the most affected. According to our findings and data reported in the literature, we proposed a mechanism based on neuroprotection that involves accumulation of cholesteryl esters esterified to PUFAs in astrocytes. Collectively, our findings suggest that lipids play a crucial role in modulation of cellular process linked to thiol metabolism and neurodegeneration.

Keywords: Lipids, lipid peroxidation, thiols, oxidative stress, amyotrophic lateral sclerosis, mass spectrometry.

LIST OF ACRONYMS AND ABBREVIATIONS

AAPH - 2 -2-azobis(2-methylpropionamidine) dihydrochloride;

AD - Alzheimer’s disease

AdA - adrenic acid

ALA - α-linolenic acid

ALS - Amyotrophic lateral sclerosis

ARA - arachidonic acid

Cer - ceramide

CL - cardiolipin

CNS - central nervous system

COX - cyclooxygenases

DAG - diacylglycerol

DHA - docosahexaenoic acid

EPA - eicosapentaenoic acid

ER - endoplasmic reticulum

FFA - free fatty acids

GalC - galactosylceramide

GlcC - glucosylceramide

GP - glycerophospholipid

GSH - glutathione

HHE - 4-hydroxy-2-hexenal

HNE - 4-hydroxy-2-nonenal

LA - linoleic acid

LOX - lipoxygenases

MUFA - monounsaturated fatty acid

NAC - N-acetylcysteine

NEM - N-ethylmaleimide

PC - phosphatidylcholine

PD - Parkinson's disease

PE - phosphatidylethanolamine

PG - phosphatidylglycerol

PI - phosphatidylinositol

PS - phosphatidylserine

PUFA - polyunsaturated fatty acid

ROS - reactive oxygen species

SFA - saturated fatty acid

SM - sphingomyelins

SM - sphingomyelins

SOD1 - Cu -Zn-superoxide dismutase

TAG - triacylglycerol

TCA cycle - tricarboxylic acid cycle

UHPLC - ultra-high performance liquid chromatography

ω-acyl-Cer - ω-acyl-ceramide

SUMMARY

1. INTRODUCTION

1.1. Lipid diversity in mammalian cells

Lipids encompass a diverse group of compounds soluble in organic solvents and insoluble in water. According to their molecular characteristics, lipids can be subdivided in several classes of which glycerophospholipids (GPs), glycerolipids, sphingolipids, free fatty acids (FFA) and sterols are some of the best known components (Fahy *et al*. 2005, 2009). GPs are composed by two fatty acids bonded to a glycerol backbone at *sn*-1 and *sn*-2 positions. At *sn-1* position, the fatty acyl chains can be linked by an ester, ether or vinyl-ether bond. At *sn*-3 position, the glycerol backbone is substituted by a phosphoric group and a specific head group. According to the head group, GPs are generally divided into phosphatidylcholine (PC), phosphatidylethanolamine (PE), phosphatidylserine (PS), phosphatidylinositol (PI), phosphatidylglycerol (PG), cardiolipin (CL), among others (Fig. 1) (Fahy *et al*. 2005, 2009; Han and Gross 2005).

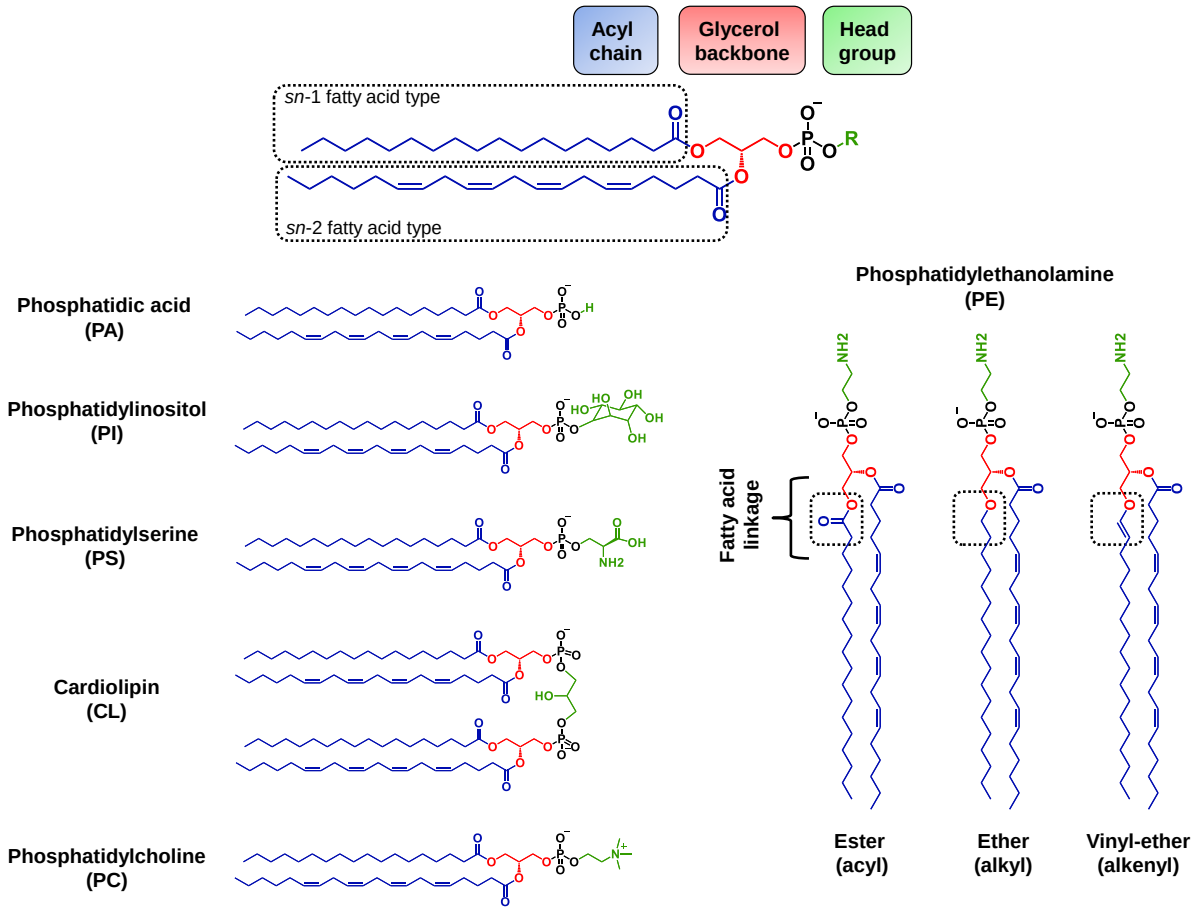

Figure 1. General structures of glycerophospholipids. According to the head group, GPs are generally divided into (PA) phosphatidic acid; (PC) phosphatidylcholine, (PE) phosphatidylethanolamine, (PS) phosphatidylserine, (PI) phosphatidylinositol, (PG) phosphatidylglycerol, (CL) cardiolipin.

Unlike GPs, the *sn*-3 position of glycerolipids can be substituted by another fatty acid, providing more hydrophobicity to this lipid class. The glycerolipids are defined as mono-, di- or triacylglycerols according to the number of fatty acids bonded to their structures (Fig. 2) (Lehner and Kuksis 1996). In mammalian cells, the term "sterols" is mainly applied to cholesterol and those products derived from it, especially 24-hydroxycholesterol and cholesteryl ester (Lutjohann and von Bergmann 2003; Schwartz *et al*. 2004). Cholesterol is composed by a sum of four fused rings containing only one double bond between the carbons 5 and 6, a hydrocarbon tail and a hydroxyl group at carbon 3 (Fig. 2) (Harayama and Riezman 2018). Sphingolipid chemical diversity is linked to the length and type of the sphingoid base, n-acyl chain and head group (Merrill 2008). The sphingoid base is composed by a hydrocarbon chain (usually 18 carbons) with presence (ceramide) or absence (dihydroceramide) of a double bond between carbons 3 and 4, and also a hydroxyl group at the carbon 2 (Pruett *et al*. 2008). Usually, the n-acyl chain found in sphingolipids is longer (from 16 to 30 carbons) and less unsaturated (one or two double bonds) than those found in GPs and glycerolipids (Harayama and Riezman 2018). Similarly to GPs, the head group of sphingolipids defines their subclasses as ceramide (Cer), sphingomyelin (SM), sphingosine-1-phosphate (CerP) galactosylceramide (GalC), glucosylceramide (GlcC), sulfatide, glycosylated ω-acyl-ceramide, among others (Fig. 3) (Fahy *et al*. 2005).

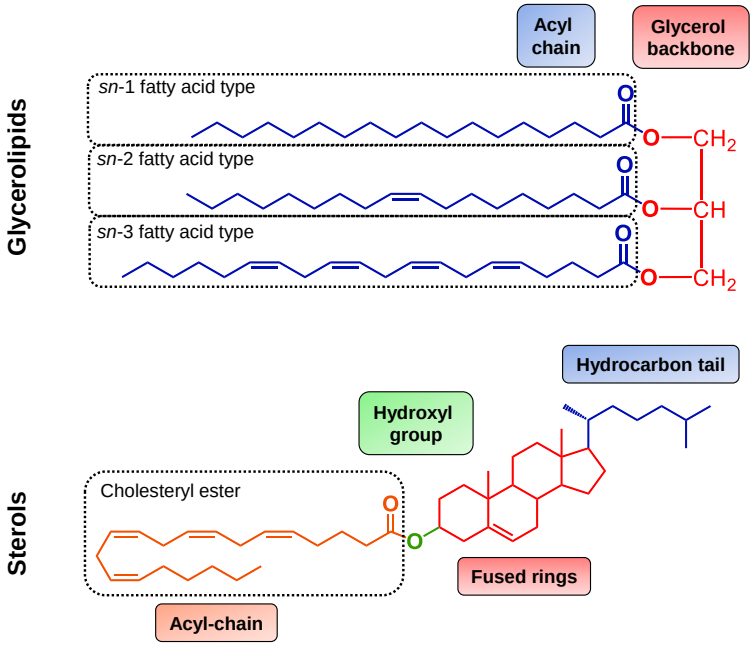

Figure 2. General structures of storage lipids. According to the number of acyl chains, glycerolipids can be divided into mono-, di- or triacylglycerols. Cholesteryl esters can be esterified with SFA, MUFA or PUFA.

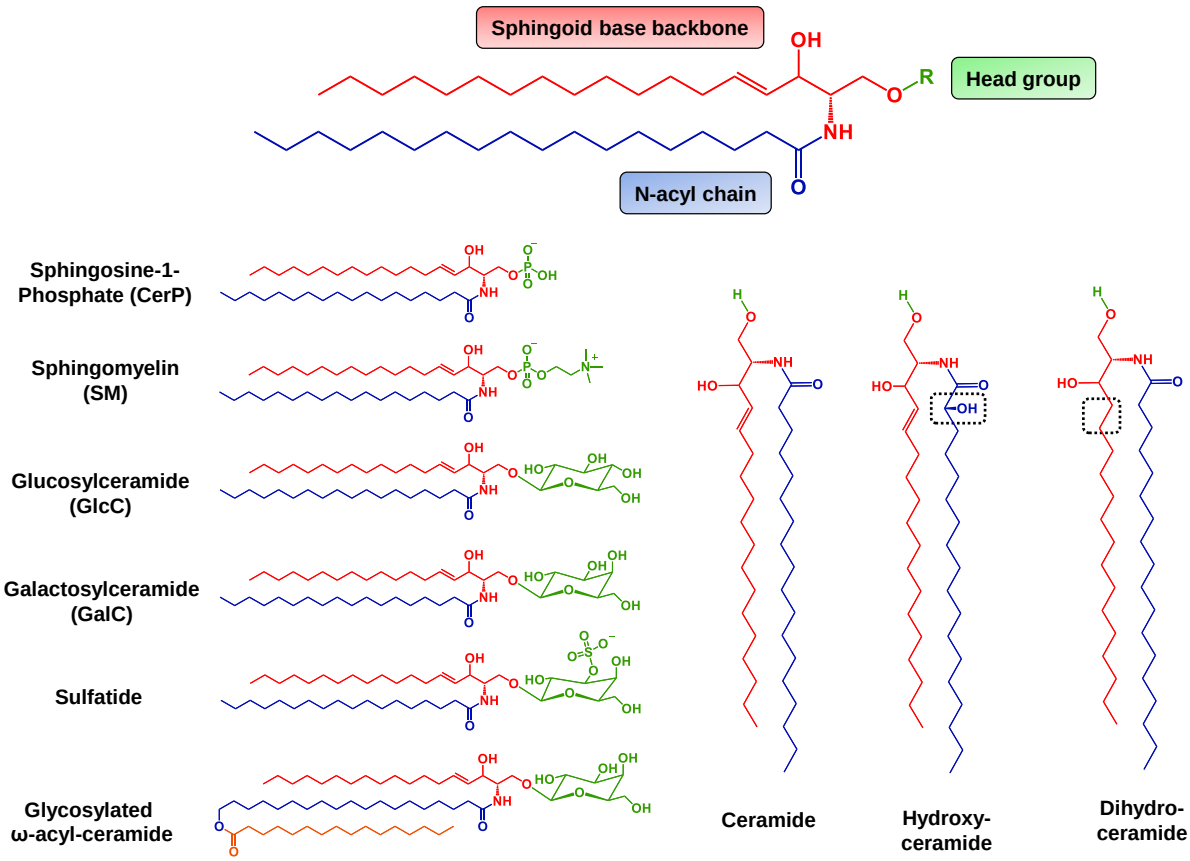

Figure 3. General structures of sphingolipids. The head group of sphingolipids defines their subclasses as (CerP) sphingosine-1-phosphate, (SM) sphingomyelin, (Cer) ceramide, (GalC) galactosylceramide, (GlcC) glucosylceramide, sulfatide and glycosylated ω-acyl-ceramide.

The molecular characteristics of fatty acids directly affect the biological properties of the lipids bonded to them. Because free fatty acids are usually toxic to the cells, especially the saturated ones, they are mainly found esterified to triacylglycerols, GPs and sterols (Cnop *et al*. 2001; Miller *et al*. 2005). Fatty acids can be classified according to degree and position of the double bonds and chain length. Regarding the chain length, fatty acids up to 36 carbons have been detected in mature spermatozoa, retina and also in the brain (Leonard *et al*. 2004). According to the number of double bonds fatty acids are subdivided into saturated (SFA; with no double bonds), monounsaturated (MUFA; one double bond) or polyunsaturated (PUFA; two or more double bonds). Usually, the *sn*-1 position of GPs is esterified to a SFA or MUFA, whereas the *sn*-2 position is more often esterified to MUFA or PUFA (Yamashita *et al*. 2014).

Among the unsaturated fatty acids, they can be further classified by the position of the double bond closest to the methyl-end group, being the omega-3 (n-3) and omega-6 (n-6) fatty acids some of the most important lipids for mammalian cells. Mammals can synthesize SFA and MUFAs, however, they do not express the enzymes responsible to catalyze the synthesis of n-3 and n-6 fatty acids. Thus, essential fatty acids like α-linolenic (ALA; C18:3n-3) and linoleic (LA; C18:2n-6) acids have to be obtained from the diet (Poudyal *et al*. 2011). From ALA, cells are able to synthesize others n-3 fatty acids like eicosapentaenoic (EPA; C20:5n-3) and docosahexaenoic (DHA; C22:6n-3) acids by reactions catalyzed by elongases and desaturases. Meanwhile, arachidonic (ARA; C20:4n-6) and adrenic (AdA; C22:4n-6) acids, two of the most important n-6 fatty acids in mammals, can be synthesized from LA by the same enzymatic machinery (Fig. 4) (Galano *et al*. 2015).

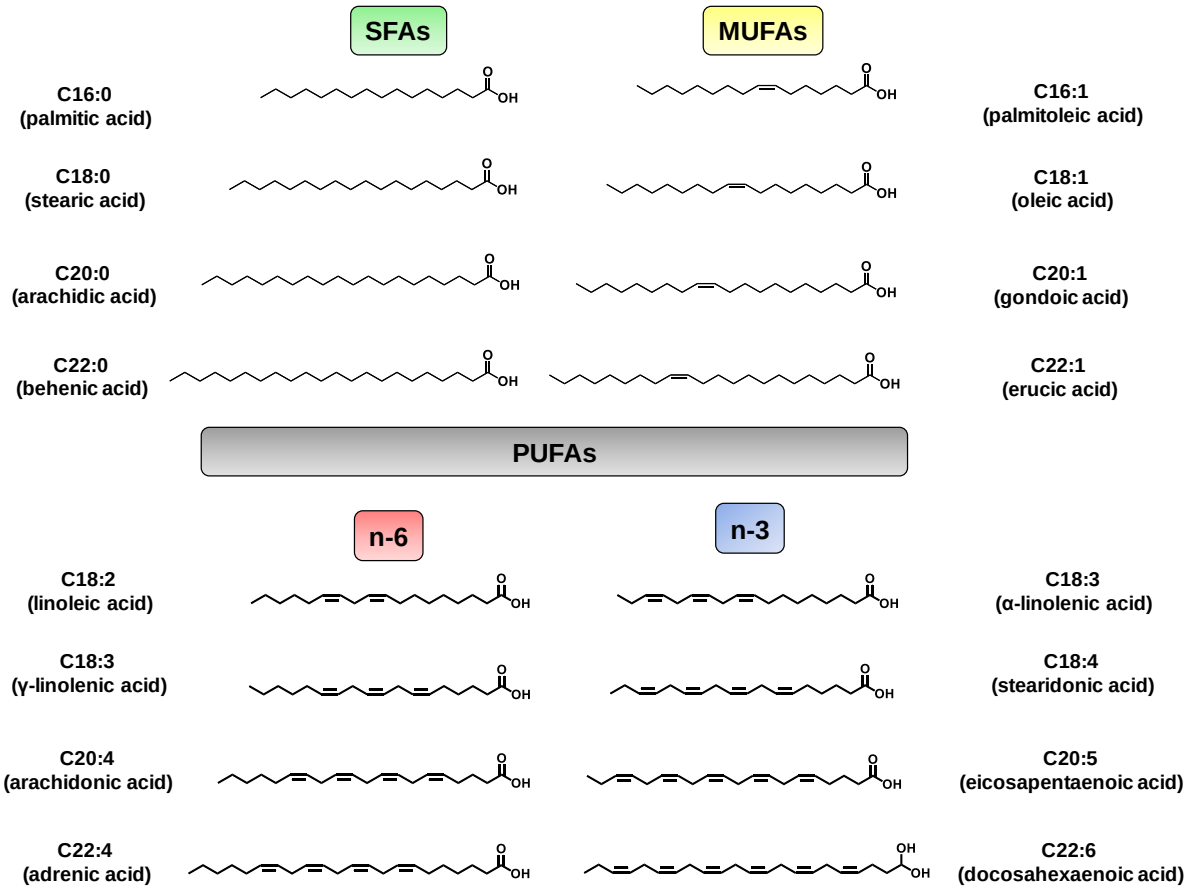

Figure 4. General structures of fatty acids. (SFAs) saturated fatty acids; (MUFAs) monounsaturated fatty acids; (PUFAs) polyunsaturated fatty acids.

1.2. Cellular localization and biological function of lipids

Lipids are the main components of plasma membrane and also organelles such as mitochondria, peroxisome and endoplasmic reticulum (ER). The majority of membranes are composed of GPs, sphingolipids and cholesterol (Van Meer *et al*. 2008). The plasma membrane is asymmetric, that is, the inner and outer leaflets do not have exactly the same lipid composition. For instance, sphingolipids are usually found at the outer leaflet of plasma membranes, whereas PS is found only in the inner leaflet (Hishikawa *et al*. 2014). Interestingly, some structures or organelles have specific lipids in their composition, as reported for cardiolipin in the inner membrane of mitochondria (Paradies *et al*. 2014).

Although the majority of lipids are found in membranes, neutral lipids like triacylglycerol and cholesteryl esters are important for storage and transport of fatty acids (Van Meer *et al*. 2008). However, the functions of lipids go beyond regulating the entrance and exit of molecules through the cell membranes and storing energy.

Lipids are reported by their ability to participate in a wide range of cellular events including inflammation, metabolism and proliferation (Hannun and Obeid 2008; Wymann and Schneiter 2008). Particularly, the association of sphingolipids and cholesterol in microdomains of the plasma membrane called lipid rafts are essential for anchorage of proteins, regulation of lipid trafficking, cell signaling and modulation of membrane fluidity (Dupree and Pomicter 2010). Sphingolipids like galactosylceramide (GalC) and sulfatides are essential for myelin stabilization, a membrane that insulates neurons, ensuing a fast transmission of the electrical signal (Aggarwal *et al*. 2011). Ceramides, for instance, are linked to cell signaling by regulation of apoptosis, cell differentiation and autophagy (Grösch *et al*. 2012). Cholesterol is an essential precursor for synthesis of steroid hormones, bile salts and important carrier of fatty acids in blood circulation (Payne and Hales 2004). Polar lipids like GPs also participate in signaling pathways linked to cell growth and differentiation, exocytosis and apoptosis as reported for PS and PI (Schink *et al*. 2013; Hishikawa *et al*. 2014; Kim *et al*. 2014).

Despite the head group of lipid subclasses determining the function and cellular localization, the molecular characteristics of the fatty acids bonded to GPs and sphingolipids may affect the biophysics properties of membranes (Dunbar *et al*. 2014). For instance, GPs esterified with short chain fatty acids or PUFAs provide more membrane fluidity than those bonded to long chain fatty acids or MUFAs (Maulucci *et al*. 2016). Furthermore, fatty acids esterified in GPs at the inner leaflet of plasma membrane can be hydrolyzed by phospholipases in response to cellular stimulus like calcium influx (Balsinde and Balboa

2005). Once released in the cytosol, FFA can modulate cellular events linked to signaling and inflammation (Balsinde and Balboa 2005). DHA itself can lead to downregulation of genes linked to expression of pro-inflammatory proteins, by activation of the peroxisome proliferator-activated receptor alpha (PPAR-α) (Forman *et al*. 1997). PUFAs can also serve as substrates for oxygenases like lipoxygenases (LOX) and cyclooxygenases (COX) leading to synthesis of biological active molecules (Phillis *et al*. 2006; Schneider *et al*. 2007). For instance, ARA and DHA are precursors of a wide range of oxygenated products called eicosanoids and docosanoids, respectively. Some of the most known eicosanoids are prostaglandins, leukotrienes, thromboxanes and prostacyclins (Fig. 5) (Wang *et al*. 2014). Eicosanoids derived from ARA are mostly related to inflammatory and allergic processes, platelet aggregation and recruitment of immune cells (Ricciotti and Fitzgerald 2011). On the other hand, docosanoids have been described as anti-inflammatory molecules, with maresins, neuroprotectins and resolvins among the most known (Fig. 6) (Bazan *et al*. 2010; Serhan 2014). Maresin 1 and its sulfide conjugates are reported by their ability to induce tissue regeneration in planaria (Serhan *et al*. 2012; Dalli *et al*. 2016). Another well-characterized enzymatic product of DHA is neuroprotectin D1, which possesses a protective role in the CNS reducing stress pathways that lead to cell death and increasing cell survival (Serhan 2014). Nonetheless, PUFAs are only not oxidized by enzymatic pathways, but also by free radicals via autoxidation processes. As a consequence, a wide range of non-stereospecific oxidized products can be formed and contribute to the modulation of several cellular processes (Leonarduzzi *et al*. 2000; Yin *et al*. 2011).

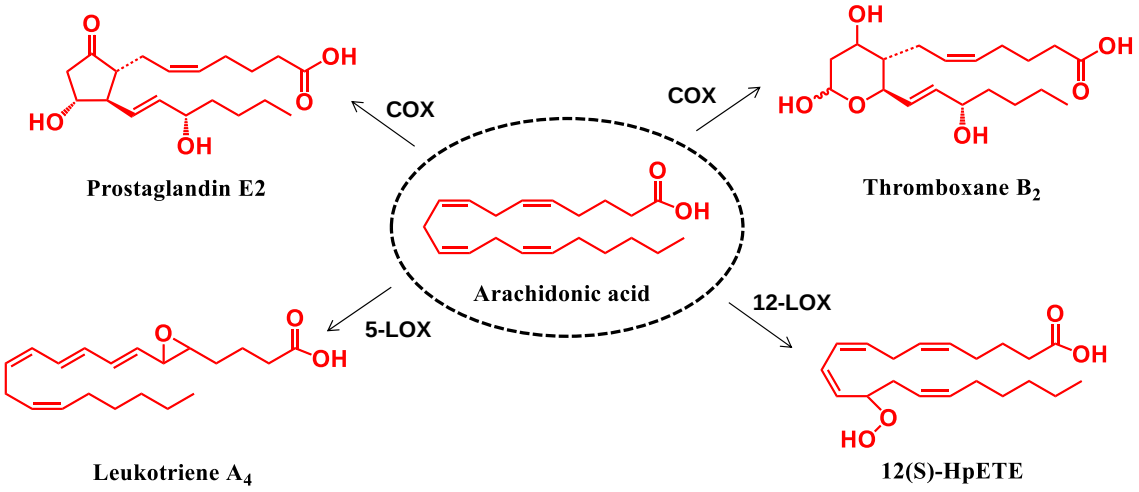

Figure 5. Eicosanoids derived from ARA.

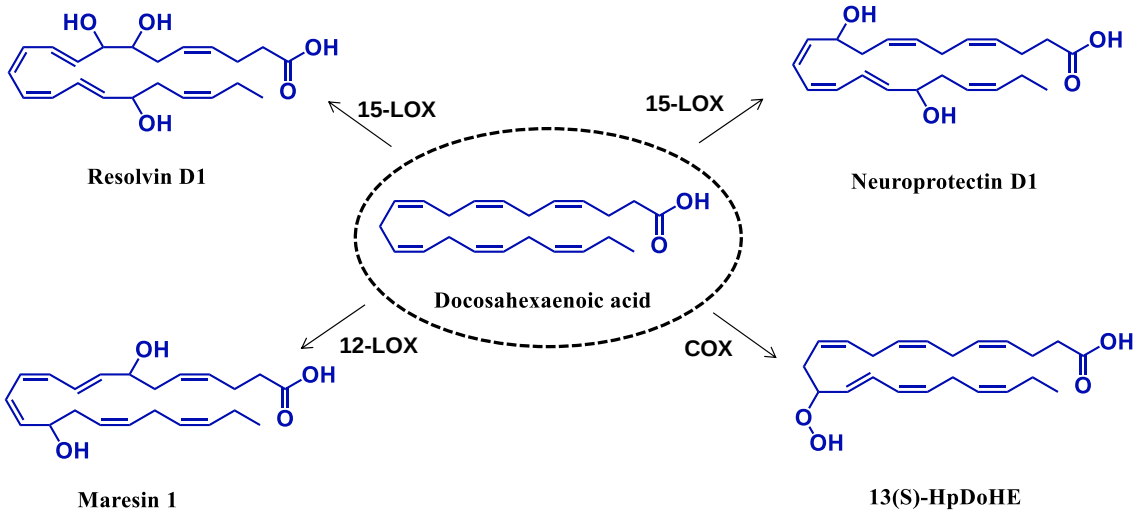

Figure 6. Docosanoids derived from DHA.

1.3. Reactive oxygen species (ROS), lipid peroxidation and oxidative stress

The term "reactive oxygen species" (ROS) is applied to molecules derived from oxygen metabolism, which possess high reactivity, such as the radicals hydroxyl ($HO^{\bullet}$) and superoxide anion ($O_2^{\bullet-}$), as well as non-radical molecules like hydrogen peroxide (H_2O_2) (Valko *et al*. 2007). Endogenously, ROS such as superoxide anion can be formed by oxidant enzymes such as NADPH oxidase and cytochrome P450 enzymes (CYP), in response to pathogens and xenobiotics, respectively (Robertson *et al*. 2004; Chrissobolis and Faraci

2008). Since approximately 85–90% of oxygen is used by mitochondria (Barber *et al*. 2006), it is during the transfer of electron in the mitochondrial respiratory chain where the highest production of superoxide anion usually occurs (Finkel and Holbrook 2000). Among the most accepted hypothesis, leakage of electrons from the intermediate semiquinone radical from ubiquinone can readily transfer an electron to oxygen, leading to formation of superoxide anion (Finkel and Holbrook 2000). Also, stimulation of lipid β-oxidation in mitochondria may contribute for leakage of electrons, since it requires more oxygen than glucose for its total oxidation (Schönfeld and Reiser 2013). The superoxide anion can be readily converted to hydrogen peroxide in a reaction catalyzed by the mitochondrial enzyme Mn-superoxide dismutase (SOD2) (Fukai and Ushio-Fukai 2011). If the hydrogen peroxide is not degraded by peroxidases, it may cross membranes and propagate oxidation beyond mitochondria (Fukai and Ushio-Fukai 2011). In reaction catalyzed by ferrous ion (Fe^{2+}), hydrogen peroxide can be converted into hydroxyl radical ($HO^{\bullet}$), the most reactive oxidant generated in biological systems (Niki 2009). At low concentrations, free radicals such as superoxide anion can play a pivotal role in cell defense against pathogens (Garthwaite and Boulton 1995; Chrissobolis and Faraci 2008). However, at high concentrations, free radicals can oxidize proteins, DNA and lipids. Consequently, cellular events linked to cell death and tissue dysfunction can be triggered (Murphy *et al*. 2011).

Because PUFAs like DHA and ARA are highly unsaturated, they are common targets of oxidation by ROS, in a process called autoxidation or lipid peroxidation (Fig. 7) (Yin *et al*. 2011). Oxidation of unsaturated fatty acids can lead to formation of a wide range of non-stereospecific and complex oxidized products (Yin *et al*. 2011). The first step of lipid peroxidation is the abstraction of a bis-allylic hydrogen in the lipid structure by a free radical, yielding a lipid radical (L•). Next, this lipid radical can easily react with oxygen, generating a lipid peroxyl radical (LOO•) (Niki 2009). The lipid peroxyl radical, in turn, is able to abstract

a proton from another PUFA triggering a chain reaction (Spiteller 2006). Still, lipid peroxyl radical can undergo intra-molecular cyclization yielding isofuranes or react with more oxygen molecules, yielding complex cyclic hydroperoxy-endoperoxide structures (Yin *et al*. 2011). The propagation of lipid peroxidation can be stopped by antioxidant molecules like α-tocopherol (vitamin E) resulting in the formation of lipid hydroperoxides (LOOH) (Gaschler and Stockwell 2017). Lipid hydroperoxides, in turn, can be readily reduced to less toxic alcohol derivatives by thiol and selenium groups of intracellular antioxidants, like glutathione (GSH) and glutathione peroxidase 4 (GPX4) (Ursini *et al*. 1982; Yuan and Kaplowitz 2009). Furthermore, lipid hydroperoxides can be converted into reactive ketones or even broken into short-chain aldehydes like 4-hydroxy nonenal (4-HNE), malondialdehyde (MDA) and acrolein (Siddiqui *et al*. 2008).

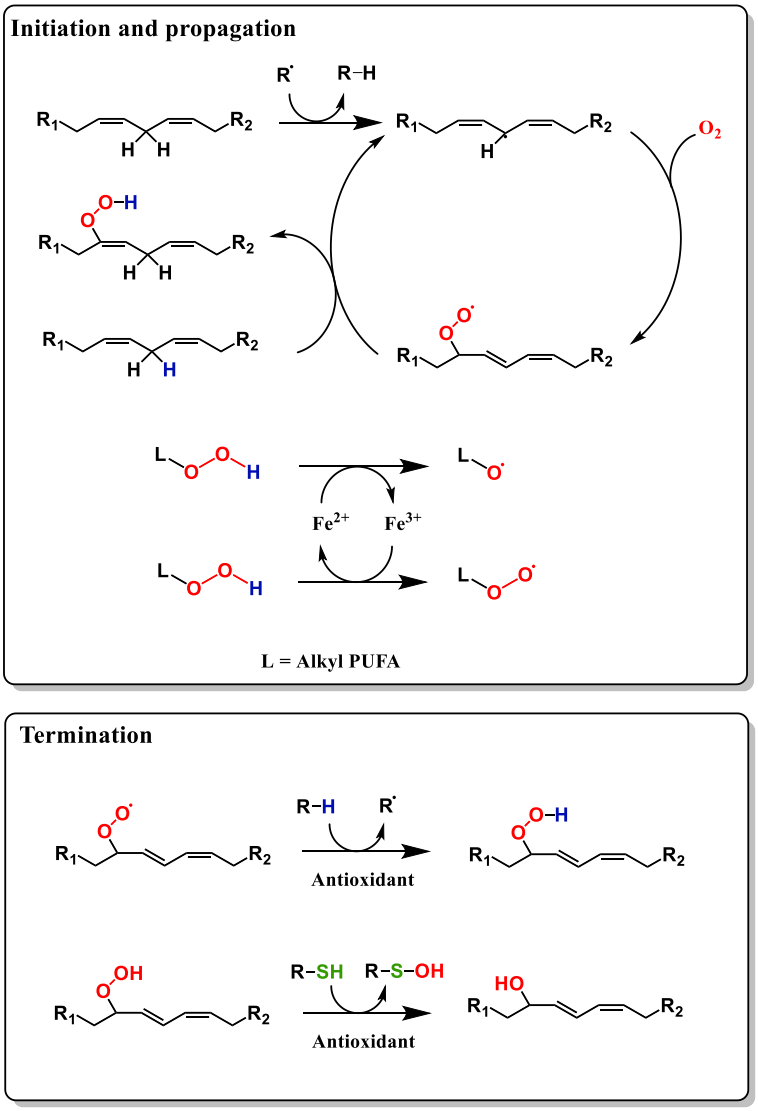

Figure 7. Mechanism of lipid peroxidation of PUFAs.

A considerable amount of side-chains of GPs is composed of PUFAs, which are very susceptible to oxidation by ROS. As a consequence, oxidation of these lipids can contribute to alterations in permeability and stability of membranes (Catalá 2009). Oxidized lipids are well known to augment oxidative stress by shifting the balance between production of oxidants and the antioxidant capacity of cells to eliminate these reactive molecules (Circu and Aw 2010). Oxidized lipids are also known to promote modification of proteins by reacting with histidine, lysine and cysteine residues (Hauck and Bernlohr 2016). Chemical modifications of

proteins may result in alterations of folding and biological function, leading to loss of cellular homeostasis (Hauck and Bernlohr 2016).

Thiol groups usually participate in processes that involve enzymatic activity, signal transduction, protein folding and antioxidant system (Winterbourn and Hampton 2008; Hansen and Winther 2009). Therefore, chemical modification of cysteine residues may modulate these cellular events and trigger the onset of pathological conditions (Fra *et al*. 2017; Valle and Carrì 2017). In a recent study performed by our group, it was demonstrated that DHA and its hydroperoxides induce SOD1 aggregation (Appolinário *et al*. 2015), a hallmark of amyotrophic lateral sclerosis (ALS) (Valentine *et al*. 2005). In this study, it was demonstrated that protein aggregation is tightly linked to the cysteine residues of SOD1 (Cys6 and Cys111). More recently, it has been proposed that accumulation of lipid hydroperoxides in the presence of metal ions induces ferroptosis, a regulated form of cell death linked to pathological conditions, like cancer (Yang and Stockwell 2016; Stockwell *et al*. 2017).

Ferroptosis is characterized by the loss of the activity of glutathione peroxidase 4 (GPX4), a selenocysteine enzyme responsible for reducing toxic lipid hydroperoxides (Yang and Stockwell 2016). In this context, some oxidized lipids can be important for activation of signaling pathways linked to antioxidant system. For instance, ketones derived from DHA are reported as modulators of Nrf2 pathway, which lead to upregulation of genes linked to synthesis of glutathione and others antioxidants (Groeger *et al*. 2010). In experiments performed with β-amyloid proteins, it was demonstrated that 4-hydroxy-2-nonenal (HNE), an α,β-unsaturated aldehyde derived from lipid peroxidation of n-6 PUFAs, induces amyloid β protein aggregation, common in Alzheimer's disease (AD) (Liu *et al*. 2008). On the other hand, 4-hydroxy-2-hexenal (HHE), an analogue aldehyde derived from n-3 PUFAs, does not induce peptide aggregation likely because its aliphatic chain is shorter by three methylene groups when compared to HNE (Liu *et al*. 2008). Although it is clear that chemical

modification of thiol groups of proteins and peptides by oxidized lipids modulates redox pathways, the role of autoxidized products of PUFAs in modifying thiols is still unknown. In chapter 1 of this thesis we investigate the mechanisms by which cyclic endoperoxides derived from ARA and DHA may modify cysteine residues of peptides (glutathione) and proteins (SOD1).

1.4. Neurodegenerative diseases and alterations in the lipidome

Neurodegeneration is a process that occurs in the central nervous system (CNS) characterized by loss of neuronal structure and function. Neurodegenerative disorders are generally age-dependent, such as in Alzheimer's disease (AD), multiple sclerosis, Parkinson's disease (PD) and amyotrophic lateral sclerosis (ALS), negatively affecting mental and physical functions (Chen *et al*. 2016). The majority of neurodegenerative diseases shares a common etiology, being the causes and molecular mechanisms involved in neurodegeneration usually similar (Pierpaoli 2005). Among them, chronic inflammation and oxidative stress, which are both strongly linked to the metabolism of lipids (Andersen 2004; Halliwell 2006). It is well described that aging is clearly associated with increased production of ROS, leading to the development of chronic oxidative stress (Poon *et al*. 2004; Halliwell 2006). As consequence, oxidative stress may lead to alterations in the lipid metabolism of the CNS by regulation of pathways linked to lipid synthesis, transport and also peroxidation (Cutler *et al*. 2002; Adibhatla and Hatcher 2007; Arima *et al*. 2015).

As part of this thesis, we focused in understanding the mechanisms involved in lipid metabolism of an ALS rodent model. ALS is a neurodegenerative disorder characterized by death of motor neurons in brain and spinal cord. Dysfunction and death of motor neurons lead to progressive muscle weakness, atrophy and paralysis followed by death between 3 and 5 years after symptoms onset (Gros-Louis *et al*. 2006). In a case study performed in USA, it was reported that the incidence of ALS is about 5 cases per 100,000 people per year and ALS

was more common among males between 60–69 years old (Mehta *et al*. 2016). Although the etiology of ALS is not totally known, it is described that about 10% of the causes of ALS are familiar with the majority being sporadic cases. From the familial ALS cases, 20% are associated with mutations in the gene encoding the Cu,Zn-superoxide dismutase (SOD1) (Naini *et al*. 2002).

SOD1 is a cytosolic metalloenzyme that plays a key role in antioxidant system, converting superoxide anion into hydrogen peroxide and molecular oxygen, similarly to SOD2 localized in mitochondria (García-Ramírez *et al*. 2008). Among the hypothesis associated to development of ALS by mutation of SOD1 gene, it is reported that mutant SOD1 catalyze the synthesis of oxidant agents by gain of peroxidase activity (Liu *et al*. 1999). Also, mutant SOD1 can undergo self oligomerization, leading to formation of cytotoxic aggregates (Bruijn *et al*. 2004). Although the mechanisms are still unclear, it is reported that neuronal mitochondrial dysfunction and protein aggregation contribute to ROS production in ALS (Jaarsma *et al*. 2000; Vandoorne *et al*. 2018). In ALS, it is proposed that ROS can inhibit glutamate uptake through the EAAT2 transporter in glial cells leading to calcium accumulation in mitochondria and ROS production in neurons (Barber *et al*. 2006). Thus, alterations in lipid metabolism may be expected in ALS, either by direct oxidation of unsaturated fatty acids or by modulation of enzymes linked to synthesis and degradation of lipids.

It is reported that in ALS, oxidation of PUFAs leads to protein modification by short chain aldehydes like HNE, derived from oxidation of omega-6 fatty acids (Pedersen *et al*. 1998; Perluigi *et al*. 2005). Also, decreased DHA content in phospholipids such as PC further suggests oxidation of this lipid subclass (Arima *et al*. 2015). In addition, eicosanoids derived from ARA, like prostaglandin E2 (PGE2), are increased in ALS (Almer *et al*. 2002). PGE2, in turn, can stimulate the release of glutamate from astrocytes leading to increased influx of

calcium and superoxide anion production in neurons of the CNS (Bezzi *et al*. 1998). Moreover, it was demonstrated that inhibition of COX-2 prolongs survival in a model of ALS mouse (Drachman *et al*. 2002). Together, these findings suggest that oxygenases like COX play an important role in the pathogenesis of ALS by increasing the levels of pro-inflammatory compounds like PGE2.

Targeted lipidomics analysis of spinal cord of ALS mouse model revealed alterations in the metabolism of ceramides and storage lipids like cholesteryl esters (Cutler *et al*. 2002). As suggested by these authors, ceramide synthesis by cleavage of sphingomyelin leads to synthesis of cholesteryl ester in ALS via acyl-CoA: cholesterol acyltransferase (ACAT). Ceramides and glucosylceramides are increased in cerebrospinal-fluid, spinal cord tissue and skeletal muscle of ALS patients and rodent models (Dodge *et al*. 2015; Henriques *et al*. 2015; Blasco *et al*. 2017). Furthermore, it has been demonstrated that glycosylated ceramides slow down the symptom progression of the disease in a rodent model of ALS (Dodge *et al*. 2015). Taken together, the data reported in the literature suggest that alterations in sphingolipid metabolism in CNS are directly associated with ALS. Nevertheless, it is clear that a more detailed characterization of the lipidome in the CNS will be required to a deeper understanding of alterations in lipid metabolism linked to neurodegenerative disorders such as ALS.

1.5. Analytical techniques for analysis of lipids

As described in the section 1.1, lipids comprise a large class of biomolecules characterized by high diversity in chemical structures and biological functions. Thus, the development of robust techniques for accurate identification and quantification of lipid are required to capture this variety of structures. One of the simplest methods used to characterize lipids, and still very useful today, is thin layer chromatography (TLC) (Carrasco-Pancorbo *et al*. 2009). Using TLC, it is possible to separate, identify and quantify lipid subclasses such as

TAG, specific phospholipids and sphingolipids. Here, subclasses are isolated and analyzed as a whole rather than individual lipids. Other assays based on enzymatic reactions coupled to chromophore groups are used to identify lipid classes like glycerolipids (Warnick 1986). Nuclear magnetic resonance (NMR) can be also used for characterization of purified lipids, but this method requires high purity and milligram amounts of target compounds, making this technique unsuitable for whole lipidome analysis (Carrasco-Pancorbo *et al*. 2009). Techniques based on liquid (LC) or gas (GC) chromatography are frequently used for lipid analysis. However, LC analysis coupled to UV/detection provides low specificity for lipid identification, especially when the compounds display absorbance at similar wavelengths. Although GC coupled to mass spectrometry (MS) is a powerful tool for quantitative and qualitative (structural elucidation) analysis of fatty acids and sterols, it is limited to volatile lipids entering the gas phase and those amenable to derivatization (Quehenberger *et al*. 2011). With the discovery of the electrospray ionization technique (ESI), non-volatile lipids such as phospholipids and sphingolipids could be finally loaded as intact molecules into a MS (Pulfer and Murphy 2003). This technique has emerged as the main tool for analysis of cellular lipidome due its capacity to provide accurate information about the mass and fragmentation profile of the analytes (Wenk 2005).

Analysis of a vast number (hundreds to thousands) of molecular species of lipids by mass spectrometry are usually performed by direct infusion or coupled to ultra-high performance liquid chromatography (UHPLC) (Wenk 2010). Although lipidomics analysis performed by direct infusion in MS are usually faster and provide general information about sample composition, this approach can suffer interferences like ion suppression caused by co-elution of compounds and low resolution for identification of isobaric compounds (Carrasco-Pancorbo *et al*. 2009). Despite the drawback for method optimization and time of analysis, liquid chromatography coupled to MS (UHPLC-MS/MS) represents an alternative to improve

both sensitivity and specificity of lipid analysis through separation of the compounds according to their chemical characteristics. Another challenge in working with ESI-MS is that each compound tends to ionize with distinct efficiencies. To cope with this issue, the use of internal standards can correct for loss of analytes during sample preparation and distinct ionization efficiencies, making the analysis of lipids by ESI-MS semi-quantitative. The semi-quantitation of lipids is due to their structural diversity and the unlikelihood of using internal standards for each compound. Finally, MS is usually a technique that requires high investment for maintenance and high expertise.

Although there are some relevant challenges in the use of UHPLC-MS/MS, it is the most robust technique for a comprehensive analysis of lipids. The identification based on fragmentation profiles of analytes reduces drastically the false discovery rates providing a precise identification of compounds. Also, a large number of analytes can be analyzed in a single run in untargeted and targeted analysis, even those molecules present in very low picogram concentrations. Thus, UHPLC-MS/MS emerged as a powerful tool for analysis of cellular lipidomes and has been providing essential information about the roles of lipids in biological systems.

2. OBJECTIVE

2.1. General objective

Investigate redox-triggered events in lipid biology.

2.2. Specific objectives

Chapter 1: Elucidate mechanisms by which auto-oxidized ARA and DHA may modify cysteine residues of peptides (GSH) and proteins (SOD1).

Chapter 2: Characterize lipidome alterations in brain and spinal cord of a rodent model of amyotrophic lateral sclerosis (ALS).

CHAPTER 1

Hydroxy-endoperoxides derived from Polyunsaturated Fatty Acids Reacts with Thiols Producing Conjugates

Adriano B. Chaves-Filho, Marcos Y. Yoshinaga, Lucas S. Dantas, Larissa R. Diniz, and Sayuri Miyamoto*.

Department of Biochemistry, Institute of Chemistry, University of São Paulo, São Paulo, Brazil.

*Corresponding author: Instituto de Química, Departamento de Bioquímica, Universidade de São Paulo, CP 26077, CEP 05513-970, São Paulo, Brazil.

E-mail: miyamoto@iq.usp.br

Abstract

Polyunsaturated fatty acids (PUFA) are converted to a series of oxygenated cyclic products upon enzymatic and non-enzymatic oxidation. Even though the mechanisms by which poly-oxygenated cyclic products are formed is well described, their reactivity towards biomolecules, particularly those containing thiol groups are less explored. Using an untargeted high resolution LC-MS/MS approach, we identified a series of glutathione (GSH)-conjugates with poly-oxygenated cyclic products derived from docosahexaenoic (DHA) and arachidonic (ARA) acid. MS/MS spectra obtained from GSH-conjugates revealed that GSH are bonded to hydroxy-endoperoxides through a thioperoxide (RS-OR) linkage. Here, we suggest that hydroxy-endoperoxides undergo a nucleophilic attack by the thiolate anion to form a sulfenate ester bond. In experiments performed with GSH and DHA in the presence of the radical initiator AAPH, we observed conjugates of DHA covalently linked to GSH, likely derived from a thiol-ene reaction where thiyl radical (GS·) reacts with DHA double bonds. Therefore, a mechanism of reaction involving cyclic endoperoxides and thiolate anion from GSH is proposed. Assays performed with the enzyme superoxide dismutase 1 suggest that the reactive thiol groups of proteins are also a target for modification by hydroxy-endoperoxides. In summary, our data reveal novel DHA and ARA oxidation products that can modify the thiol group of GSH and proteins yielding conjugates potentially relevant in redox and inflammatory processes.

Keywords: Docosahexaenoic acid, arachidonic acid, hydroxy-endoperoxide, glutathione, thiols, mass spectrometry.

1. Introduction

Arachidonic (C20:4n-6, ARA) and docosahexaenoic (C22:6n-3, DHA) acids are two of the most abundant polyunsaturated fatty acids (PUFAs) found in mammalian cells. Usually, they are found esterified at *sn*-2 position of membrane phospholipids.[1,2] Upon their release by activated phospholipases, ARA and DHA may serve as substrates for oxygenases, such as lipoxygenases (LOX), cyclooxygenases (COX) and cytochrome P450 monooxygenase.[3] The enzymatic products derived from ARA and DHA are commonly known by the general terms “eicosanoids” and “docosanoids", respectively.[4] Leukotrienes, prostaglandins and thromboxanes are subclasses of eicosanoids that play an important role in inflammatory processes by promoting neutrophil recruitment, inducing allergic reactions and platelet aggregation.[5–7] Docosanoids have received increased scientific attention due to their role as anti-inflammatory agents. Among the latter, resolvins, maresins and neuroprotectins are implicated in the inhibition of neuron death by apoptosis, in tissue regeneration and downregulation of pro-inflammatory mediator levels.[8–10]

ARA and DHA are highly unsaturated lipids and may thus readily undergo oxidation, thereby yielding peroxyl radicals, which in turn can be converted into hydroperoxides or into a wide range of cyclic endoperoxides.[11] Since these primary oxidation products are relatively unstable, they may be cleaved into short chain metabolites containing reactive carbonyl groups.[12] Ketones and aldehydes derived from PUFAs are remarkably reactive and may form adducts with cysteine, lysine and histidine residues of proteins, via mechanisms like Michael addition and Schiff base formation.[13–15] Thiol groups usually participate in processes that involve enzymatic activity, signal transduction, protein folding and antioxidant system.[16] Therefore chemical modification of cysteine residues may modulate these cellular events and trigger the onset of pathological conditions.[17,18]

Oxidative stress and chronic inflammation are hallmarks of neurodegenerative diseases, such as amyotrophic lateral sclerosis (ALS), Parkinson's (PD) and Alzheimer's (AD) diseases, and may contribute to formation of reactive compounds derived from ARA and DHA.[19–22] These latter fatty acids are the most abundant PUFAs in the brain,[23] and their oxidation modulates signaling pathways linked to cell defense, as reported for the Nrf2-Keap1 pathway and the upregulation of antioxidant proteins genes.[15] Thiol groups of peptides like glutathione (GSH), an intracellular antioxidant, can also serve as substrate for enzymatic synthesis of bioactive conjugates with eicosanoids or docosanoids, namely leukotriene C_4 (LTC_4) and MCTR1, respectively. Although the latter compounds are both linked to a molecule of GSH, LTC_4 is related to allergic response in pulmonary diseases,[7] whereas MCTR1 has been implicated in promoting tissue regeneration.[24] That is, chemical modifications of peptides and proteins may trigger differential biological effects according to the oxidized PUFAs linked to them.

Thus far, modifications of thiol groups by ketones and aldehydes derived from PUFAs have been relatively well studied.[15,25,26] However, to the best of our knowledge, chemical modifications of peptides or proteins by cyclic PUFA's oxidation products have never been reported. Here, we investigate the mechanisms by which auto-oxidized ARA and DHA may modify cysteine residues of a peptide (GSH) and a protein (SOD1).

2. Experimental section

2.1. Chemicals and reagents

L-glutathione reduced, docosahexaenoic and arachidonic acids were purchased from Sigma (St. Louis, USA). The leukotriene C_4 was obtained from Cayman (Ann Arbor, USA). Proteomic grade trypsin and RapiGest SF surfactant were acquired from Promega (Madison, USA) and Waters (Milford, USA), respectively. 2,2'-Azobis(2-methylpropionamidine)

dihydrochloride (AAPH) was obtained from Wako (Osaka, Japan). Solvents (HPLC grade) were purchased from J.T. Baker (Avantor Performance Materials, Mexico). All other reagents were purchased from Sigma (St. Louis, USA). Aqueous solutions were prepared with ultrapure water purified by a Direct-Q3 system (Merck Millipore, Germany).

2.2. Incubation between GSH and PUFAs

Samples were prepared with 10 mM GSH in presence of Methanol (10 %, *v/v*), 100 μM DHA or 100 μM ARA previously stored at -20 ºC for at least 5 years. All incubations were performed in 200 mM sodium phosphate buffer (pH 7.4) for 1h at 37 ºC. After that, incubations were analyzed by LC-MS/MS.

2.3. LC-MS/MS method for analysis of GSH-adducts

Samples were analyzed by ESI-TOF-MS (Triple TOF 6600, Sciex, Concord, US) interfaced with a high-performance LC (UHPLC Nexera, Shimadzu, Kyoto, Japan). The GSH-adducts were separated chromatographically through a C18 column (Kinetex C18 100A, 100 x 2.1 mm, 2.6 μm, Phenomenex Inc., Torrance, CA) with a flow rate of 0.2 mL min^{-1}. The auto injector and column temperature were maintained at 4 ºC and 25 ºC, respectively. The mobile phase A consisted of water, while mobile phase B was composed of acetonitrile. Mobile phases A and B contained formic acid (at a final concentration of 0.005 %). The linear gradient during analysis was as follows: hold at 1 % B from 0-5 min.; from 1 to 80 % B over 7 min., hold at 80 % B from 7-12 min., decreased from 80 to 1 % B during 12-13 min., and hold at 1 % B from 13-20 min. The injection volume was set at 5 μL.

The ESI-TOF-MS was operated in negative ionization mode, and the scan range set at a mass-to-charge ratio of 200-2000 Da. Data for RSH-adducts identification was obtained by Information Dependent Acquisition (IDA®). Data acquisition was performed with a period cycle time of 0.650 s with 0.100 s acquisition time for MS1 scan and 0.050 s acquisition time to obtain the top 10 precursor ions. Data acquisition was performed using Analyst® 1.7.1 with

an ion spray voltage of -4.5 kV, cone voltage at -80 V and collision energy was set at -30 eV. The curtain gas was set at 25 psi, nebulizer and heater gases at 45 psi and interface heater of 450 °C. The mass spectra were analyzed with PeakView®. For semi-quantification, the area of each GSH adduct was obtained by MS data from MultiQuant®.

2.4. Purification of auto-oxidized fatty acids by HPLC-DAD

Highly oxidized DHA or ARA stored at -20 ºC for at least 5 years were purified using LC system coupled to a diode array detector (DAD) (HPLC Prominence, Shimadzu, Kyoto, Japan). The fractions were separated chromatographically using a semi-preparative C18 column (Luna C18, 250 x 10 mm, 5.0 µm, Phenomenex Inc., Torrance, CA) with a flow rate of 4.7 mL min^{-1}. The auto injector and column temperature were maintained at 4 ºC and 25 ºC, respectively. The mobile phase A consisted of water, while mobile phase B was composed of acetonitrile. Mobile phases A and B contained formic acid (at a final concentration of 0.005 %). The linear gradient during analysis were as follows: hold at 70 % B from 0-15 min.; from 70 to 99 % B over 16 min., hold at 99 % B from 16-23 min., decreased from 99 to 70 % B during 23-24 min., and hold at 70 % B from 24-30 min. Fractions were collected in a single injection each (100 µL) of 10 mM DHA or 10 mM ARA, according to their absorption spectrum in UV/Vis. After collected, lipid fractions (F1 to F9) were partially dried under N_2 gas to remove the acetonitrile. The fraction correspondent to the non-oxidized lipid (F9) was dried under N_2 gas and dissolved in methanol.

2.5. LC-MS/MS method for characterization of cyclic endoperoxides derived from DHA and ARA

The oxidized lipids were separated chromatographically through a C18 column (Acquity UHPLC BEH C18 100A, 100 x 2.1 mm, 1.7 µm, Waters, Milford, USA) with a flow rate of 0.2 mL min^{-1}. The auto injector and column temperature were maintained at 4 ºC and 30 ºC, respectively. The mobile phase A consisted of water, while mobile phase B was

composed of acetonitrile. Mobile phases A and B contained formic acid (at a final concentration of 0.005 %). The linear gradient during analysis were as follows: hold at 1 % B from 0-2 min.; increased from 1 to 40 % B over 3 min., from 40 to 55 % B during 3-11 min., increased from 55 to 90 % B during 11-12 min., hold at 90 % B from 12-14 min., decreased from 90 to 1 % B during 14-15 min., and hold at 1 % B from 15-20 min. The injection volume was set at 5 μL. The ESI-TOF-MS was operated in negative ionization mode, and the scan range set at a mass-to-charge ratio of 200-1000 Da. Data for oxidized lipids identification was obtained by Product Ion analysis. Data acquisition was performed with a period cycle time of 0.385 s with 0.025 s acquisition time for MS1 scan and 0.010 s acquisition time to obtain precursor ions. Data acquisition was performed using Analyst® 1.7.1 with an ion spray voltage of -4.5 kV and the cone voltage at - 80 V. The curtain gas was set at 25 psi, nebulizer and heater gases at 45 psi and interface heater of 450°C.

2.6. Stability assay of GSH-adducts

Samples were prepared with 1 mM GSH in presence of DHA-F3 (10 %; *v/v*) or ARA-F2 (10 %; *v/v*). All incubations were performed in 200 mM sodium phosphate buffer (pH 7.4) for 1h at 37 ºC. After incubation, GSH-adducts were extracted using solid-phase extraction (Discovery® DSC-18 SPE 500 mg column, Sigma) and eluted using methanol.[4] Samples were dried under N_2 gas and suspended 200 mM sodium phosphate buffer (pH 7.4). Purified GSH-adducts and LTC_4 (500 ng/mL) were added with H_2O (control; final pH 7.4), HCl (0.2 %, *v/v*; final pH 3.0) or NaOH (153 mM; final pH 11.0). After that, the GSH-adducts and the oxidized lipids derived from them were analyzed by LC-MS/MS as described in items *2.3* and *2.5*, respectively**.**

2.7. Human Recombinant SOD1 Expression and Purification and Preparation of apo-SOD1 WT

The enzyme was expressed in *Escherichia coli* and purified as previously described.[27] Purified protein was repeatedly washed and concentrated by ultrafiltration filter cut off 30 kDa (Amicon Ultra Centrifugal Filter) in 5 mM phosphate buffer pH 7.4, treated with Chelex-100. Apo-form was prepared from SOD1 by repeated dialysis against: (1) 50 mM acetate buffer pH 3.8 containing 10 mM EDTA, (2) 50 mM acetate buffer pH 3.8 containing 100 mM NaCl to remove EDTA and (3) finally, against Milli-Q grade water, treated with Chelex-100 resin to remove traces of transition metals.[27]

2.8. SOD1 Incubation, enzymatic digestion and peptide analysis

SOD1 WT (10 µM) in apo form was incubated in 50 mM phosphate buffer (pH 7.4) containing 150 mM NaCl and 100 µM DTPA for 1 h at 37 ºC in the presence of 100 µM ARA. Control was performed in presence of methanol (10 %, v/v). SOD1 samples were digested for 18 h with proteomic grade trypsin (Promega) in a 1:100 (w/w) ratio at 37 ºC with aid of RapiGest SF Surfactant (Waters, Milford, USA). The resulting peptides were analyzed by LC-MS/MS using a nanoAcquity UPLC system (Waters, United States) coupled to a TripleTOF 6600 mass spectrometer (Sciex, United States). The peptides were separated chromatographically through a C18 column (Acquity UPLC C18 100A, 20 mm x 180 µm, 5.0 µm, Waters, Milford, USA) with a flow rate of 0.4 µL min^{-1}. The auto injector and column temperature were maintained at 4 ºC and 35 ºC, respectively. The mobile phase A consisted of water, while mobile phase B was composed of acetonitrile. Mobile phases A and B contained formic acid (at a final concentration of 0.1 %). The linear gradient during analysis was as follows: from 1 to 35 % B over 60 min., from 35 to 90 % B over 61 min., hold at 90 % B from 61-73 min., decreased from 90 to 1 % B during 73-74 min., and hold at 1 % B from 74-97 min. The injection volume was set at 1 µL. Data for modified peptides identification was

obtained by Information Dependent Acquisition (IDA®). The search for modified peptides were performed by Mascot software and confirmed by checking the MS/MS spectra in PeakView®. All mass assignments were performed using < 10 ppm as acceptable error.

2.9. Incubation of GSH with N-ethylmaleimide (NEM)

First, 1 mM GSH was incubated with H_2O (control) or 5 mM NEM for 15 min at 37 ºC. After that, the ARA-F2 (10 %; *v/v*) was added in the samples and incubated for 15 min at 37 ºC. The levels of GSH-adducts were checked by LC-MS/MS.

2.10. Incubation with N-acetylcysteine (NAC)

Incubations were performed with 10 mM NAC in presence or absence of 100 µM DHA. All incubations were performed in 200 mM sodium phosphate buffer (pH 7.4) for 1h at 37 ºC. After that, incubations were analyzed by LC-MS/MS for identification of NAC-adducts.

2.11. Incubation between GSH and DHA in presence of a free radical generator.

Incubations were prepared with 10 mM GSH and 100 µM DHA in presence of 50 mM 2,2-Azobis(2-methylpropionamidine) dihydrochloride (AAPH), a free radical-generating compound. All incubations were performed in 200 mM sodium phosphate buffer for 1h at 37 ºC. After that, incubations were analyzed by LC-MS/MS.

2.12. Data analysis

All data are presented as average ± standard deviation (SD). Means were compared using GraphPad Prism Software (La Jolla, USA) and differences were considered significant at $p < 0.05$.

3. Results and discussions

3.1. GSH forms several adducts with oxygenated PUFA

To identify GSH-PUFA adducts we performed an untargeted analysis using high resolution LC-MS/MS (Figure 1). Our global analysis identified several high-molecular weight ions with *m/z* values above 650 Da (between 7.5 and 8.5 min, grey filled circles) with intermediate polarity between GSH (1.5 min) and DHA (12 min) or ARA (12.5 min). MS/MS data obtained for these species revealed that they are adducts formed by the conjugation of one molecule of GSH (*m/z* 306.0765) with oxygenated derivatives of DHA (*m/z* 327.2330) or ARA (*m/z* 303.2330).

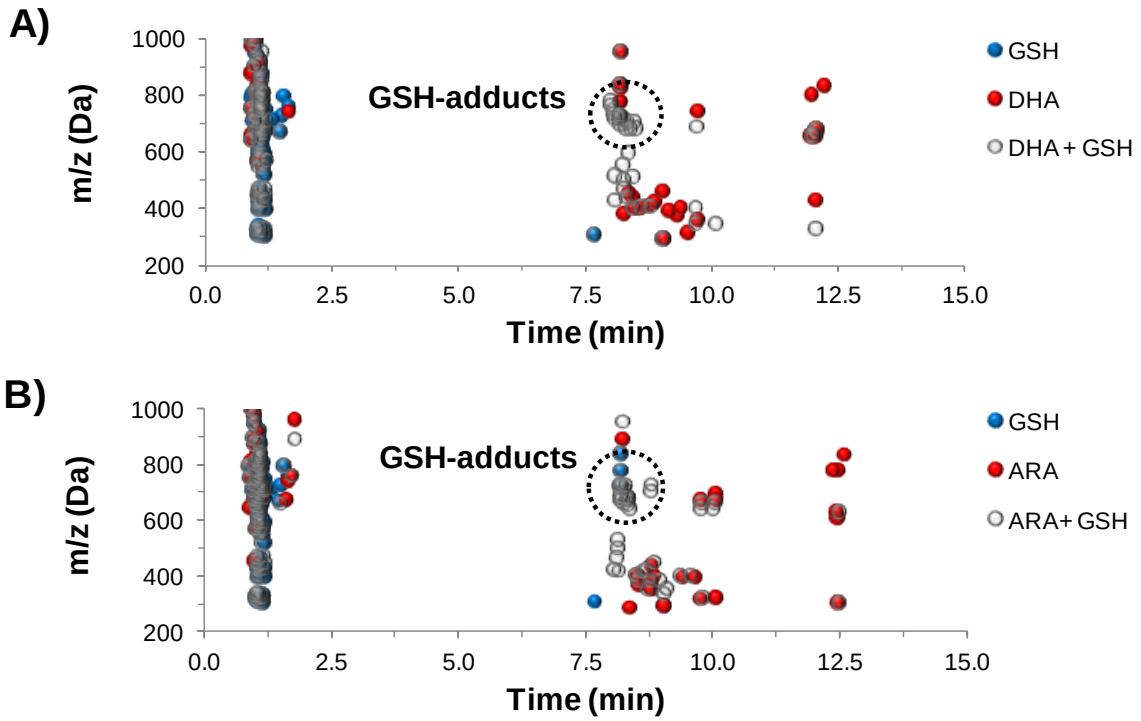

Figure 1. Incubations with PUFA and GSH yield new high molecular weight conjugates. Incubations were performed in 200 mM phosphate buffer (pH 7.4) with 100 µM DHA (A) or 100 µM ARA (B) in presence or absence of 10 mM GSH. Only precursor ions with total ion count (TIC) above 3 x 10^4 are shown in the figure. Each point in the map represents an ion selected for auto fragmentation. Untargeted MS/MS data was acquired by information dependent analysis (IDA).

Detailed MS/MS spectra analysis, showed that they share a common fragment ion at *m/z* 306.0765 as the most abundant ion, which corresponds to the mass-to-charge ratio of GSH (Figure S1). By looking to this fragment we have identified seven GSH-oxygenated DHA adducts (GSH-DHA-O_x), and five GSH-oxygenated ARA adducts (GSH-ARA-O_x). Adducts differed to each other by an increment of 16 Da indicating the incorporation of one oxygen atom in the molecular structure of the adducts. Semi-quantitative analysis of GSH-adducts, demonstrated that oxygenated forms containing 3, 4 and 5 oxygen atoms are more abundant compared to those having more than 6 oxygens (Figure 2). The successive increment in oxygen atoms led us to conclude that GSH-adducts are formed by the reaction of GSH with a series of oxygenated fatty acid intermediates that typically arises from free radical mediated lipid peroxidation. For PUFAs like ARA and DHA that contains more than three double bonds, the radical chain reaction involves a series of successive peroxyl radical cyclization and oxygen addition reactions, yielding monocyclic peroxides and serial cyclic peroxides.[11]

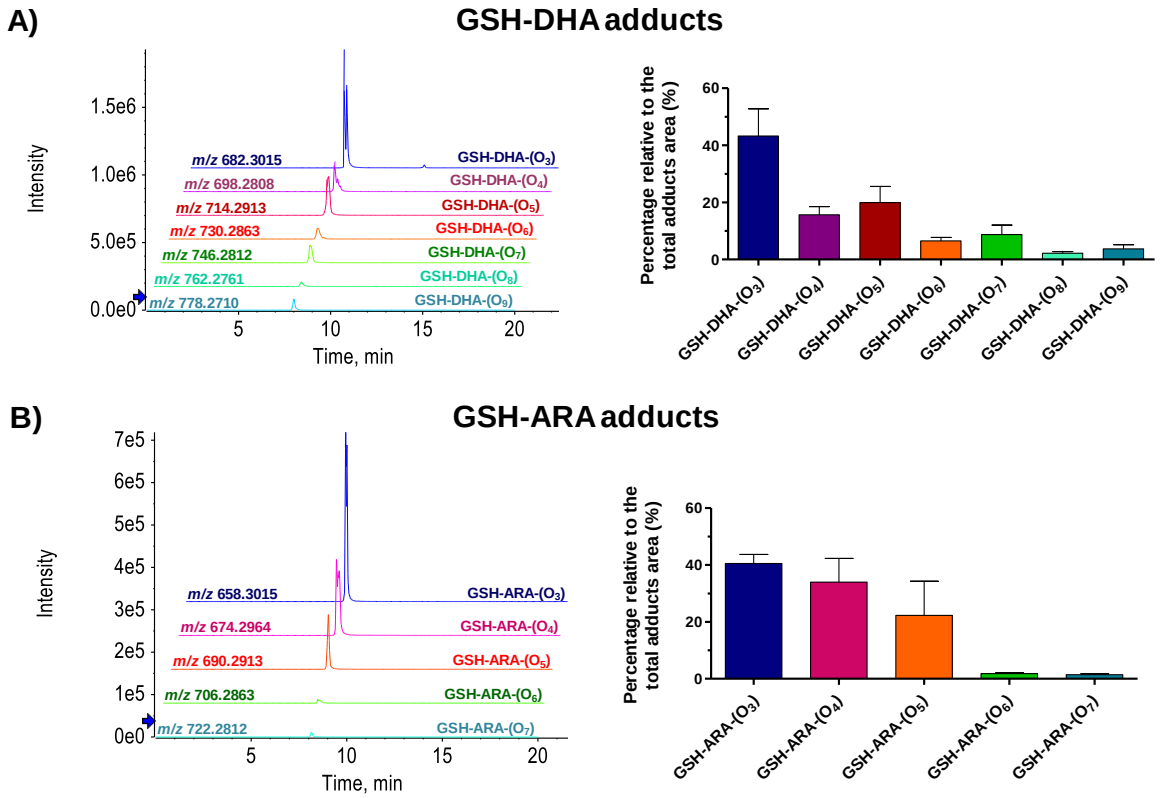

Figure 2. GSH-adducts found in incubations are characterized by increment of oxygen atoms in the PUFAs structure. The extracted-ion chromatogram (XIC) and area of each GSH-adduct was plotted for incubations with 100 µM DHA (A) or 100 µM ARA (B) in presence of 10 mM GSH. The sum of all GSH-adducts was defined as 100 % and the relative percentage of each adduct was calculated. Data were expressed as average ± standard deviation (n = 3).

Although the mechanisms associated with formation of GSH-adducts derived from highly oxidized PUFAs remain unclear, some of the glutathione conjugates derived from enzymatic pathways are well described. One of the most known GSH-adduct is the leukotriene C_4 (LTC_4), an enzymatic product derived from oxidative metabolism of ARA synthesized by neutrophils and macrophages.[28] The discovery of the first leukotrienes in 1938 represented a milestone in understanding the role of PUFAs regulating biological functions, particularly those associated with inflammation and respiratory disorders.[29,30] It was only recently, however, that 13,14-epoxy-Maresin, an enzymatic product derived from DHA, was

reported as the precursor of an enzymatic GSH-adduct.[24] In subsequent investigations, the GSH-Maresin adduct namely 13-glutathionyl-14-hydroxy docosahexaenoic acid (MCTR1) and derivatives thereof were reported as powerful tissue-regenerating mediators produced by macrophages.[31,32] In addition to these enzymatic GSH-adducts, glutathione conjugates with ketones derived from DHA were implicated in multi-drug resistant protein-mediated export and a redox signaling role.[15] In summary, data from the literature support the key role of glutathione conjugates with PUFAs as modulators of inflammatory and redox processes.

3.2. GSH-adducts display MS/MS spectra that contrast to a similar enzymatically-derived adduct (LTC_4)

To provide detailed information on the GSH adducts formed with oxygenated DHA or ARA we carried out a comprehensive structural study. For this purpose, we initially focused on the characterization of the less oxygenated derivatives, namely GSH-DHA-(O_3) (Figure 3A) and GSH-ARA-(O_3) (Figure 3B). MS/MS spectra of these GSH-adducts showed fragment ions that can be attributed to the oxidized DHA-(O_3) (*m/z* 375.2177) and ARA-(O_3) (*m/z* 351.2177) and fragments at *m/z* 553.2589 and *m/z* 529.2589 derived from the cleavage of the peptide bond of GSH-DHA-(O_3) and GSH-ARA-(O_3). More importantly, the ion at *m/z* 306.0765 is the most prominent fragment in both adducts, suggesting that the bond between oxidized PUFAs and GSH is labile and can be easily broken during MS/MS experiments.

To check whether the GSH-oxygenated fatty acid adducts are somehow similar to the known enzymatically generated GSH adduct, we have compared their MS/MS profile to that of LTC_4 (Figure 3C). In contrast to the novel GSH-adducts identified in this study, MS/MS spectrum of LTC_4 clearly displays a fragment ion at *m/z* 272.0888 as the most abundant ion (Figure 3C). This fragmentation pattern of LTC_4 suggests that the bond between the sulfur and carbon atoms (from GSH and ARA, respectively) is not labile enough to be cleaved generating a major fragment ion at *m/z* 306.0765 as in GSH-DHA-(O_3) and GSH-ARA-(O_3)

(Figure 3A and 3B). Moreover, a fragment corresponding to the intact oxidized ARA bonded to a sulfur atom from GSH is observed at *m/z* 351.1999 (Figure 3C), which is absent in the novel GSH-adducts. For instance, in MS/MS spectrum of GSH-ARA-O_3 it is possible to observe a fragment ion at *m/z* 351.2195, which originates from the presence of 2 oxygen atoms (*m/z* 351.2177, Figure 3B) instead of a sulfur atom in the ARA (*m/z* 351.1999).

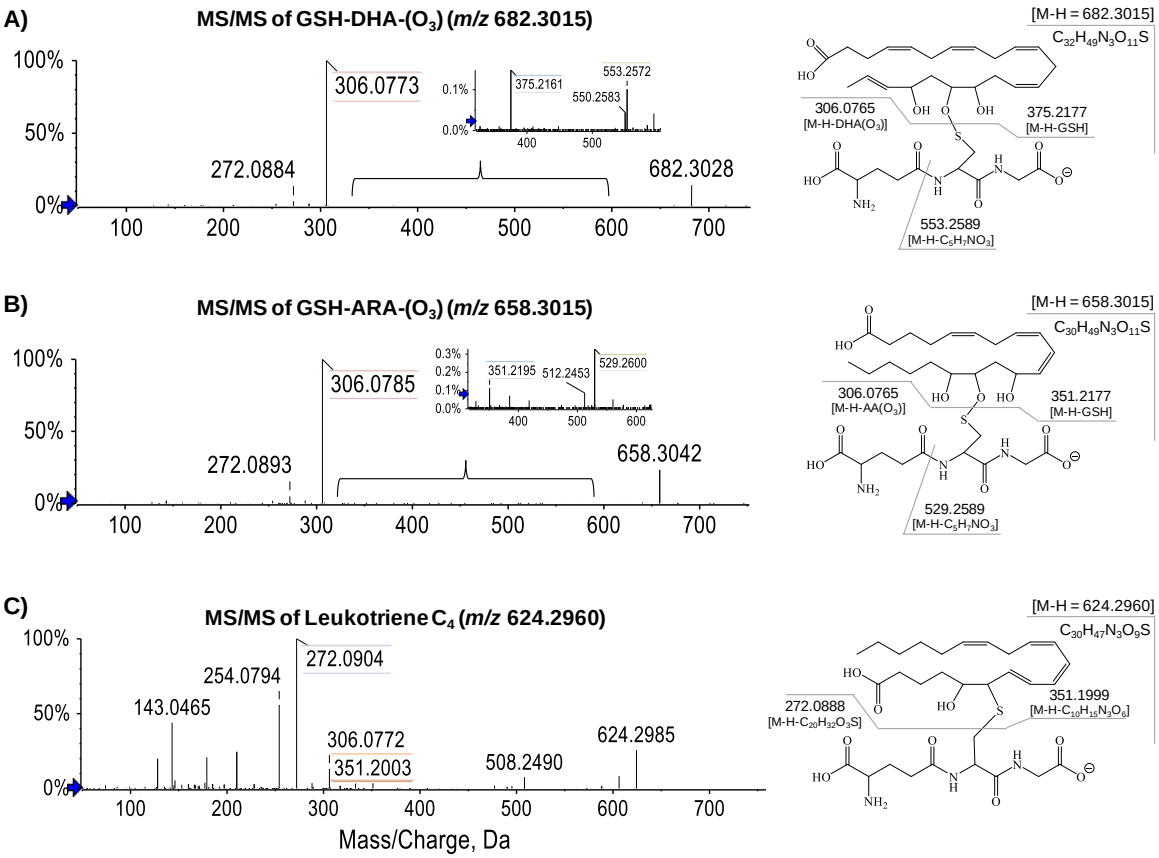

Figure 3. GSH-adducts display MS/MS spectra that contrast to LTC$_4$. The fragmentation profile of GSH-DHA-(O_3) (A), GSH-ARA-(O_3) (B) and Leukotriene C_4 (C) were obtained using the same parameters for ionization and fragmentation during LC-MS/MS analysis (Declustering Potential = 80 V; Collision energy = 25 eV).

Our findings thus suggest that the covalent linkage between GSH and DHA-(O_3) or ARA-(O_3) is characteristic of a sulfur-oxygen chemical bond (also known as sulfanate ester bond), which is more labile if compared to the sulfur-carbon bond present in LTC$_4$. To ensure

that the thiol group participates directly in the formation of GSH-adducts, we used n-ethylmaleimide (NEM), an organic compound that blocks the chemical activity of thiol groups (Figure S2). Pre-incubation of 1 mM GSH with 5 mM NEM clearly avoided formation of adducts, confirming that thiol participates directly in the reaction.

3.3. Proposed mechanisms for cyclization of lipid peroxyl radicals and reaction between cyclic endoperoxides and thiol groups

Taking into account the detection of a series of poly-oxygenated GSH-fatty acid adducts we have envisaged a scheme whereby they could be formed. Scheme 1 illustrates how oxidized products derived from ARA (and other PUFAs in general) could serve as precursors of GSH-adducts according to mechanisms of lipid peroxyl cyclization described in the literature.[11] After abstraction of a PUFA's hydrogen atom (Scheme 1 - Step 1), the resulting carbon centered lipid radical can react with oxygen yielding a peroxyl radical (Scheme 1 - Step 2). This peroxyl radical may abstract a hydrogen atom from another lipid to produce lipid hydroperoxides (Scheme 1 - Step 3) or undergo a *5-exo* cyclization step to yield a cyclic peroxide (1,2-dioxolane) containing a carbon-centered radical (Scheme 1 - Step 4). Sequentially, this radical reacts with another oxygen molecule yielding a peroxyl radical (Scheme 1 - Step 5). From then on, this radical could either abstract a hydrogen atom from another lipid to form a relatively stable hydroperoxide-endoperoxide (hydroperoxy-1,2-dioxolane) product (red and green arrows, Scheme 1 - Step 6) or undergo bicyclization (the isoprostane pathway, not shown here) and/or additional *5-exo* cyclizations (blue arrow, Scheme 1 - Step 7) yielding serial hydroperoxy-endoperoxide products (Scheme 1 - Step 8).[11] The higher the number of double bonds present in the PUFA, the more oxygen atoms can be added to its structure. Thus PUFA´s cyclization reactions generate oxygenated compounds containing hydroperoxy-endoperoxide groups that can be reduced into hydroxy-endoperoxides by reducing agents, like GSH (Scheme 1 - Step 9). Furthermore, the cyclic

endoperoxide may undergo a nucleophilic attack by thiolate anion (GS^-). Similar mechanism has been proposed for the conversion of prostaglandin H_2 (PGH_2) to prostaglandin D_2/E_2.[33] In this process (Scheme 1 - Step 10), the hydroxyl group adjacent to the endoperoxide may pull the electronic density, and as a consequence the closest oxygen atom in the cyclic structure becomes more susceptible to react with thiolate anion. The proposed cyclization mechanism supports the diversity of PUFA-derived GSH-adducts with additions of up to seven oxygen atoms for ARA and nine for DHA (Figure 2, Figure S1).

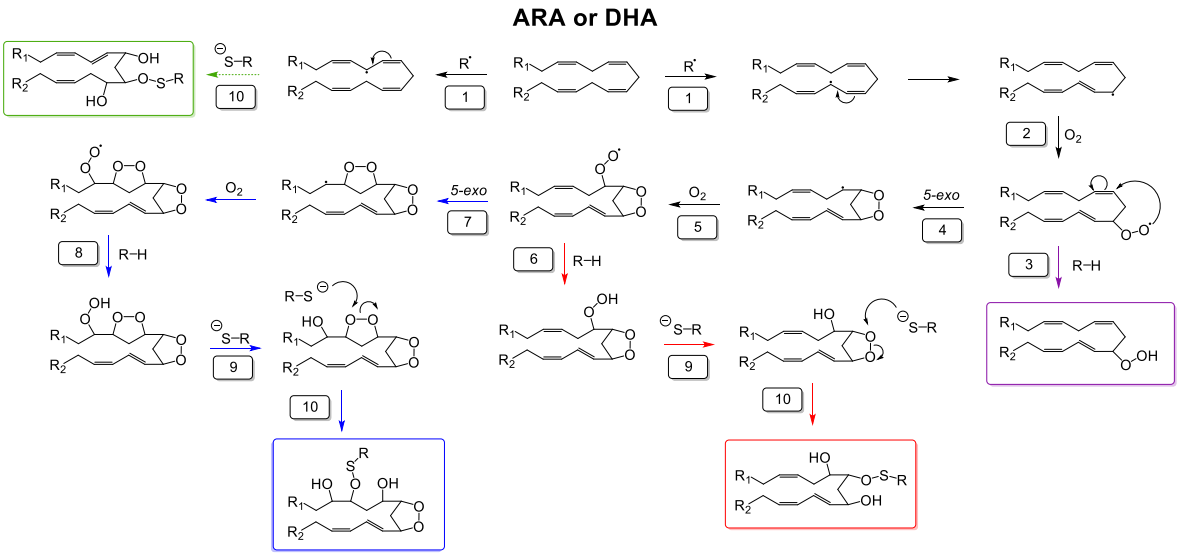

Scheme 1. Proposed mechanisms for cyclization of lipid peroxyl radicals and reaction between hydroxyl-endoperoxides and thiolate anions (RS^-).

According to theoretical studies, GS^- is more nucleophilic than GSH to react with cyclic endoperoxides given the relatively higher energy of activation necessary to start the reaction.[33] Due the low reactivity of the thiol in GSH (pKa = 8.8),[34] the formation of GSH-adducts in physiological pH is not highly favorable. However, since GSH is usually reported at millimolar concentration in mammalian cells,[35,36] even very small amounts of GS^- could react with cyclic peroxides. Additionally, enzymes like Glutathione S-transferase (GST),

which converts GSH into $GS^{\cdot}$,[37] could be a new target for studies with cyclic endoperoxides as a new substrate.

3.4. Highly polar autoxidation products of PUFA are the precursors of GSH-adducts

In order to get more details about the oxygenated PUFA substrates conjugated to GSH-adducts we performed an extensive study involving fractionation and purification of the oxidized fatty acids. For this purpose, we have isolated 9 fractions from oxidized DHA and ARA (Figure 4A) by HPLC-DAD coupled to a fraction collector. The most polar fractions (F1 to F4, named as DHA-$O_{3or>}$ and ARA-$O_{3or>}$) have a wide ultraviolet absorption from 200 to 350 nm, indicating the presence of resonance structures, like conjugated dienes, trienes and tetraenes. Fractions (F5 to F8) displaying intermediate polarity are composed by mono-hydro(pero)xides (DHA-O_{1or2} and ARA-O_{1or2}), which have maximum absorption at 235 nm consistent with the presence of conjugated dienes. The fractions F9 correspond to the non-oxidized/intact forms of DHA and ARA. All individual fractions were incubated with GSH and then analyzed by LC-MS/MS to search for GSH-adducts (Figure 4B). Unlike fractions F1 to F4, the fractions F5 to F9 did not react with GSH confirming that only highly polar oxidized PUFA fractions are precursors of GSH-adducts (data not shown). Relative quantification of all GSH-adducts generated in presence of fractions F1 to F4 (Figure 4C) showed that incubations performed with DHA-F1 and DHA-F2 yields two of the most oxidized GSH-adducts (GSH-DHA-O_6 and GSH-DHA-O_7). In contrast, the highest levels of the less oxygenated GSH-adducts (GSH-DHA-O_3 and GSH-DHA-O_4) were observed in DHA-F3 and DHA-F4 fractions. Similar results were found for ARA purified fractions, indicating that highly polar fractions contains poly-oxygenated fatty acids, most probably hydroxy-endoperoxides, capable to react with GSH.

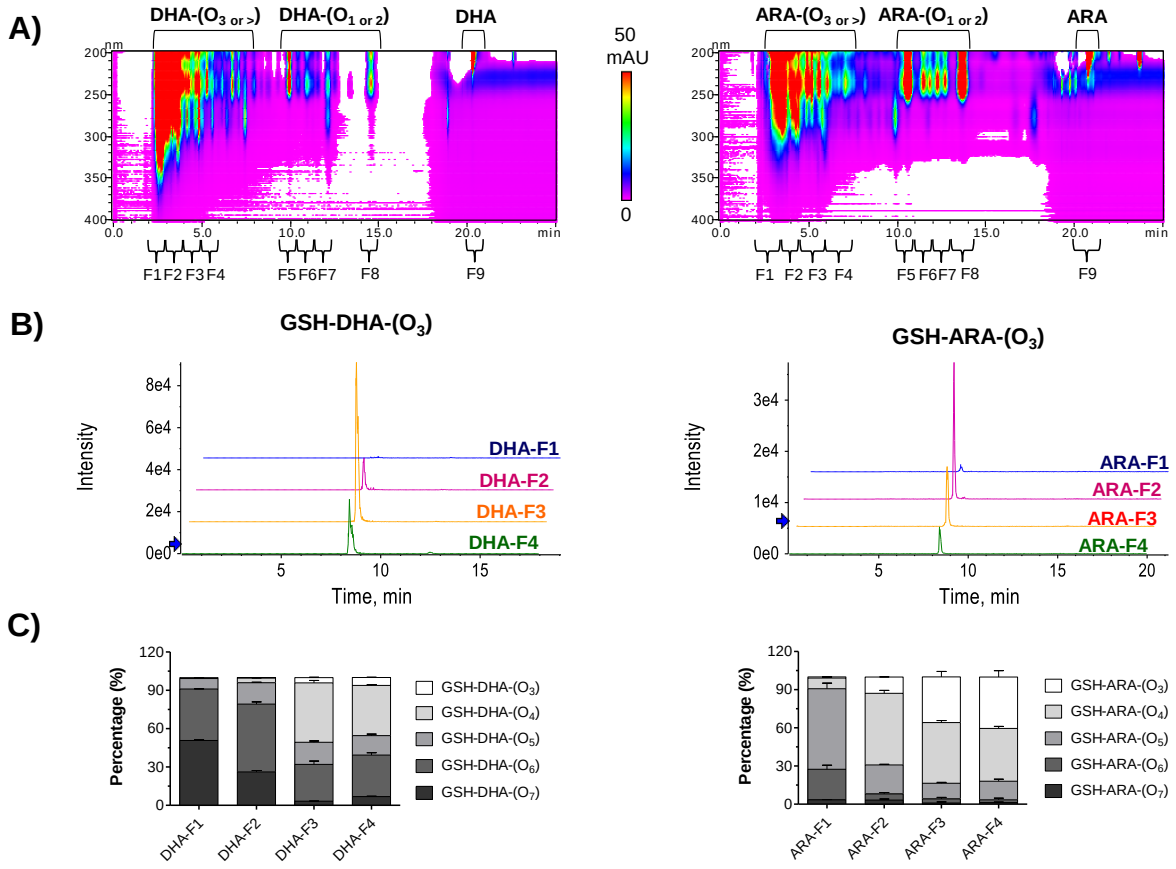

Figure 4. Highly polar autoxidation products of PUFA are the precursors of GSH-adducts. (A) Purification of auto-oxidized DHA and ARA was performed by HPLC-UV/Vis. (B) Collected fractions of oxidized DHA and ARA (10 %; *v/v*) were incubated in presence of 1 mM GSH. (C) Profile of GSH adducts formed after incubation with DHA or AA fractions. The profile and levels of GSH-adducts were analyzed by LC-MS/MS. Data were expressed as average ± standard deviation (n = 2).

3.5. Instability of GSH-adducts in basic pH suggests a mechanism of reaction based on thiol-oxygen binding

To investigate the pH stability of the adducts, we first purified GSH-adducts from DHA-F3 and ARA-F2. These fractions were chosen because they contained the highest concentration of the tri-oxygenated adduct (GSH-DHA-O_3 and GSH-ARA-O_3) (Figure 4C). The purified adducts were submitted to different pH conditions and compared to LTC_4 (Figure 5). At pH 3.0, the GSH-DHA-(O_x) and GSH-ARA-(O_x) adducts remained stable,

whereas the levels of LTC_4 decreased drastically by the acidic treatment relative to control conditions at pH 7.4. On the other hand, at basic conditions (pH 11.0) the GSH-DHA-O_x and GSH-ARA-O_x adducts were readily degraded, whereas LTC_4 remained stable, confirming the instability of the sulfanate ester bond (RS-OR) to base-catalyzed hydrolysis.[33]

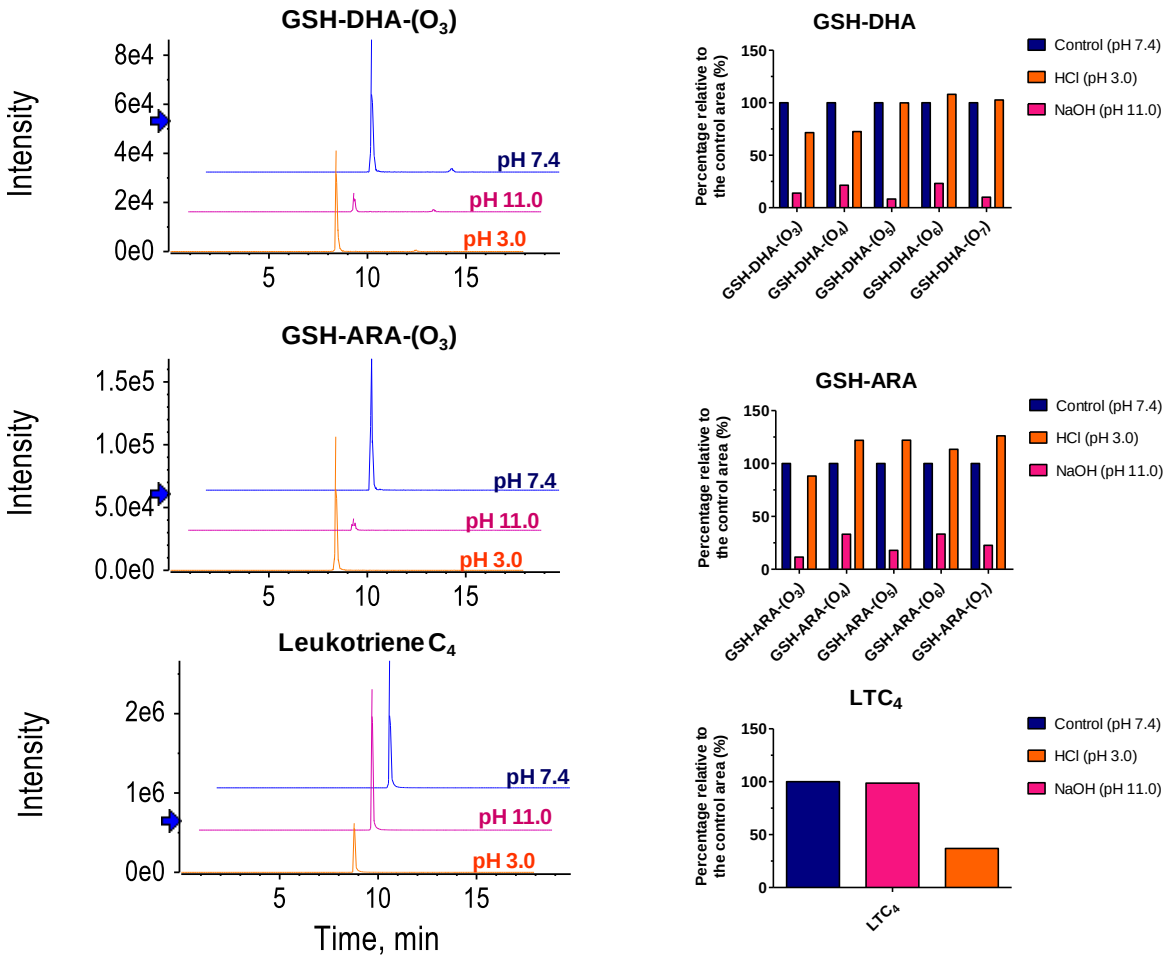

Figure 5. Instability of GSH-adducts in basic pH suggests a mechanism of reaction based on S-O bond formation. Incubations were performed with DHA-F3 (10 %; *v/v*) (A) or ARA-F2 (10 %; *v/v*) (B) in presence of 1 mM GSH. After incubation, GSH-adducts were purified from samples by SPE-C18 column. Purified GSH-adducts and LTC_4 (C) were added with H_2O (control), HCl (0.2 %; *v/v*) or NaOH (153 mM).

Next, we aimed to get more detailed information on the structure of oxygenated fatty acids attached to GSH by LC-MS/MS. Since the MS/MS spectra of the whole adduct gave

limited information, we thought first to induce the release of the oxygenated fatty acid by alkaline hydrolysis at pH 11.0 and them analyze the MS/MS spectra of the released product (Figure 6). For both DHA-(O_3) and ARA-(O_3), MS/MS spectra showed major fragment ions related to water molecule loss(es) and cleavage of the α-carbon adjacent to the carbonyl group (followed by and additional decarboxylation). These fragment ions in DHA-O_3 correspond respectively to the ions at *m/z* 357.2071 [M-H-H_2O], 339.1966 [M-H-2H_2O], 287.1653 [M-H-H_2O-C_4H_7O] and *m/z* 243.1754 [M-H-CO_2-H_2O-C_4H_7O]. Correspondingly, the most intense fragment ions observed in the ARA-O_3 MS/MS spectrum were the ions *m/z* 333.2071 [M-H-H_2O], *m/z* 315.1966 [M-H-2H_2O], *m/z* 221.1183 [M-H-$C_7H_{14}O_2$] and *m/z* 177.1285 [M-H-CO_2-$C_7H_{14}O_2$]. The structure of ARA-O_3 characterized herein resembles the structure of a recently identified dioxolane A3 (DXA_3).[38] DXA_3 is generated in platelets from prostaglandin G2 via COX 1 and it could act as a neutrophil activator.[38] Corroborating the oxidation origin of ARA-O_3, its fragmentation pattern (Figure 6B) is remarkably different from the isomeric, but enzymatically-derived DXA_3.[38]

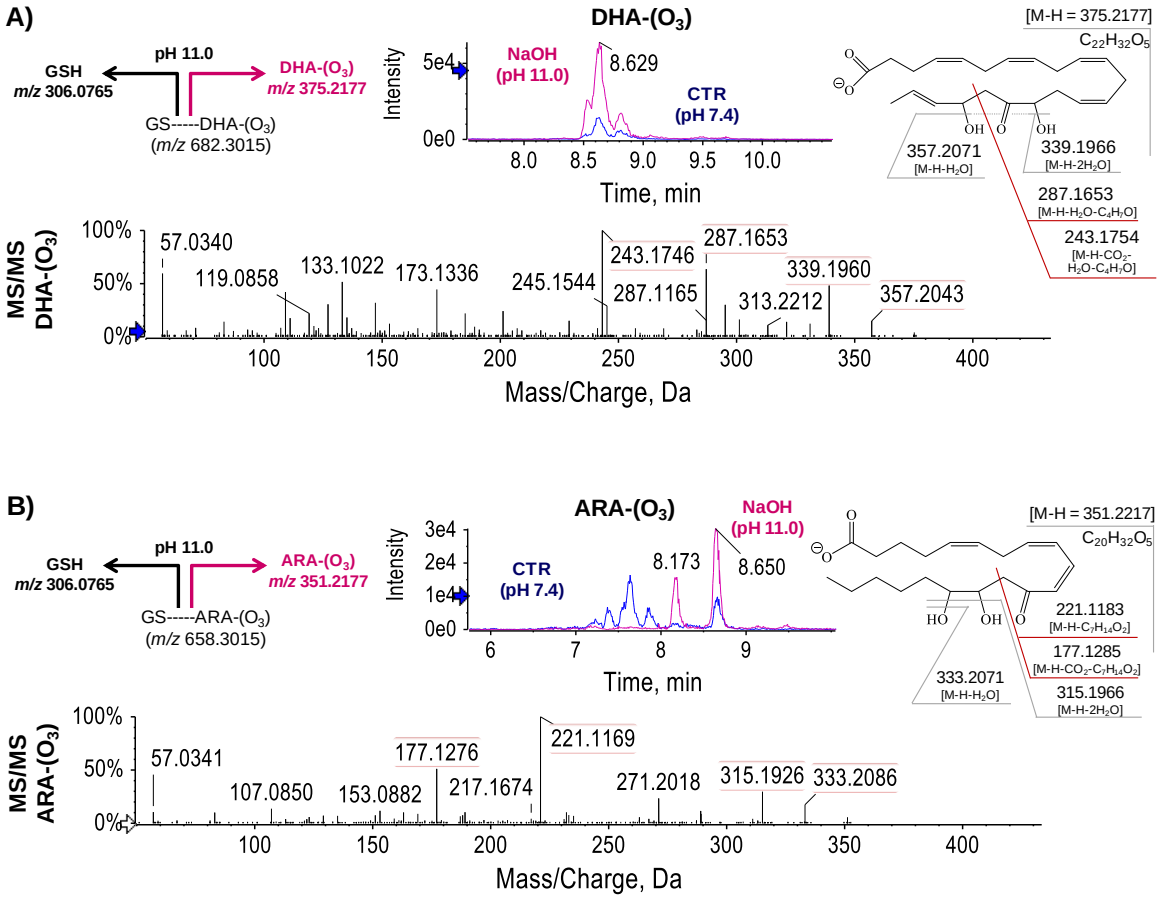

Figure 6. The cleavage of GSH-adducts induced in basic pH yields free oxidized lipids derived from hydroxy-endoperoxides. Incubations were performed in 200 mM sodium phosphate buffer (pH 7.4) containing DHA-F3 (10 %; *v/v*) (A) or ARA-F2 (10 %; *v/v*) (B) in presence of 1 mM GSH. After incubation, GSH-adducts were purified from samples by SPE-C18 column and then incubated with H_2O (control) or NaOH (153 mM). Specific fragments for DHA-(O_3) and ARA-(O_3) are highlighted in red lines.

To summarize the results obtained up to here, we propose sequential steps involved in the formation of thiol adducts and their cleavage at pH 11.0 (Scheme 2). As mentioned above, the thiolate anion reacts with the hydroxyl-endoperoxide to form a mixed sulfide via a nucleophilic attack. In the presence of hydroxide anions, there is a deprotonation of the carbon holding the sulfur-oxygen bond, which undergoes a heterolytic cleavage thereby yielding a free GSH and an oxidized PUFA with a ketone and hydroxyl group instead of the cyclic structure. This proposed mechanism is built on studies performed with enzymes such as

the microsomal PGE_2 synthase-1, which uses GSH to react with the cyclic endoperoxide present in PGH_2.[39] These authors verified that the sulfur-oxygen bond cleavage of the GSH-PGH_2 conjugate is mediated by the bidentate complex Asp49 with Arg126, in which Asp49 acts as a hydroxide anion, deprotonating PGH_2 and yielding PGE_2 as end product. In another study, the enzyme lipocalin type prostaglandin D synthase catalyzes the conversion of PGH_2 into PGD_2, an isomer of PGE_2, by the same GSH-dependent mechanism.[40]

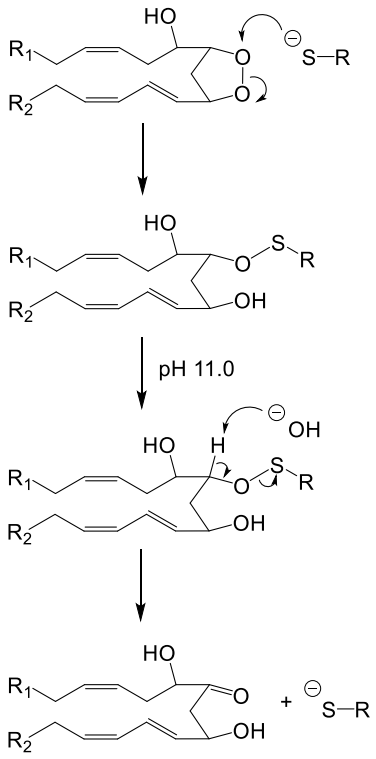

Scheme 2. Proposed mechanism for GSH-adduct formation and its cleavage under alkaline conditions.

3.6. Are thiols in proteins and small peptides also reactive toward hydroxy-endoperoxides?

Because GSH has low reactivity against hydroxy-endoperoxides due its high pKa, we sought to evaluate the capacity of these oxidized PUFAs to modify cysteine groups of proteins containing thiol groups. For this purpose, we incubated the SOD1 enzyme in

presence or absence of ARA. After incubation, SOD1 was digested by trypsin and the peptides were analyzed by nano-LC-ESI-TOF-MS/MS (Figure 7). The SOD1 is a dimeric protein that contains in each monomer four cysteine groups (Cys), two of them (Cys6 and Cys111) present as free residues, and the other two participate of intramolecularly conjugated by a disulfide bond (Cys57 and Cys146).[41]

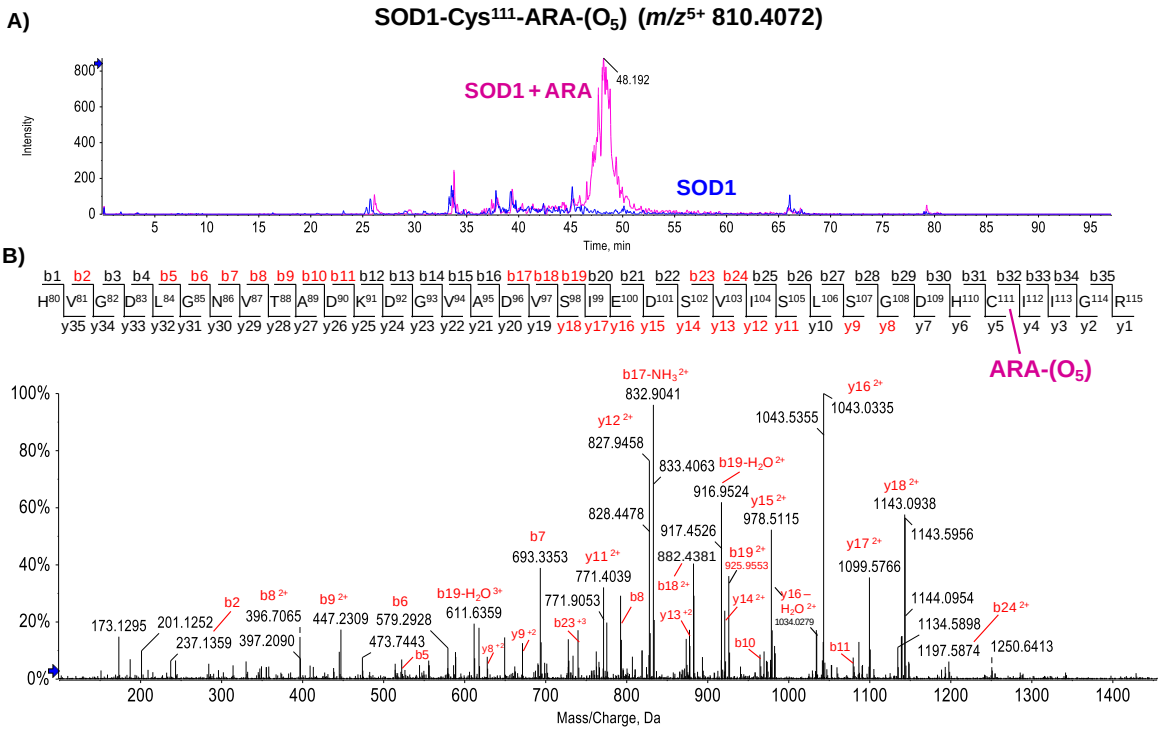

Figure 7. Proteomic analysis show that ARA-(O_5) can modify the most reactive cysteine of SOD1. (A) Extracted-ion chromatogram (XIC) of the SOD1 peptide modified by ARA-(O_5) (m/z^{5+} 810.4072 ± 5 mDa). (B) MS/MS spectrum of the peptide H^{80}VGDLGNVTADKDGVADVSIEDSVISLSGDHCIIGR^{115} modified by ARA-(O_5) at Cys111.

Relative to the control, we identified a modification of only one peptide at Cys111 in SOD1, which is described as the most susceptible cysteine residue to oxidation due its exposure to solvent.[42] This modification, namely SOD1-Cys111-ARA-(O_5) (m/z^{5+} 810.4072) is a product of reaction with penta-oxygenated ARA (Figure 7B), which is one of the three

most abundant hydroxy-endoperoxide in ARA sample (Figure 1A). By comparing theoretical fragments of the modified peptide against experimental fragments, we were able to attribute the most abundant fragments ("b" and "y", with an acceptable error of ≤ 10 ppm) to the SOD1-Cys111-ARA-(O_5) structure.

Thiol groups of proteins usually participate in physiological and pathological processes that involve enzymatic activity and protein folding.[16] In pathological conditions like ALS, SOD1 oligomerization/aggregation is reported to be dependent on cross-linking between intermolecular disulfide bonds.[43] In a recent study, our group has proposed that DHA can induce SOD1 thiol-mediated aggregation.[44] In retrospect, hydroxy-endoperoxides derived from DHA's oxidation as observed here could contribute for triggering SOD1 aggregation. Although protein aggregation is a hallmark of neurodegenerative diseases, some authors have suggested that biological event induced by lipids could be rather important for ubiquitin-proteasome system activation, leading to degradation of misfolded proteins.[45] Also, it was reported that ketones, derived from enzymatic oxidation of omega-3 PUFAs, activate the Nrf2 pathway and it may be assigned to the chemical modification of reactive cysteine residues in Keap1 protein.[15] Modifications of thiol groups in Keap1 results in the release of nuclear factor Nrf2, which leads to the expression of enzymes linked to antioxidant defenses such as SOD1, glutathione S-transferase (GST) and heme oxygenase-1.[46,47]

In addition to SOD1, we also performed experiments with n-acetylcysteine (NAC), a small antioxidant peptide, in presence of DHA. Corroborating the results observed with GSH, untargeted MS analysis revealed several NAC-adducts (Figure S3A). Relative quantification of NAC conjugates showed the tri-oxygenated, NAC-DHA-(O_3), and penta-oxygenated, NAC-DHA-(O_5), as the most abundant conjugates (Figure S3B). We analyzed the MS/MS spectra of NAC-DHA-(O_3) and NAC-DHA-(O_4), and identified the fragments corresponding to DHA-O_3 (*m/z* 375.2177) and DHA-O_4 (*m/z* 391.2126), respectively (Figure S3C). In

MS/MS spectra of both adducts we could attribute the fragment ion *m/z* 162.0230 to the intact mass of NAC. In summary, while our data supports the fact that hydroxy-endoperoxides could react with cysteines groups in peptides and also protein, it worth noting that the efficiency of adduct formation depends directly on the reactivity of the thiol group, particularly since not all cysteine residues in SOD1 were modified.

3.7. Experiments with free radical generator induced formation of GSH adducts dependent on thiyl radical

In order to improve the yields of GSH-adducts and better understand the contribution of radical mechanisms to their formation, we performed incubations with GSH and DHA in the presence of AAPH, a free radical-generating azo compound. Untargeted MS analysis of incubations with AAPH revealed new conjugates of GSH with non-oxidized DHA (GS-DHA; *m/z* 634.3168) and also two others molecules with addition of one (GS-DHA-(O_1); *m/z* 650.3117) or two (GS-DHA-(O_2); *m/z* 666.3066) oxygen atoms (Figure 8). For the GS-DHA adduct, major fragment ions suggest that DHA is covalently bounded to GSH: *m/z* 505.2742 [M-H-$C_5H_7NO_3$], *m/z* 361.2207 [M-H-$C_{20}H_{32}O_3S$] and *m/z* 272.0888 [M-H-$C_{20}H_{32}O_3S$] (Figure 8A). Similarly, the GS-DHA-(O_1) and GS-DHA-(O_2) adducts displayed fragment ions at *m/z* 521.2691 [M-H-$C_5H_7NO_3$], *m/z* 377.2156 [M-H-$C_{20}H_{32}O_3S$] and *m/z* 272.0888 [M-H-$C_{20}H_{32}O_4S$] (Figure 8B), and at *m/z* 537.2640 [M-H-$C_5H_7NO_3$], *m/z* 393.2105 [M-H-$C_{20}H_{32}O_3S$] and *m/z* 272.0888 [M-H-$C_{20}H_{32}O_5S$] (Figure 8C). This fragmentation pattern resembles more the MS/MS spectrum of LTC_4 (Figure 3C) than the ones of GSH-adducts described for the oxidation products (Figure 3A). Furthermore, the fragment ions *m/z* 272.0888, *m/z* 254.0782 and *m/z* 143.0462, all derived from the GSH structure, are also characteristic ions in the MS/MS spectrum of LTC_4. Taken together, these data suggest that GSH in the AAPH experiments, where high flux of radicals is generated, GSH can be bound covalently to DHA and its oxidation products through a sulfur-carbon bond. Our findings thus

support the proposition that the mechanism of reaction between GSH and hydroxy-endoperoxides does not involve a radical mechanism, but instead a nucleophilic attack of the anion thiolate on the oxygen atom of the peroxide group.

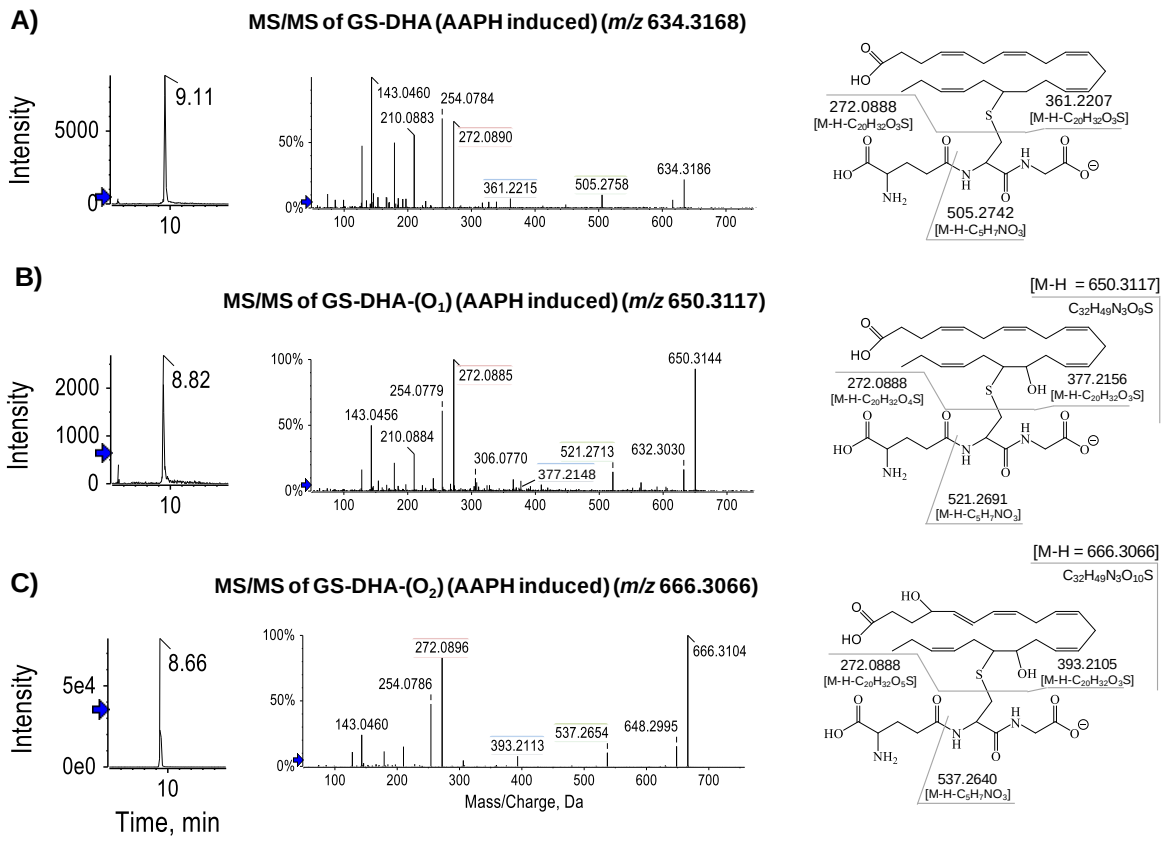

Figure 8. Oxidation induced by AAPH yields GSH-adducts via thiol-ene reaction. Incubations were performed with 10 mM GSH and 100 μM DHA in presence of 50 mM AAPH.

To better understand how adducts can be formed between DHA and GSH in the presence of AAPH, we proposed a mechanism illustrated in Scheme 3. When exposed to heating, AAPH can be converted into two radicals molecules (6.5×10^{-7} s^{-1}),[48,49] which can be converted in peroxyl radicals (2.9×10^{9} M^{-1} s^{-1}) in the presence of oxygen.[50] As previously reported, thiyl radicals can be formed from GSH in presence of peroxyl radicals (Scheme 3 - Step 1) (1.2×10^{2} M^{-1} s^{-1}).[51] After initiation, thiyl radicals ($GS^{\bullet}$) can react with each other to

form GSSG (Scheme 3 - Step 2) (1.5 x 10^9 M^{-1} s^{-1}) or even react with molecular oxygen in a reversible process, as reported for 2-mercaptoethanol in H_2O (Scheme 3 - Step 3) (K_{ad} = 2 x 10^9 M^{-1} s^{-1}; K_{frag} = 6 x 10^5 s^{-1}).[52] Since the reverse reaction between thiyl radicals and oxygen is rather fast, thiyl radicals may be added into double bonds of lipids to form a carbon centered radical via a reversible process, namely thiol-ene reaction (Scheme 3 - Step 4).[53] The resulting radical may follow three pathways. First, it can abstract a hydrogen atom from another molecule of thiol to yield a thio-ether product (Scheme 3 - Step 5),[53] which corresponds to the identified GS-DHA adduct (Scheme 3 - Structure A, Figure 8A). Second, the carbon centered radical may react with oxygen yielding a peroxyl radical, a reaction known as thiol-olefin cooxidation (Scheme 3 - Step 6).[54] After formation of a peroxyl radical, hydrogen abstraction from the thiol may result in a hydroperoxide (Scheme 3 - Step 7), as illustrated by the GS-DHA-OOH (Scheme 3 - Structure B). The GS-DHA-OOH may be readily reduced by a GSH molecule or undergo rearrangements into the corresponding hydroxide sulfoxides at room temperature (Scheme 3 - Step 8),[53] thereby yielding a GS-DHA-(O_1) adduct (Scheme 3 - Structure C), which was detected in the AAPH experiments (Figure 8B). Finally, it has been reported that the carbon centered radical may suffer *cis/trans* isomerization, yielding a stereospecific product (Scheme 3 - Step 9).[55]

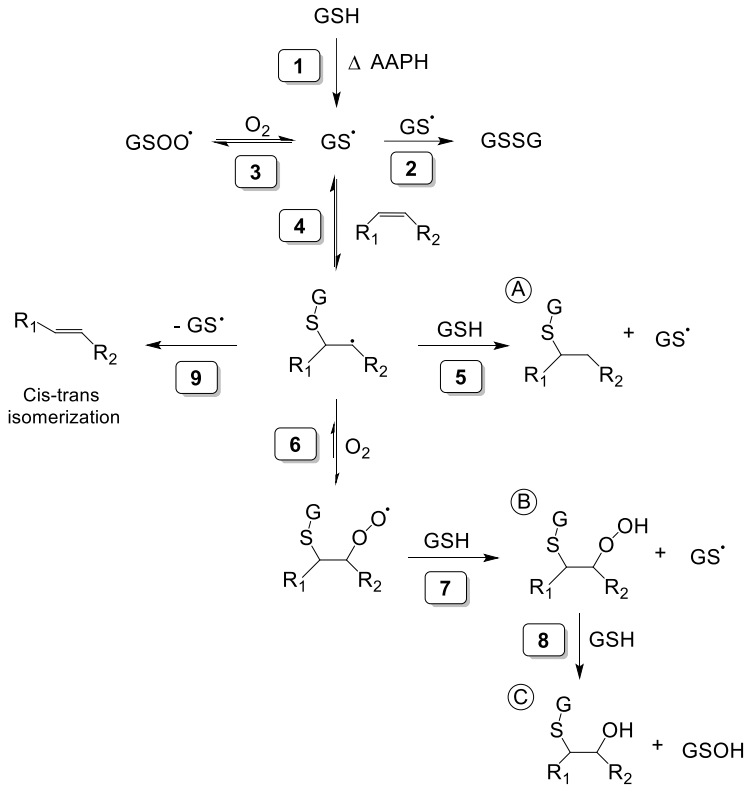

Scheme 3. Proposed mechanism for thiol-ene reaction. (A) GSH-DHA; (B) GSH-DHA-(O_2); (C) GSH-DHA-(O_1).

4. Conclusion

In the present study, we investigated the reactivity of cyclic endoperoxides derived from the autoxidation of ARA and DHA with thiol groups of peptides and proteins. Detailed inspection of MS/MS spectra of GSH-adducts revealed that GSH and DHA-($O_{3or>}$) or ARA-($O_{3or>}$) are likely bonded through a labile sulfur-oxygen chemical bond. We suggest that the reaction between GSH and hydroxy-endoperoxides involves a nucleophilic attack by the thiolate anion instead of a radical addition mechanism. In experiments performed with the SOD1 protein we identified a modification in the cysteine residue (Cys-111) by penta-oxygenated ARA-(O_5), supporting the idea that reactive thiols in proteins could be modified by the cyclic peroxides described herein. Collectively, our findings bear evidence of chemical modifications of thiol groups induced by hydroxy-endoperoxides, which may modulate the

formation of GSH conjugates, protein aggregation and redox system, as reported for the enzymatically oxidized PUFA's.

Associated content

Supporting information

(1) Supplementary Figures.

Notes

The authors declare no competing financial interest.

Acknowledgments

The authors would like to thank to Fernando Coelho from the University of São Paulo for the technical assistance on SOD1 preparations. This work was supported by Fundação de Amparo à Pesquisa do Estado de São Paulo (FAPESP) Grants 08/57721-0, 10/50891-0 and 13/07937-8, Conselho Nacional de Desenvolvimento Científico e Tecnológico (CNPq) Grant 573530/2008-4 and Pro-Reitoria de Pesquisa da Universidade de São Paulo (PRPUSP) Grant 2011.1.9352.1.8. The authors are members of INCT Redoxoma (FAPESP/CNPq/CAPES), NAP Redoxoma (PRPUSP), and the CEPID Redoxoma (FAPESP).

Abbreviations

DHA, docosahexaenoic acid; ARA, arachidonic acid; GSH, glutathione; AAPH, 2,2-azobis(2-methylpropionamidine) dihydrochloride; NEM, N-ethylmaleimide; NAC, N-acetylcysteine; SOD1, superoxide dismutase 1.

References

(1) Hulbert, A. J.; Kelly, M. A.; Abbott, S. K. Polyunsaturated Fats, Membrane Lipids and Animal Longevity. *J. Comp. Physiol. B Biochem. Syst. Environ. Physiol.* **2014**, *184* (2), 149–166.

(2) Bascoul-Colombo, C.; Guschina, I. A.; Maskrey, B. H.; Good, M.; O'Donnell, V. B.; Harwood, J. L. Dietary DHA Supplementation Causes Selective Changes in Phospholipids from Different Brain Regions in Both Wild Type Mice and the Tg2576 Mouse Model of Alzheimer's Disease. *Biochim. Biophys. Acta - Mol. Cell Biol. Lipids* **2016**, *1861* (6), 524–537.

(3) Wang, D.; Dubois, R. N. Eicosanoids and Cancer. *Nat. Rev. Cancer* **2010**, *10* (3), 181–193.

(4) Yang, R.; Chiang, N.; Oh, S. F.; Serhan, C. N. *Metabolomics-Lipodomics of Eicosanoids and Docosanoids Genarated By Phagocytes*; 2011; Vol. Chapter 14.

(5) Harizi, H.; Corcuff, J. B.; Gualde, N. Arachidonic-Acid-Derived Eicosanoids: Roles in Biology and Immunopathology. *Trends Mol. Med.* **2008**, *14* (10), 461–469.

(6) Ricciotti, E.; Fitzgerald, G. A. Prostaglandins and Inflammation. *Arterioscler. Thromb. Vasc. Biol.* **2011**, *31* (5), 986–1000.

(7) Liu, M.; Yokomizo, T. The Role of Leukotrienes in Allergic Diseases. *Allergol. Int.* **1970**, *64* (1), 17–26.

(8) Serhan, C. N.; Chiang, N.; Van Dyke, T. E. Resolving Inflammation: Dual Anti-Inflammatory and pro-Resolution Lipid Mediators. *Nat. Rev. Immunol.* **2008**, *8* (5), 349–361.

(9) Serhan, C. N. Pro-Resolving Lipid Mediators Are Leads for Resolution Physiology. *Nature* **2014**, *510* (7503), 92–101.

(10) Kuda, O. Bioactive Metabolites of Docosahexaenoic Acid. *Biochimie* **2017**, *136*, 12–20.

(11) Yin, H.; Xu, L.; Porter, N. A. Free Radical Lipid Proxidation: Mechanisms and Analysis. *Chem. Rev.* **2011**, *111* (10), 5944–5972.

(12) Ayala, A.; Muñoz, M. F.; Argüelles, S. Lipid Peroxidation: Production, Metabolism, and Signaling Mechanisms of Malondialdehyde and 4-Hydroxy-2-Nonenal. *Oxid. Med. Cell. Longev.* **2014**, *2014*.

(13) Refsgaard, H. H.; Tsai, L.; Stadtman, E. R. Modifications of Proteins by

Polyunsaturated Fatty Acid Peroxidation Products. *Proc Natl Acad Sci U S A* **2000**, *97* (2), 611–616.

(14) Liu, L.; Komatsu, H.; Murray, I. V. J.; Axelsen, P. H. Promotion of Amyloid β Protein Misfolding and Fibrillogenesis by a Lipid Oxidation Product. *J. Mol. Biol.* **2008**, *377* (4), 1236–1250.

(15) Groeger, A. L.; Cipollina, C.; Cole, M. P.; Woodcock, S. R.; Bonacci, G.; Rudolph, T. K.; Rudolph, V.; Freeman, B. A.; Schopfer, F. J. Cyclooxygenase-2 Generates Anti-Inflammatory Mediators from Omega-3 Fatty Acids. *Nat. Chem. Biol.* **2010**, *6* (6), 433–441.

(16) Hansen, R. E.; Winther, J. R. An Introduction to Methods for Analyzing Thiols and Disulfides: Reactions, Reagents, and Practical Considerations. *Anal. Biochem.* **2009**, *394* (2), 147–158.

(17) Fra, A.; Yoboue, E. D.; Sitia, R. Cysteines as Redox Molecular Switches and Targets of Disease. *Front. Mol. Neurosci.* **2017**, *10* (June), 1–9.

(18) Valle, C.; Carrì, M. T. Cysteine Modifications in the Pathogenesis of ALS. *Front. Mol. Neurosci.* **2017**, *10* (January), 1–8.

(19) Montine, T. J.; Morrow, J. D. Fatty Acid Oxidation in the Pathogenesis of Alzheimer's Disease. *Am. J. Pathol.* **2005**, *166* (5), 1283–1289.

(20) Mouchlis, V. D.; Chen, Y.; McCammon, J. A.; Dennis, E. A. Membrane Allostery and Unique Hydrophobic Sites Promote Enzyme Substrate Specificity. *J. Am. Chem. Soc.* **2018**, jacs.7b12045.

(21) Chen, X.; Guo, C.; Kong, J. Oxidative Stress in Neurodegenerative Diseases. *Neural Regen. Res.* **2012**, *7* (5), 376–385.

(22) Liu, Z.; Zhou, T.; Ziegler, A. C.; Dimitrion, P.; Zuo, L. Oxidative Stress in Neurodegenerative Diseases: From Molecular Mechanisms to Clinical Applications. *Oxid. Med. Cell. Longev.* **2017**, *2017* (Figure 1).

(23) Muskiet, F. A. J.; van Goor, S. A.; Kuipers, R. S.; Velzing-Aarts, F. V.; Smit, E. N.; Bouwstra, H.; Janneke Dijck-Brouwer, D. A.; Rudy Boersma, E.; Hadders-Algra, M. Long-Chain Polyunsaturated Fatty Acids in Maternal and Infant Nutrition. *Prostaglandins Leukot. Essent. Fat. Acids* **2006**, *75* (3), 135–144.

(24) Dalli, J.; Chiang, N.; Serhan, C. N. Identification of 14-Series Sulfido-Conjugated Mediators That Promote Resolution of Infection and Organ Protection. *Proc. Natl. Acad. Sci.* **2014**, *111* (44), E4753–E4761.

(25) Dalle-Donne, I.; Giustarini, D.; Colombo, R.; Rossi, R.; Milzani, A. Protein

Carbonylation in Human Diseases. *Trends Mol. Med.* **2003**, *9* (4), 169–176.

(26) Grimsrud, P. A.; Xie, H.; Griffin, T. J.; Bernlohr, D. A. Oxidative Stress and Covalent Modification of Protein with Bioactive Aldehydes. *J. Biol. Chem.* **2008**, *283* (32), 21837–21841.

(27) Benov, L.; Beyer, W.; Stevens, R.; Fridovich, I. Purification and Characterization of the Cu,zn Sod from Escherichia Coli. *Free Radic. Biol. Med.* **1996**, *21* (1), 117–121.

(28) Maclouf, J. A.; Murphy, R. C. Transcellular Metabolism of Neutrophil-Derived Leukotriene A4by Human Platelets. A Potential Cellular Source of Leukotriene C4. *J. Biol. Chem.* **1988**, *263* (1), 174–181.

(29) Hammarstrom, S. Leukotrienes. *Annu. Rev. Biochem.* **1983**, *52*, 355–377.

(30) Feinmark, S. J.; Cannon, P. J. Endothelial Cell Leukotriene C4 Synthesis Results from Intercellular Transfer of Leukotriene A4 Synthesized by Polymorphonuclear Leukocytes. *J. Biol. Chem.* **1986**, *261* (35), 16466–16472.

(31) Dalli, J.; Sanger, J. M.; Rodriguez, A. R.; Chiang, N.; Spur, B. W.; Serhan, C. N. Identification and Actions of a Novel Third Maresin Conjugate in Tissue Regeneration: MCTR3. *PLoS One* **2016**, *11* (2), 4–15.

(32) Dalli, J.; Vlasakov, I.; Riley, I. R.; Rodriguez, A. R.; Spur, B. W.; Petasis, N. A.; Chiang, N.; Serhan, C. N. Maresin Conjugates in Tissue Regeneration Biosynthesis Enzymes in Human Macrophages. *Proc. Natl. Acad. Sci.* **2016**, *113* (43), 12232–12237.

(33) Yamaguchi, N.; Naiki, T.; Kohzuma, T.; Takada, T.; Sakata, F.; Mori, S. Theoretical Studies on Model Reaction Pathways of Prostaglandin H2 Isomerization to Prostaglandin D2/E2. *Theor. Chem. Acc.* **2011**, *128* (2), 191–206.

(34) Mishanina, T. V.; Libiad, M.; Banerjee, R. Biogenesis of Reactive Sulfur Species for Signaling by Hydrogen Sulfide Oxidation Pathways. *Nat. Chem. Biol.* **2015**, *11* (7), 457–464.

(35) Yuan, L.; Kaplowitz, N. Glutathione in Liver Diseases and Hepatotoxicity. *Mol. Aspects Med.* **2009**, *30* (1–2), 29–41.

(36) Dringen, R. Metabolism and Functions of Glutathione in Brain. *Prog. Neurobiol.* **2000**, *62*, 649–671.

(37) Strange, R. C.; Spiteri, M. A.; Ramachandran, S.; Fryer, A. A. Glutathione-S-Transferase Family of Enzymes. *Mutat. Res. Mol. Mech. Mutagen.* **2001**, *482* (1–2), 21–26.

(38) Hinz, C.; Aldrovandi, M.; Uhlson, C.; Marnett, L. J.; Longhurst, H. J.; Warner, T. D.;

Alam, S.; Slatter, D. A.; Lauder, S. N.; Allen-Redpath, K.; et al. Human Platelets Utilize Cycloxygenase-1 to Generate Dioxolane A3, a Neutrophil-Activating Eicosanoid. *J. Biol. Chem.* **2016**, *291* (26), 13448–13464.

(39) Sjögren, T.; Nord, J.; Ek, M.; Johansson, P.; Liu, G.; Geschwindner, S. Crystal Structure of Microsomal Prostaglandin E_2 Synthase Provides Insight into Diversity in the MAPEG Superfamily. *Proc. Natl. Acad. Sci. U. S. A.* **2013**, *110* (10), 3806–3811.

(40) Kumasaka, T.; Aritake, K.; Ago, H.; Irikura, D.; Tsurumura, T.; Yamamoto, M.; Miyano, M.; Urade, Y.; Hayaishi, O. Structural Basis of the Catalytic Mechanism Operating in Open-Closed Conformers of Lipocalin Type Prostaglandin D Synthase. *J. Biol. Chem.* **2009**, *284* (33), 22344–22352.

(41) Valentine, J.; Doucette, P.; Potter, S. Copper-Zinc Superoxide Dismutase and Amyotrophic Lateral Sclerosis. *Annu. Rev. Biochem.* **2005**, *74*, 563–593.

(42) Cozzolino, M.; Amori, I.; Pesaresi, M. G.; Ferri, A.; Nencini, M.; Carrì, M. T. Cysteine 111 Affects Aggregation and Cytotoxicity of Mutant Cu,Zn-Superoxide Dismutase Associated with Familial Amyotrophic Lateral Sclerosis. *J. Biol. Chem.* **2008**, *283* (2), 866–874.

(43) Furukawa, Y.; Fu, R.; Deng, H.-X.; Siddique, T.; O'Halloran, T. V. Disulfide Cross-Linked Protein Represents a Significant Fraction of ALS-Associated Cu, Zn-Superoxide Dismutase Aggregates in Spinal Cords of Model Mice. *Proc. Natl. Acad. Sci.* **2006**, *103* (18), 7148–7153.

(44) Appolinário, P. P.; Medinas, D. B.; Chaves-Filho, A. B.; Genaro-Mattos, T. C.; Cussiol, J. R. R.; Netto, L. E. S.; Augusto, O.; Miyamoto, S. Oligomerization of Cu,Zn-Superoxide Dismutase (SOD1) by Docosahexaenoic Acid and Its Hydroperoxides in Vitro: Aggregation Dependence on Fatty Acid Unsaturation and Thiols. *PLoS One* **2015**, *10* (4), 1–15.

(45) Kim, Y. J.; Nakatomi, R.; Akagi, T.; Hashikawa, T.; Takahashi, R. Unsaturated Fatty Acids Induce Cytotoxic Aggregate Formation of Amyotrophic Lateral Sclerosis-Linked Superoxide Dismutase 1 Mutants. *J. Biol. Chem.* **2005**, *280* (22), 21515–21521.

(46) Nguyen, T.; Nioi, P.; Pickett, C. B. The Nrf2-Antioxidant Response Element Signaling Pathway and Its Activation by Oxidative Stress. *J. Biol. Chem.* **2009**, *284* (20), 13291–13295.

(47) Kensler, T. W.; Wakabayashi, N.; Biswal, S. Cell Survival Responses to Environmental Stresses Via the Keap1-Nrf2-ARE Pathway. *Annu. Rev. Pharmacol. Toxicol.* **2007**, *47* (1), 89–116.

(48) Viner, R. I.; Ferrington, D. A.; Aced, G. I.; Miller-Schlyer, M.; Bigelow, D. J.; Schöneich, C.; Schoneich, C. In Vivo Aging of Rat Skeletal Muscle Sarcoplasmic Reticulum Ca-ATPase. Chemical Analysis and Quantitative Simulation by Exposure to Low Levels of Peroxyl Radicals. *Biochim. Biophys. Acta* **1997**, *1329*, 321–335.

(49) Porter, N. A.; Lehman, L. S.; Weber, B. A.; Smith, K. J. Unified Mechanism for Polyunsaturated Fatty Acid Autoxidation. Competition of Peroxy Radical Hydrogen Atom Abstraction, Beta-Scission, and Cyclization. *J. Am. Chem. Soc.* **1981**, *103* (21), 6447–6455.

(50) O'Donnell, V. B.; Chumley, P. H.; Hogg, N.; Bloodsworth, a; Darley-Usmar, V. M.; Freeman, B. a. Nitric Oxide Inhibition of Lipid Peroxidation: Kinetics of Reaction with Lipid Peroxyl Radicals and Comparison with Alpha-Tocopherol. *Biochemistry* **1997**, *36* (49), 15216–15223.

(51) Ho, S. C.; Chiu, S. J.; Hu, T. M. Comparative Kinetics of Thiol Oxidation in Two Distinct Free-Radical Generating Systems: SIN-1 versus AAPH. *Free Radic. Res.* **2012**, *46* (10), 1190–1200.

(52) Zhang, X.; Zhang, N.; Schuchmann, H. P.; Von Sonntag, C. Pulse Radiolysis of 2-Mercaptoethanol in Oxygenated Aqueous Solution. Generation and Reactions of the Thiylperoxyl Radical. *J. Phys. Chem.* **1994**, *98* (26), 6541–6547.

(53) Dénès, F.; Pichowicz, M.; Povie, G.; Renaud, P. Thiyl Radicals in Organic Synthesis. *Chem. Rev.* **2014**, *114*, 2587–2693.

(54) Kharasch, M. S.; Nudenberg, W.; Mantell, G. J. Reactions of Atoms and Free Radicals in Solution. XXV. the Reactions of Olefins with Mercaptans in the Presence of Oxygen. *J. Org. Chem.* **1951**, *16* (4), 524–532.

(55) Chatgilialoglu, C.; Ferreri, C.; Guerra, M.; Samadi, A.; Bowry, V. W. The Reaction of Thiyl Radical with Methyl Linoleate: Completing the Picture. *J. Am. Chem. Soc.* **2017**, *139* (13), 4704–4714.

Supporting information

Hydroxy-endoperoxides derived from Polyunsaturated Fatty Acids Reacts with Thiols Producing Conjugates

Adriano B. Chaves-Filho, Marcos Y. Yoshinaga, Lucas S. Dantas, Larissa R. Diniz, and Sayuri Miyamoto*

1. Supplementary Figures

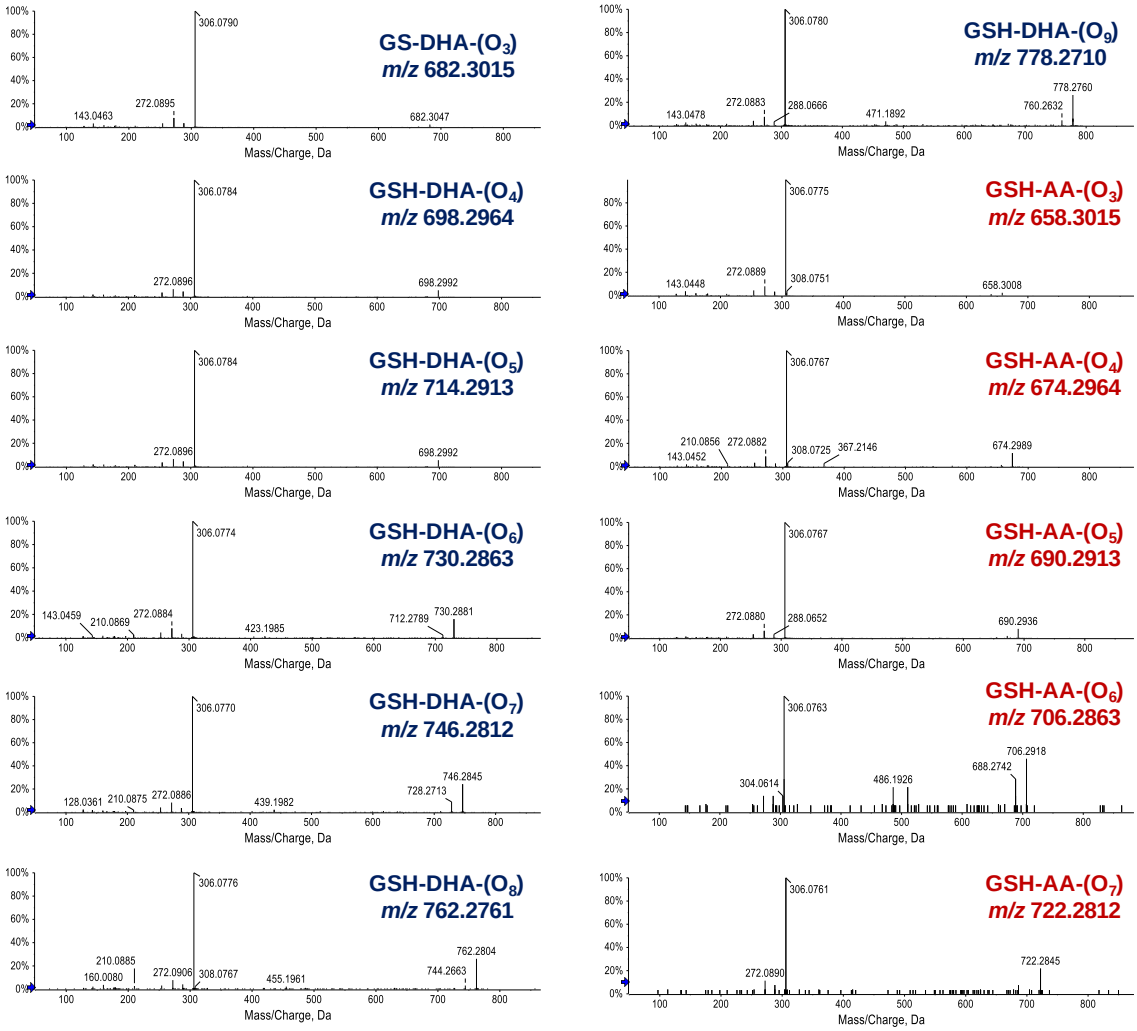

Figure S1. MS/MS spectrum of GSH-adducts shares the fragment ion correspondent to GSH. The MS/MS spectrum of GSH-adducts were plotted for incubations with 100 µM DHA (blue) or 100 µM ARA (red) in presence of 10 mM GSH.

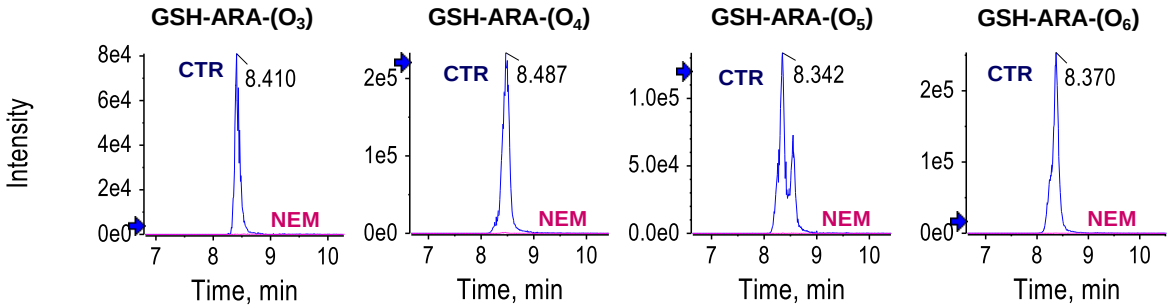

Figure S2. NEM avoid GSH-adducts formation when preincubated with GSH. Incubations were performed with 1 mM GSH in presence or absence of 5 mM NEM for 15 min at 37 ºC. After that, the ARA-F2 (10 %; *v/v*) was added in the samples and incubated for 15 min at 37 ºC.

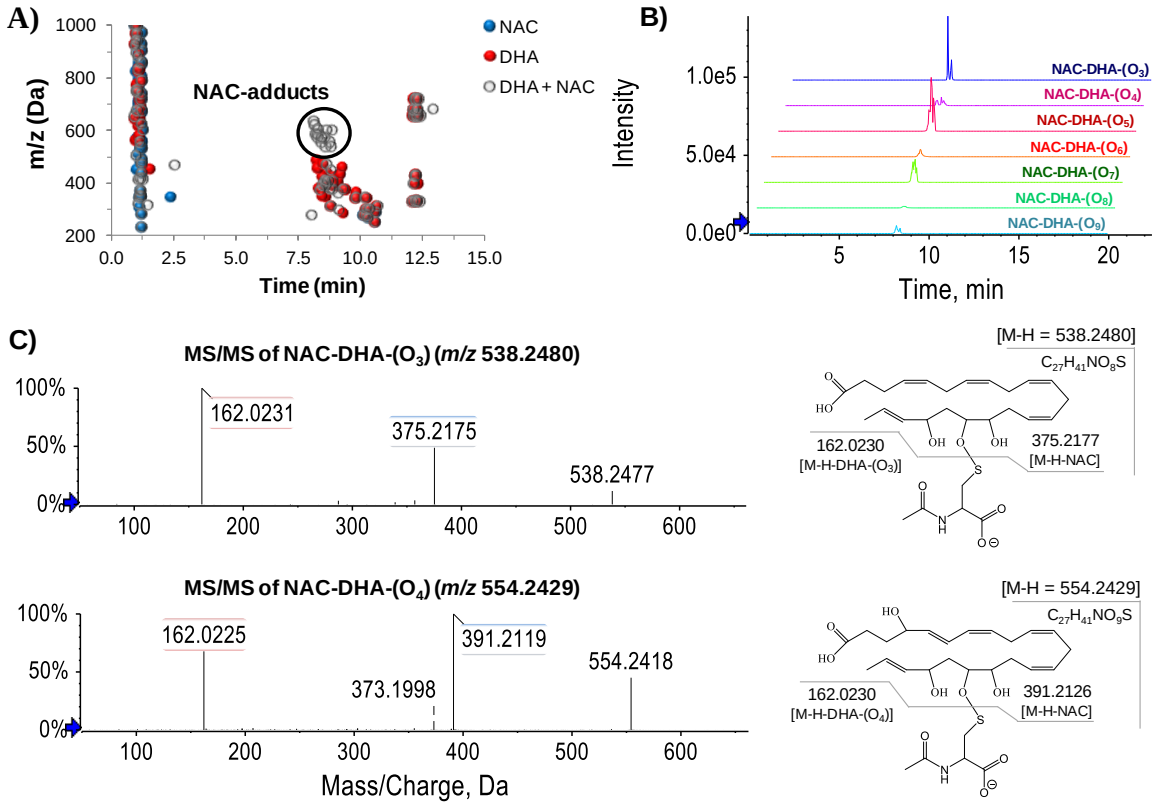

Figure S3. Formation of NAC-adducts confirms that small molecules which contain thiol groups can be modified by cyclic endoperoxides. (A) Untargeted MS/MS data acquired by

information dependent analysis (IDA). (B) Extracted-ion chromatogram (XIC) and area of NAC-adducts. (C) MS/MS spectra of NAC-adducts. Incubations were performed with 100 µM DHA in presence or absence of 10 mM NAC. Only species with total ion count (TIC) above 3×10^4 are shown in the figure.

CHAPTER 2

Altered lipid metabolism in CNS reflecting increased oxidative stress in amyotrophic lateral sclerosis

Adriano B. Chaves-Filho[1], Marcos Y. Yoshinaga[1], Isabella F.D. Pinto[1], Lucas S. Dantas[1], Alex Inague[1], Rodrigo L. de Faria[1], Ohara Augusto[1], Isaías Glezer[2], Sayuri Miyamoto[1,*]

[1]Instituto de Química, Departamento de Bioquímica, Universidade de São Paulo, Brazil.

[2]Departamento de Bioquímica, Escola Paulista de Medicina, Universidade Federal de São Paulo, Brazil.

*Corresponding author: Instituto de Química, Departamento de Bioquímica, Universidade de São Paulo, CP 26077, CEP 05513-970, São Paulo, Brazil.

E-mail: miyamoto@iq.usp.br

Abstract

Lipids are essential components of the central nervous system (CNS) because they participate in a wide range of membrane structures, including lipid rafts, and also modulate cellular events such as differentiation, autophagy and apoptosis. Thus, alterations in the metabolism of lipids in CNS, induced by aging and/or increased oxidative stress, may lead to development of neurodegenerative disorders. Using a rodent model of amyotrophic lateral sclerosis (ALS), a neurodegenerative disease that affects motor neurons, we performed an untargeted lipidomics analysis in brain and spinal cord tissues of asymptomatic and symptomatic ALS rats ($SOD1^{G93A}$). Our results revealed that major lipidome alterations in the brain were linked to higher amounts of sulfatides, galactosyl-ceramides and glycosylated ω-acyl-ceramides associated with aged animals rather than disease. In contrast, drastic alterations of ceramides, cardiolipin and cholesteryl esters were exclusively found in the spinal cord of ALS symptomatic rats. Increased cholesteryl esters and decreased cardiolipin (CL) levels are consistent with recent literature demonstrating the role of neuron-to-glial lipid transport for neuroprotection against elevated oxidative stress in neurons. Here, we demonstrate that a precise analysis of molecular lipid species may provide valuable information on the role of lipid metabolism in aging and neurodegenerative diseases.

Keywords: Lipidomics, Amyotrophic lateral sclerosis, cholesterol ester, sphingolipids, neurodegeneration, mass spectrometry.

1. Introduction

The central nervous system (CNS) is characterized by the presence of high amounts and wide variety of lipids (1). According to their molecular characteristics and cellular localization, lipids play a critical role in the CNS through control of membrane fluidity (2), improving transmissions of electrical signals and serving as precursors for various second messengers (1). Although molecular alterations in CNS at different stages of life are part of the physiological development (3), aging can modulate alterations in the lipidome, especially in response to increased reactive oxygen species (ROS) (4, 5). As consequence, the alteration of lipid metabolism in CNS could contribute to the onset of neurodegenerative disorders (6).

For instance, levels of phospholipids such as phosphatidylethanolamine (PE) esterified to docosahexaenoic (DHA; C22:6n-3) and arachidonic (ARA; C20:4n-6) acids are decreased in the hippocampus of patients with Alzheimer's disease (AD) (7). Because polyunsaturated fatty acids such as DHA and ARA are highly susceptible to peroxidation, their depletion may indicate increased oxidative stress during AD. Increased sphingolipid content with age in the CNS has been attributed to myelination of neurons as the brain develops (8). Not surprisingly, impairment of motor neurons in neurodegenerative diseases has been associated with significant alterations in the metabolism of sphingolipid, as reported in Parkinson's disease, multiple sclerosis and amyotrophic lateral sclerosis (ALS) (9–12). Dysregulation of cholesterol homeostasis in the brain (especially high concentrations of both cholesterol and cholesteryl esters) is also being increasingly linked to neurodegeneration (13, 14). Given this association, it is proposed that inhibition of synthesis of cholesteryl ester may serve as therapeutic target for AD treatment (15, 16).

In this paper, the focus is ALS, a neurodegenerative disorder characterized by loss of motor neurons in CNS. Symptomatic stage of ALS leads to muscular atrophy, paralysis and death at most 5 years after onset of symptoms (17). Among the familiar cases described for

ALS, G93A mutation in the gene of the antioxidant enzyme Cu/Zn-superoxide dismutase ($SOD1^{G93A}$) is one of the most studied models (18). The putative mechanisms involved in ALS disease progression consist of protein aggregation and gain of toxic function of mutant SOD1, abnormal production of ROS and alterations in mitochondrial functions (19, 20). Lipidome alterations in ALS have been mainly investigated through targeted analysis of sphingolipids and cholesterol. Historically, a pioneer study by Cutler *et al*. (2002) revealed aberrant synthesis of ceramides based on targeted analysis of sphingolipids in spinal cord of ALS mice model (21). In addition, these authors suggested that ceramide synthesis by cleavage of sphingomyelin leads to modulation of enzymes linked to synthesis of cholesteryl esters in ALS. Alterations in sphingolipid metabolism were emphasized in studies of the skeletal muscle and spinal cord of SOD1 mice model (12, 22, 23). These authors evidenced an increase in hydroxylated ceramide and others sphingolipids like GalC and GlcC in advanced stages of ALS.

Although relatively well-studied, the CNS in ALS has never been investigated by an untargeted lipidomic approach based on accurate mass identification. Using this technique, we sought to capture further details in lipidome alteration in response to disease progression. For this purpose, we performed an untargeted mass spectrometry-based lipidomics analysis in brain and spinal cord tissues from $SOD1^{G93A}$ symptomatic and asymptomatic rats. Our analysis revealed drastic changes in lipid metabolism in the CNS both according to aging and disease progression. We propose a model in which lipid metabolism alteration in motor neurons of the spinal cord reflects the increased oxidative stress associated with ALS.

2. Materials and methods

2.1. Chemicals and reagents

The lipids used as internal standards N-decanoyl-D-erythro-sphingosine (Ceramide d18:1/10:0), 1-heptadecanoyl-2-hydroxy-sn-glycero-3-phosphocoline (LPC 17:0), 1,2-diheptadecanoyl-sn-glycero-3-phosphate (PA 17:0/17:0), 1,2-diheptadecanoyl-sn-glycero-3-phosphocholine (PC 17:0/17:0), 1,2-diheptadecanoyl-sn-glycero-3-phosphoethanolamine (PE 17:0/17:0), 1,2-diheptadecanoyl-sn-glycero-3-phospho-(1'-rac-glycerol) (PG 17:0/17:0) and N-heptadecanoyl-D-erytro-sphingosylphosphorylcholine (SM d18:1/17:0) were obtained from Avanti Polar Lipids, Inc. (Alabaster, AL. USA). Ammonium formate and ammonium acetate were obtained from Sigma-Aldrich (St Louis, MO, USA). All organic solvents were of HPLC grade obtained from Sigma-Aldrich (St Louis, MO, USA).

2.2. Animals

Male Sprague Dawley rats overexpressing $SOD1^{G93A}$ obtained from Taconic were used in this study. Genotyping was performed for detecting exogenous hSOD1 transgene, by amplification of ear DNA at 20 days of age by PCR. Rats were housed under controlled laboratory conditions, including room temperature, a 12 hour light/12 hour dark cycle with food and water *ad libitum*. Asymptomatic $SOD1^{G93A}$ rats (ALS-Asymp.; n = 7) and their wild type (WT) control (CTR-Asymp.; n = 7) were sacrificed at 73 ± 4 days of age, while symptomatic $SOD1^{G93A}$ rats (ALS-Symp.; n = 13) and their WT control (CTR-Symp.; n = 15) were sacrificed at 122 ± 6 days of age. The criteria for sacrifice of symptomatic $SOD1^{G93A}$ rats were loss of 15% of maximum body weight. Rats were fasted for 6 h and anesthetized by isoflurane inhalation at dose of 4% for induction and 2% for maintenance. Motor cortex and spinal cord were collected and stored at -80 ºC until further processing. All procedures were performed in accordance with the local Animal Care and Use Committee (Comissão de Ética em Cuidados e Uso Animal) (Permit number: 14/2013).

2.3. Lipid extraction

Lipid extraction was performed according to the method established by Yoshida *et al*. (2008) (24). Motor cortex and spinal cord tissues (200 mg) were homogenized in ice by using a tissue grinder in 1 mL of 10 mM phosphate buffer (pH 7.4) containing deferoxamine mesylate 100 μM. Briefly, 100 μL of motor cortex or spinal cord (20 mg) were mixed with 400 μL of phosphate buffer, 400 μL of ice-cold methanol and 100 μL of internal standards (Supplementary Table 1). Next, 1.5 mL of chloroform/ethyl acetate (4:1) was added to the mixture, which was thoroughly vortexing for 30 s. After centrifugation at 1500 g for 2 min at 4 °C, the lower phase containing the total lipid extract (TLE) was transferred to a new tube and dried under N_2 gas. Dried TLE were redissolved in 100 μL of isopropanol and the injection volume was set at 1 μL.

2.4. Lipidomics analysis

TLE were analyzed by ESI-TOFMS (Triple TOF 6600, Sciex, Concord, US) interfaced with a high-performance LC (UHPLC Nexera, Shimadzu, Kyoto, Japan). The samples were loaded into a CORTECS® (UPLC® C18 column, 1.6 μm, 2.1 mm i.d. x 100 mm) with a flow rate of 0.2 mL min-1 and the oven temperature maintained at 35 °C. For RPLC, mobile phase A consisted of water/acetonitrile (60:40), while mobile phase B composed of isopropanol/acetonitrile/water (88:10:2). Mobile phases A and B contained ammonium acetate or formic acid (at a final concentration of 10 mM) for experiments performed in negative or positive ionization mode, respectively. The linear gradient during RPLC were as follows: from 40 to 100% B over the first 10 min., hold at 100% B from 10-12 min., decreased from 100 to 40% B during 12-13 min., and hold at 40% B from 13-20 min.

The MS was operated in both positive and negative ionization modes, and the scan range set at a mass-to-charge ratio of 200-2000 Da. Data for lipid molecular species identification and quantification was obtained by Information Dependent Acquisition

(IDA®). Data acquisition was performed with a period cycle time of 1.05 s with 100 ms acquisition time for MS1 scan and 25 ms acquisition time to obtain the top 36 precursor ions. Data acquisition was performed using Analyst® 1.7.1 with an ion spray voltage of -4.5 kV and 5.5 kV (for negative and positive modes, respectively) and the cone voltage at +/- 80 V. The curtain gas was set at 25 psi, nebulizer and heater gases at 45 psi and interface heater of 450 °C.

2.5. Data processing

The MS/MS data was analyzed with PeakView®, and lipid molecular species were identified by an in-house manufactured Excel-based macro. Area of each lipid species were obtained by MS data from MultiQuant®. For quantification, the area ratio of each lipid species was calculated by the peak area of each lipid species divided by the peak area of the corresponding internal standard. The concentration of each lipid species was calculated by the area ratio multiplied by the internal standard amount. The total amount of lipids was expressed in µg/g of tissue extracted. Data are presented as mean ± SEM (calculated by summing of the individual lipid species within each class).

2.6. Statistical analysis

All statistical analyses were performed with Metaboanalyst (website: www.metaboanalyst.ca). In brief, data were log transformed, and the statistical significance ($p < 0.05$) evaluated by one-way ANOVA followed by Turkey's post-test. Next, we performed a heatmap analysis using only lipids that were statistically altered in the different groups. For the comparison of ALS symptomatic rats with their respective controls, we conducted a t-test ($p < 0.05$) and evaluated the differences through a volcano plot. Throughout our analysis, we followed the protocols by Xia and others (25).

3. Results

3.1. Sphingolipids are modulated according to aging and slightly with disease progression in motor cortex of SOD1^{G93A} rats

Alterations in the lipid metabolism of the CNS are usually associated with development of neurodegenerative process. In order to investigate how lipids are affected in a model of ALS, we performed a comprehensive lipidomics analysis of motor cortex and spinal cord from asymptomatic (73 ± 3 days old) and symptomatic (122 ± 6 days old) ALS rats, and their respective age matched control groups. Using non-targeted lipidomics approach we identified and quantified 285 molecular lipid species in the motor cortex, which were sorted into 26 lipid subclasses (Fig. 1A). Among the major lipid classes, glycerophospholipids (n = 120) followed by sphingolipids (n = 78), glycerolipids (n = 63) and fatty acids (n = 14) showed the most diversity of individual lipid molecular species. Together, plasmenyl and diacyl phosphatidylethanolamine (pPE and PE) encompass about 70% in mass of the total identified lipid molecular species in motor cortex of SOD1^{G93A} rats (Fig. 1B). The remaining 30% of lipids are mainly composed of phosphatidylserine (PS), diacylglycerol (DAG), free fatty acids (FFA), among others.

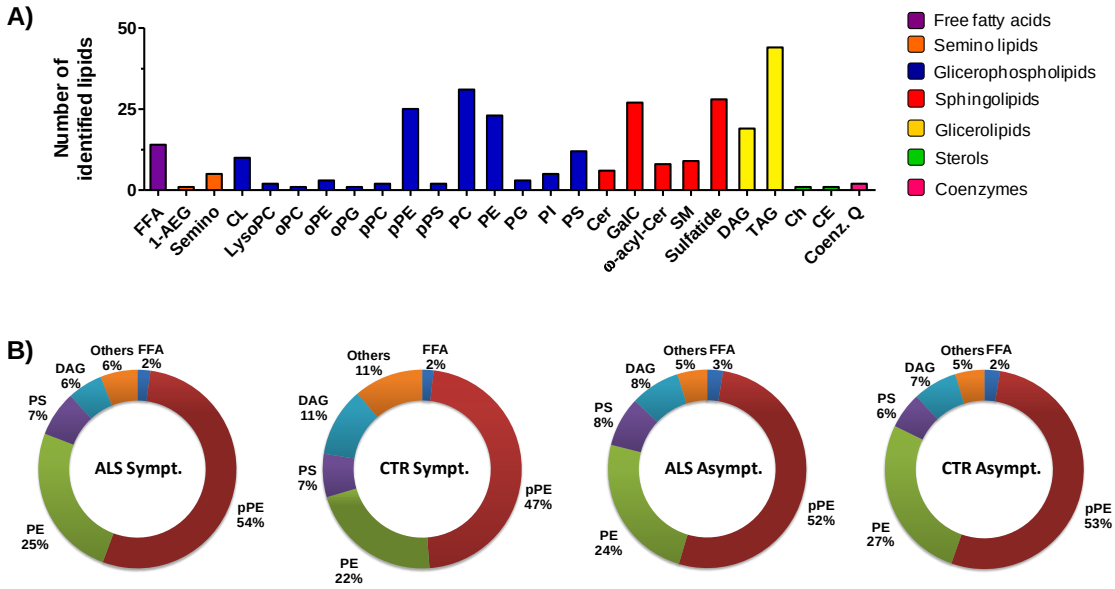

Figure 1. Profile of the lipid molecular species identified in motor cortex of SOD1^{G93A} transgenic rat model. (A) Number of the identified lipid molecular species sorted into their respective lipid subclasses. (B) Relative percentage of lipid subclasses identified in motor cortex.

Heatmap of motor cortex lipidome shows that 31 lipid molecular species are altered when all experimental groups were compared (Fig. 2). The increased levels of galactosyl ceramides (GalC; 14 species), sulfatide (10 species) and glycosylated ω-acyl-Ceramides (ω-acyl-Cer; 8 species) in both ALS and CTR symptomatic groups suggest that age is an important factor for lipidome alterations in motor cortex and not the disease per se. The altered lipids show high diversity in composition of sphingosine base, hydroxylation and chain length (Fig S1). Once our data suggest that sphingolipids are positively modulated, especially in older animals, we investigated the components of this lipid class. Among them, GalC, glycosylated ω-acyl-Cer and sulfatide are increased in the ALS and CTR symptomatic groups (Fig. S2). Furthermore, GalC and glycosylated ω-acyl-Cer are significantly increased in the ALS symptomatic group when compared to the others. This finding suggests that age is the main responsible for modulation of sphingolipid metabolism.

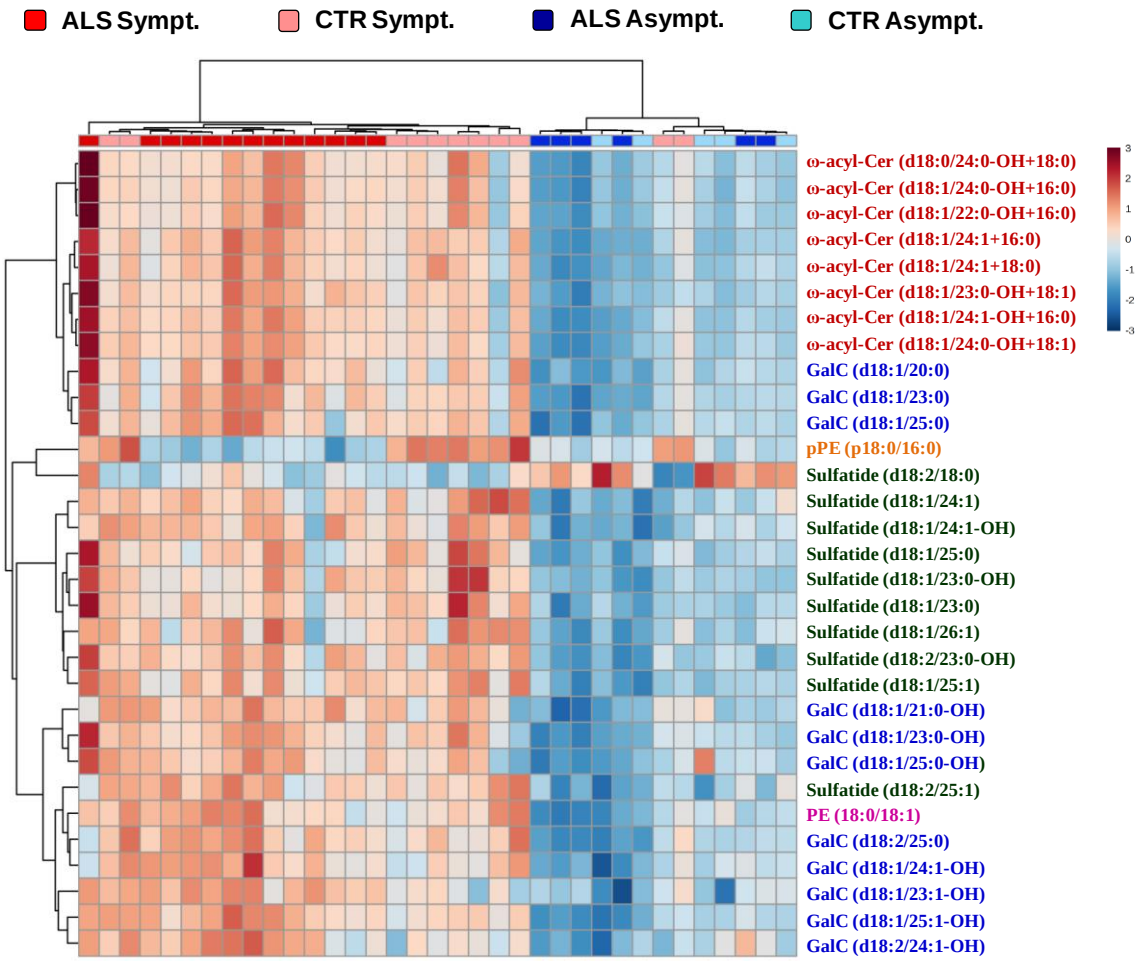

Figure 2. Heatmap of the most significantly different lipid molecular species in motor cortex of SOD1^{G93A} transgenic rat model. In total 31 lipid molecular species are shown in rows and sample in column. Statistical significance was evaluated by one way ANOVA followed by Tukey's post-test ($p < 0.05$) using Metaboanalyst. Distance was measured in Pearson, and Ward´s clustering algorithm. Each colored cell on heatmap corresponds to normalized concentrations. Log transformation was used for data normalization value.

3.2. Ceramides, cholesteryl esters and cardiolipin are altered in spinal cord of SOD1^{G93A} rats

Lipidomics analysis of spinal cord uncovered 406 molecular lipid species that could be sorted into 33 lipid subclasses. Glycerophospholipids (n = 177) followed by sphingolipids (n = 101), glycerolipids (n = 81) and seminolipids (n = 22) showed the most diversity of individual lipid molecular species found in spinal cord (Fig. 3A). Analysis of the relative

percentage of the identified lipid subclasses revealed that PE and PS encompass little more than 50 % in mass of the total identified lipid molecular species (Fig. 3B). Among the sphingolipids, the most abundant lipid subclasses are composed by sphingomyelins (SM) and sulfatides, whereas triacylglycerol (TAG) is the most abundant storage lipid.

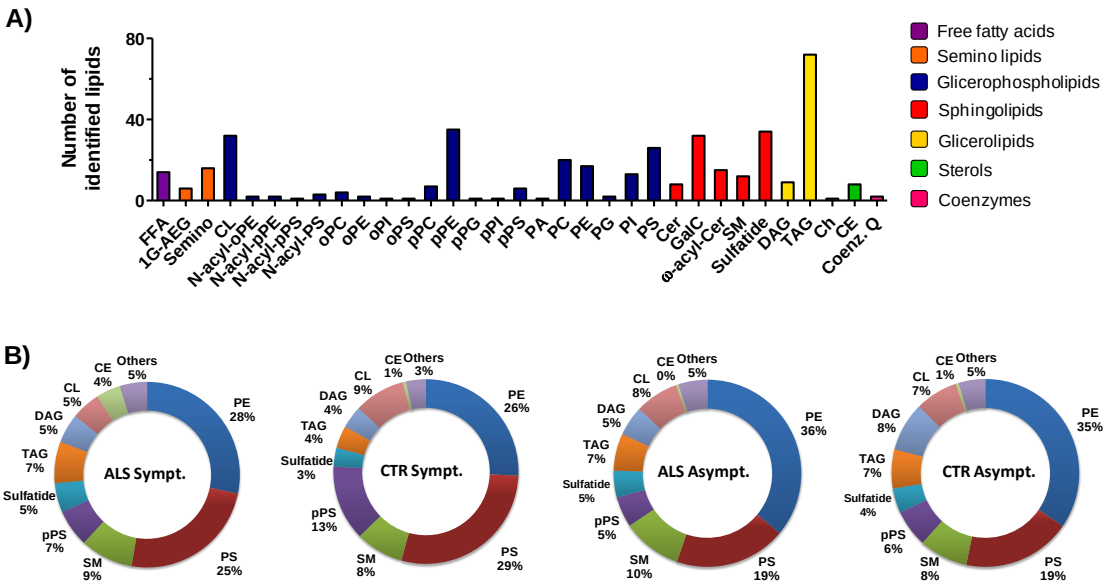

Figure 3. Profile of the lipid molecular species identified in spinal cord of SOD1^{G93A} transgenic rat model. (A) Number of the identified lipid molecular species sorted into their respective lipid subclasses. (B) Relative percentage of lipid subclasses present in spinal cord.

Heatmap of the most significant alterations in lipidome of spinal cord revealed alterations in the metabolism of sphingolipids as reported for ceramides (3 species), glycosylated ω-acyl-Cer (4 species) and SM (1 specie) (Fig. 4). While alterations in glycosylated ω-acyl-Cer and SM species seem to be increased with age, two molecular species of ceramides are increased only in ALS symptomatic rats. Notably, not only metabolism of sphingolipids is altered in the spinal cord, but also all cholesteryl esters (8 species) are drastically increased in ALS symptomatic rats, suggesting alterations in the metabolism of storage lipids. Because the main lipid alterations with age are linked to sphingolipid metabolism we investigated the total levels of glycosylated ω-acyl-Cer, ceramides and SM. As described for motor cortex, the levels of glycosylated ω-acyl-

ceramides were increased in both ALS and CTR symptomatic groups suggesting that alterations in sphingolipid metabolism are mainly associated with aging (Fig. S3).

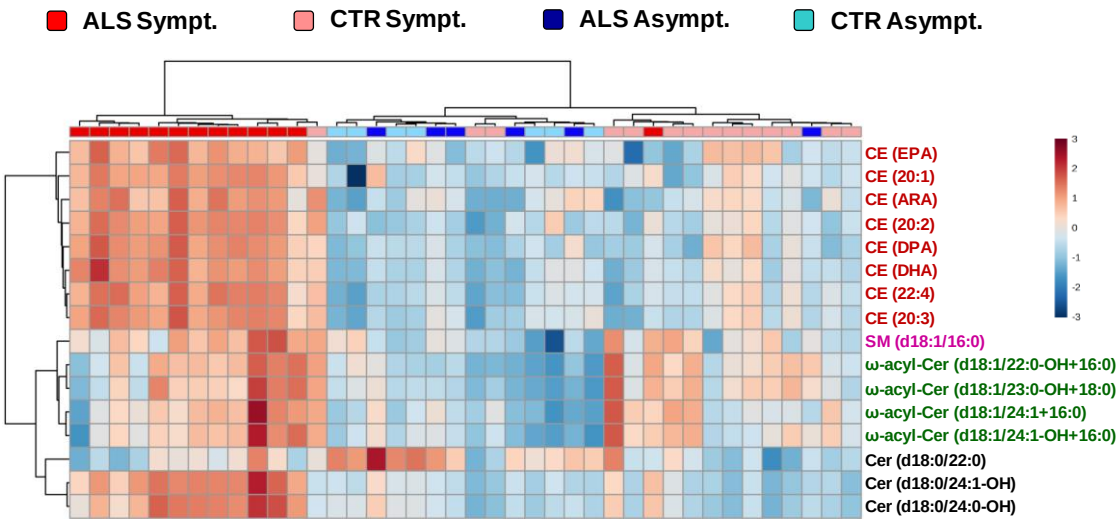

Figure 4. Heatmap of the most significantly altered lipid molecular species in spinal cord of SOD1^{G93A} transgenic rat model. In total 16 lipid molecular species are shown in rows and sample in column. Statistical significance was evaluated by one way ANOVA followed by Tukey's post-test ($p < 0.05$) using Metaboanalyst. Distance was measured in Pearson, and Ward´s clustering algorithm. Each colored cell on heatmap corresponds to normalized concentrations. Log transformation was used for data normalization value.

Since we detected a modulation of the lipid metabolism in spinal cord of ALS symptomatic rats, we investigated in more details the differences when compared to its control group through a volcano plot (Fig. 5). Analyzing these data we see a decrease in cardiolipin contents whereas cholesteryl ester contents are increased in the ALS symptomatic group. Minor alterations were detected for TAGs and ceramides. Although the total level of TAGs and ceramides were not altered in ALS symptomatic group, the molecular characteristics of ceramides were drastically changed (Fig. S4). The ratios of hydroxylated/non-hydroxylated (OH/n-OH) and very long chain/long chain (VLC/LC) ceramides were increased, whereas the ratio ceramide/dihydroceramide (Cer/dh-Cer) was

reduced in ALS symptomatic group. Therefore, the remodeling of molecular characteristics of ceramides is specific for ALS symptomatic group.

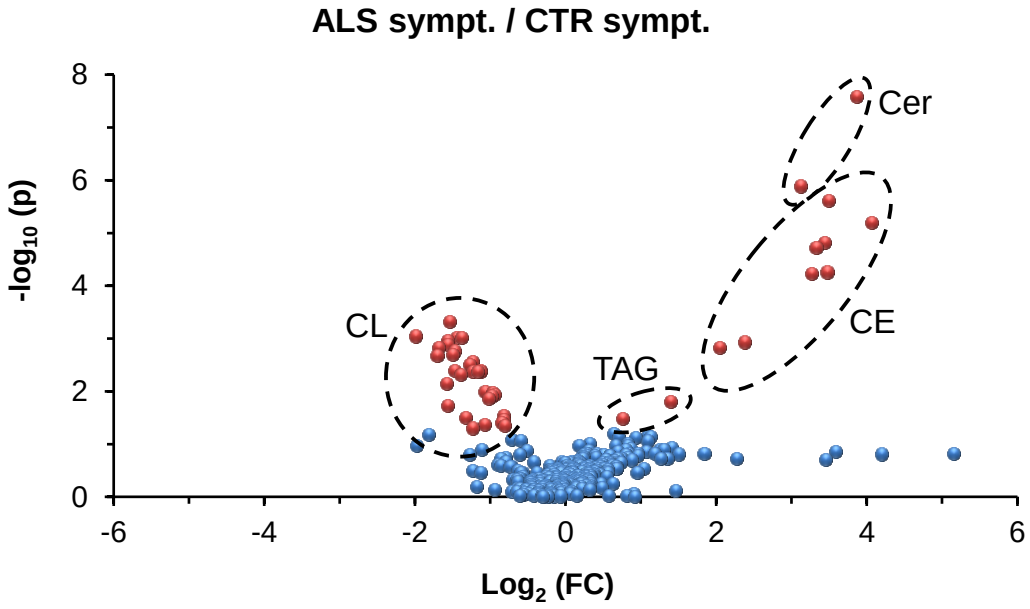

Figure 5. Volcano plot of the lipid molecular species altered in spinal cord of ALS symptomatic group. The $\log_2$ (Fold change) of ALS symptomatic / CTR symptomatic group was plotted versus the $-\log_{10}$ (p). Statistical significance was evaluated by t-test ($p < 0.05$) and fold change threshold was set as 1.5. In red are represented the significant altered lipid molecular species.

The main positive alterations in lipidome of spinal cord were found in cholesteryl esters and cardiolipins (Fig. 6). We confirmed that the total contents of cholesteryl esters were increased by 6 fold in ALS symptomatic groups (Fig. 6A). Among the composition of the fatty acids, the polyunsaturated fatty acids arachidonic (ARA; C20:4n-6), eicosapentaenoic (EPA; C20:5n-3) and adrenic (AdA; C22:4n-6) acids were the most abundant (Fig. 6B). Also, we investigated the molecular characteristics of cardiolipins, since 10 out of 32 lipid molecular species were decreased in spinal cord of ALS symptomatic rats (Fig. S5). Statistical analysis showed that total levels of cardiolipin are decreased in ALS symptomatic group when compared to its control (Fig. 6C). Also, the fatty acid composition of cardiolipin showed that

estearic (C18:0), oleic (C18:1), palmitic (C16:0), γ-linolenic (C20:3n-6) acids, ARA and DHA are decreased in ALS symptomatic rats (Fig. 6D).

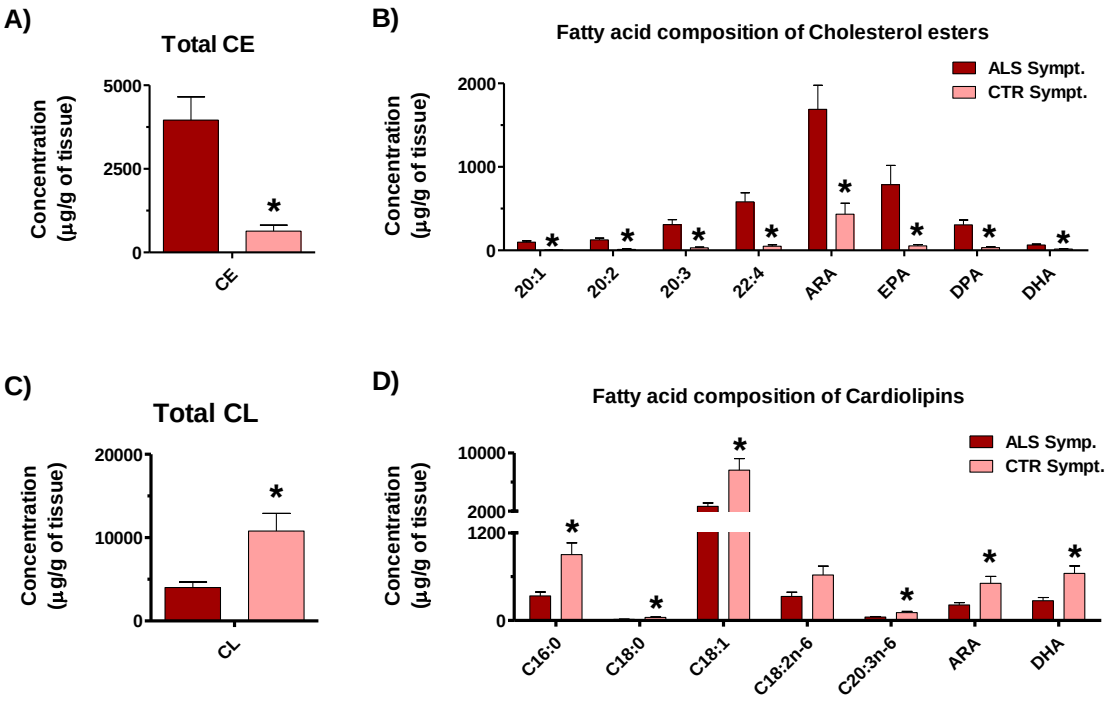

Figure 6. Profile of cholesteryl esters and cardiolipins identified in spinal cord of SOD1^{G93A} transgenic rat model. (A) Concentration of total cholesteryl esters. (B) Fatty acid composition of cholesteryl esters. (C) Concentration of total cardiolipins. (D) Fatty acid composition of cardiolipins. Data are shown as mean ± SEM. Statistical significance was evaluated by t-test ($p < 0.05$) using Metaboanalyst. (*) Different when compared to the ALS symptomatic group.

4. Discussion

Lipids play a critical role in the structure of the CNS through control of membrane fluidity, improving transmission of electrical signals and stabilizing synapses (2, 26). Alterations of lipid metabolism in neurons and glial cells (astrocytes, oligodendrocytes and microglia) modulate processes linked to aging and neurodegenerative diseases (27, 28). In order to investigate alterations in the lipidome of motor cortex and spinal cord of SOD1^{G93A} transgenic rat model for ALS, we performed an untargeted analysis using high resolution UHPLC-TOF-MS based lipidomics approach. Manual identification based on MS/MS profile

of molecular ions allowed us to identify a wide range of lipid molecular species in motor cortex (Fig. 1) and spinal cord (Fig. 3) which were sorted into 26 and 33 lipid subclasses, respectively. Whereas in the motor cortex the main alterations in sphingolipid metabolism were linked to age, the spinal cord alterations showed to be strongly associated with ALS in a symptomatic stage. Moreover, not only sphingolipids, but also cholesteryl ester and cardiolipin metabolism are modified in ALS symptomatic animals, suggesting that alterations in the mitochondrial metabolism is linked to the disease progression. Taken together, our findings suggest that spinal cord seems to be more susceptible than the motor cortex to lipid alterations during ALS symptomatic stage. However, it is important to mention that aging and neurodegenerative diseases are intimately linked and alterations in lipidome profile according to age could contribute to the onset of pathological events characteristic of most neurodegenerative process.

Alterations in the lipids from the motor cortex were mostly related to sphingolipids, namely GalC, sulfatide and glycosylated ω-acyl-Cer (Fig. 2). Despite the young age of the animals (about 70 and 120 days old), these alterations seem to be more linked to aging than to disease progression. Our findings are in line with the active production of myelin by adults, either from newly formed oligodendrocytes or new membrane production by existing cells, reflecting the constant increase in levels of sphingolipids with age (8). Interestingly, the increased content of glycosylated ω-acyl-Cer observed in motor cortex of older animals was also observed in spinal cord tissues (Figs. S2 and S3). These sphingolipids are signature lipids of the epidermis and appear to correlate with water protection in this tissue (29). To our knowledge, glycosylated ω-acyl-Cer have never been reported in the CNS and their modulation with age together with GalC and sulfatide suggest a link of these sphingolipids with myelination and brain development.

Dramatic differences in lipidome profiles were observed in the spinal cord of ALS symptomatic rats (Fig. 4). The latter comparison revealed major alterations related to cholesteryl esters and cardiolipin levels and to a minor extent to the amounts of hydroxylated dihydroceramides and TAG. Differences in the metabolism of ceramides have been repeatedly reported in spinal cord tissues of ALS patients and rodent models (12, 21–23). Hydroxylated ceramides are essential for the stability of the myelin, and a knockdown of the enzyme responsible for the hydroxylation (fatty acid 2-hydroxylase) results in neural impairments in mice (30). Ceramides have also been implicated in cellular signaling (31), and in ALS they are thought to activate the oxysterol-binding protein (OSBP) (21). According to these authors, OSBP binds and delivers oxysterols to the endoplasmic reticulum thereby activating acylcoenzyme A:cholesterol acyltransferase (ACAT) yielding cholesteryl esters as products. Accumulation of either hydroxylated ceramides or dihydroceramides could trigger cell survival events such as autophagy (32, 33). Since one of the hallmarks of ALS is the presence of cytoplasmic inclusions or SOD1 aggregates in affected motor neurons (34), the stimulation of autophagic process by these ceramides could be a potential pathway for elimination of protein aggregates and damaged organelles.

As highlighted by our data, ALS symptomatic rats display elevated levels of cholesteryl esters and decreased cardiolipin in spinal cord tissues, but not in motor cortex, as the major lipid signatures of the disease (Fig. 6). This change in cholesterol metabolism seems unrelated to alterations in the pools of free cholesterol (Fig. S6) or 24-hydroxycholesterol, the latter only observed in trace amounts in the spinal cord (data not shown). That is, it appears that cholesterol synthesis is upregulated but does not reflect in accumulation of free cholesterol neither 24-hydroxycholesterol, which is generally more soluble and can cross the brain-blood-barrier at a much faster rate than cholesterol (35). In order to understand why cholesterol synthesis is altered during ALS, we borrowed a model born in the study of

neuron-glia interaction in fruit flies (36, 37). These studies have postulated that neurons under elevated ROS shuttle lactate for lipid synthesis rather than for energy generation through the TCA cycle. As a consequence of this increased production of *de novo* synthesized lipids by neurons, lipid droplets accumulate in glial cells. Interestingly, researchers from Uruguay have recently reported that aberrant astrocytes derived from the spinal cord of rats carrying the SOD1 mutation also accumulated significant amounts of lipid droplets in their cytosol (38). Although the lipid composition of lipid droplets present in glial cells was not determined by the autors, it is tempting to suggest that the neutral lipids accumulating in the lipid droplets could be cholesteryl esters. Here, using the data provided by the above-cited authors we attempted to formulate a model (Fig. 7) based on: 1) elevated ROS in ALS leading to dysfunctional neuronal mitochondria; 2) upregulation of cholesterol synthesis due to altered lactate metabolism in neuronal mitochondria; 3) accumulation of cholesteryl esters composed of polyunsaturated fatty acids as a protective mechanism against elevated ROS in the CNS.

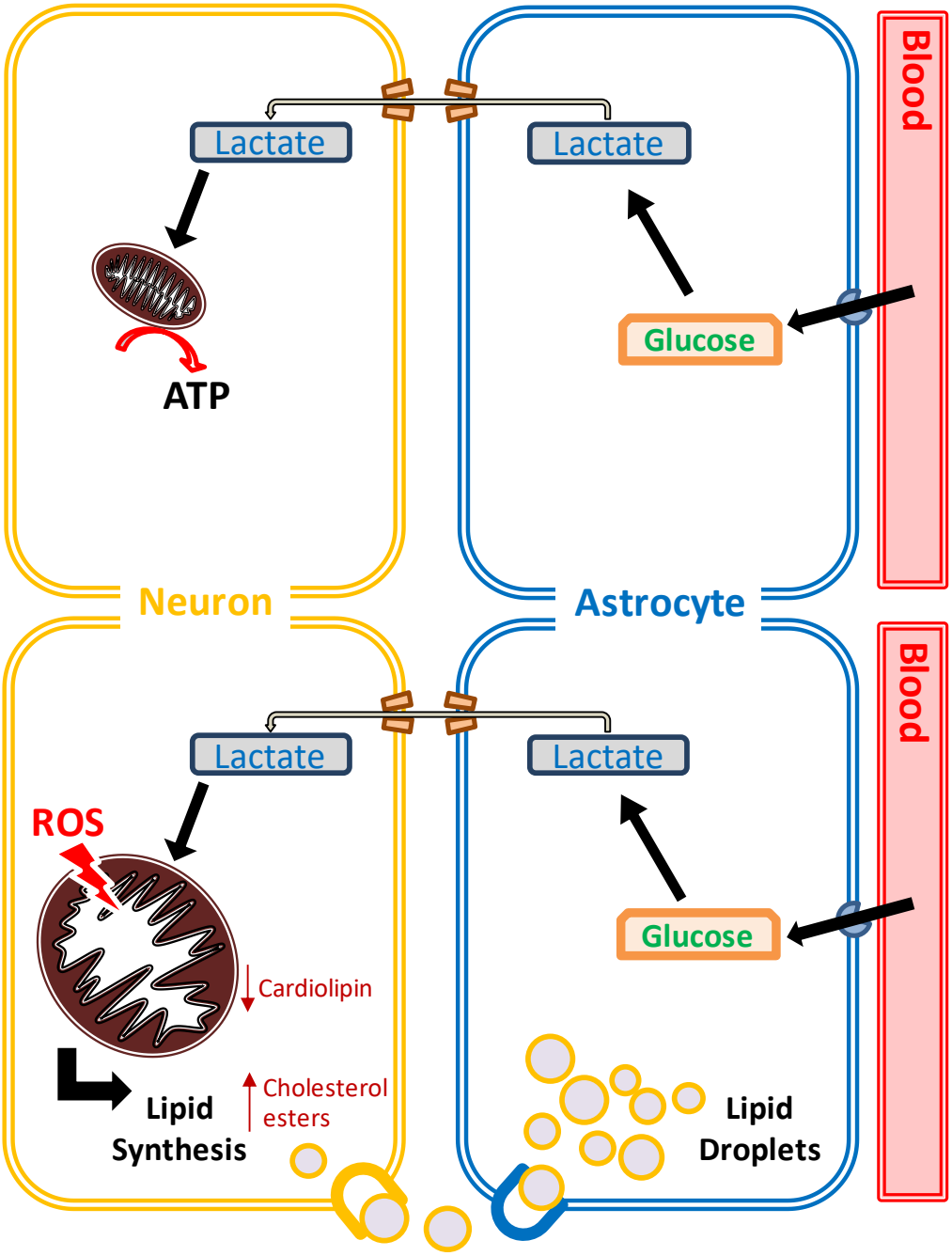

Figure 7. Proposed model for neuroprotection by accumulation of lipid droplets in astrocytes (adapted from Liu *et al.*, 2017).

A growing body of evidence implicates impaired energy metabolism in ALS patients and models (20). In this respect, ROS generation and mitochondrial dysfunction in motor neurons represent a clinical hallmark of ALS (39–42). Whether elevated ROS is caused by SOD1 gain of function, SOD1 aggregation or glutamate accumulation leading to imbalanced

calcium homeostasis in neurons remains still unanswered. Here the main point is elevated ROS negatively impacting mitochondrial function, and leading to changes that range from decreased energy metabolism to major morphological modifications. Reflecting dysfunctional mitochondria, our data reveal a significant decrease in cardiolipin levels in ALS symptomatic spinal cord when compared to control samples (Fig. 6). Cardiolipin is a major and specific phospholipid of the inner mitochondrial membrane and their functions have been primarily related to ATP production (43, 44), but especially to curvature stress control and mitochondria cristae formation (45, 46). In support of our data, abnormal mitochondrial morphology has been repeatedly observed in motor neurons of distinct familial cases of ALS models (47–51) generally consisting of mitochondria clusters, swollen mitochondria, loss of cristae and vacuoles derived from degenerating mitochondria. Given its function in structuring morphology, we suggest that a decrease in cardiolipin levels may partially reflect the loss of mitochondrial cristae and thus reflect dysfunctional mitochondria in the spinal cord of ALS symptomatic rats.

It is generally assumed that the primary source of energy in the brain is blood-born glucose, and glial cells are extremely efficient in its uptake. Glycolysis-derived lactate is provided by glial cells to neurons (52, 53) that in turn use it to fuel glycolysis. By inducing ROS formation in neurons, Liu *et al*. (2017) investigated the neuron-to-glia transport of lactate in fruit flies and mouse (37). Their data is consistent with lactate being converted to pyruvate and acetyl-CoA, with the latter generating fatty acids that are transported back to glial cells for neuroprotection. The accumulation of lipids in glial cells was evidenced by abundant lipid droplet formation, similar to data in aberrant astrocytes from the spinal cords of ALS rats (38). According to our findings, neutral lipid accumulation was observed almost exclusively as cholesteryl ester in the spinal cord of ALS symptomatic rats, with no major alterations in the pool of TAG. A pertinent question is therefore why cholesteryl ester and not

TAG are stored as neutral lipids in droplets? We hypothesize that the answer relies in part in the efficiency by which lipid droplets can be shuttled from neurons to glial cells by apolipoproteins for neuroprotection as demonstrated by Liu *et al*. (2017). As stated by these authors any defect in apolipoprotein-driven lipid transport for neuroprotection may lead to neurodegeneration.

Our data bear evidence for an accumulation of polyunsaturated fatty acids esterified to cholesteryl esters. Since mammals cannot synthesize these fatty acids, this accumulation likely reflects a protective mechanism against oxidative stress (54). That is, under elevated ROS, neuronal cells store their highly susceptible membrane-bound fatty acids as cholesteryl ester or TAG, avoiding lipid peroxidation. Once protected in lipid droplets, neutral lipids may be shuttled to and undergo fatty acids beta-oxidation in glial cells (36, 37). Whether fatty acids can be quantitatively used as fuel of energy by glial cells remains debatable (55), since beta-oxidation requires more oxygen than glucose, and may deplete the demand of oxygen by neurons (56). Furthermore, beta-oxidation also generates superoxide anion and may enhance oxidative stress, and for this reason neurons likely rely on glial cells for storing excess lipids. We suggest that a delicate balance between neuron-glia lipid transport and energy metabolism, perhaps with significant contribution of beta-oxidation in both neurons and glial cells (55), is likely relevant to this feedback loop for neuroprotection. In retrospect, any perturbation of this feedback loop may contribute to neurodegeneration. Our findings are consistent with the neuroprotective mechanism demonstrated in fruit flies (36, 37) and support the accumulation of lipid droplets as cholesteryl ester in aberrant astrocytes from the spinal cords of ALS mouse (38). The precise analysis of molecular species of lipids as presented by our study may provide additional clues to the role of oxidative stress regulating the lipid metabolism in aging and neurodegenerative diseases.

Associated content

Supporting information

(1) Supplementary Figures.

Notes

The authors declare no competing financial interest.

Acknowledgments

This work was supported by Fundação de Amparo à Pesquisa do Estado de São Paulo (FAPESP) Grants 08/57721-0, 10/50891-0 and 13/07937-8, Conselho Nacional de Desenvolvimento Científico e Tecnológico (CNPq) Grant 573530/2008-4 and Pro-Reitoria de Pesquisa da Universidade de São Paulo (PRPUSP) Grant 2011.1.9352.1.8. The authors are members of INCT Redoxoma (FAPESP/CNPq/CAPES), NAP Redoxoma (PRPUSP), and the CEPID Redoxoma (FAPESP).

Abbreviations

CNS, central nervous system; PE, phosphatidylethanolamine; DHA, docosahexaenoic acid; ARA, arachidonic acid; AD, Alzheimer's disease; ALS, Amyotrophic lateral sclerosis; SOD1, Cu,Zn-superoxide dismutase; PS, phosphatidylserine; DAG, diacylglycerol; FFA, free fatty acids; GalC, galactosylceramide; ω-acyl-Cer; ω-acyl-ceramide; SM, sphingomyelins; CL, cardiolipin; TCA cycle, tricarboxylic acid cycle; ROS, reactive oxygen species.

References

1. Adibhatla RM, Hatcher JF (2007) Role of lipids in brain injury and diseases. *Future Lipidol* 2(4):403–422.
2. Schmitt F, Hussain G, Dupuis L, Loeffler J-P, Henriques A (2014) A plural role for lipids in motor neuron diseases: energy, signaling and structure. *Front Cell Neurosci* 8(February):1–10.
3. Zhang Y, Appelkvist EL, Kristensson K, Dallner G (1996) The lipid compositions of different regions of rat brain during development and aging. *Neurobiol Aging* 17(6):869–75.
4. Poon HF, Calabrese V, Scapagnini G, Butterfield DA (2004) Free radicals and brain aging. *Clin Geriatr Med* 20(2):329–359.
5. Valko M, et al. (2007) Free radicals and antioxidants in normal physiological functions and human disease. *Int J Biochem Cell Biol* 39(1):44–84.
6. Sato N, Morishita R (2015) The roles of lipid and glucose metabolism in modulation of β-amyloid, tau, and neurodegeneration in the pathogenesis of Alzheimer disease. *Front Aging Neurosci* 7(OCT):1–9.
7. Farooqui AA, Horrocks LA, Farooqui T (2000) Glycerophospholipids in brain: Their metabolism, incorporation into membranes, functions, and involvement in neurological disorders. *Chem Phys Lipids* 106(1):1–29.
8. Bercury KK, Macklin WB (2015) Dynamics and mechanisms of CNS myelination. *Dev Cell* 32(4):447–458.
9. Brugg B, Michel PP, Agid Y, Ruberg M (1996) Ceramide induces apoptosis in cultured mesencephalic neurons. *J Neurochem* 66(2):733–739.
10. Ariga T, Jarvis WD, Yu RK (1998) Role of sphingolipid-mediated cell death in neurodegenerative diseases. *J Lipid Res* 39(1):1–16.
11. Wheeler D, Bandaru VVR, Calabresi PA, Nath A, Haughey NJ (2008) A defect of sphingolipid metabolism modifies the properties of normal appearing white matter in multiple sclerosis. *Brain* 131(11):3092–3102.
12. Henriques A, et al. (2015) Amyotrophic lateral sclerosis and denervation alter sphingolipids and up-regulate glucosylceramide synthase. *Hum Mol Genet* 24(25):7390–7405.
13. Cutler RG, et al. (2004) Involvement of oxidative stress-induced abnormalities in ceramide and cholesterol metabolism in brain aging and Alzheimer's disease. *Proc*

Natl Acad Sci 101(7):2070–2075.

14. Vance JE (2012) Dysregulation of cholesterol balance in the brain: contribution to neurodegenerative diseases. *Dis Model Mech* 5(6):746–755.
15. Huttunen HJ, Kovacs DM (2008) ACAT as a drug target for Alzheimer's disease. *Neurodegener Dis* 5(3–4):212–214.
16. Bryleva EY, et al. (2010) ACAT1 gene ablation increases 24(S)-hydroxycholesterol content in the brain and ameliorates amyloid pathology in mice with AD. *Proc Natl Acad Sci* 107(7):3081–3086.
17. Gros-Louis F, Gaspar C, Rouleau GA (2006) Genetics of familial and sporadic amyotrophic lateral sclerosis. *Biochim Biophys Acta - Mol Basis Dis* 1762(11–12):956–972.
18. Naini A, et al. (2002) Identification of a novel mutation in Cu/Zn superoxide dismutase gene associated with familial amyotrophic lateral sclerosis. *J Neurol Sci* 198(1–2):17–19.
19. Parakh S, Spencer DM, Halloran MA, Soo KY, Atkin JD (2013) Redox regulation in amyotrophic lateral sclerosis. *Oxid Med Cell Longev* 2013. doi:10.1155/2013/408681.
20. Vandoorne T, De Bock K, Van Den Bosch L (2018) Energy metabolism in ALS: an underappreciated opportunity? *Acta Neuropathol* 135(4):489–509.
21. Cutler RG, Pedersen WA, Camandola S, Rothstein JD, Mattson MP (2002) Evidence that accumulation of ceramides and cholesterol esters mediates oxidative stress - Induced death of motor neurons in amyotrophic lateral sclerosis. *Ann Neurol* 52(4):448–457.
22. Dodge JC, et al. (2015) Glycosphingolipids are modulators of disease pathogenesis in amyotrophic lateral sclerosis. *Proc Natl Acad Sci* 112(26):8100–8105.
23. Henriques A, et al. (2018) Sphingolipid Metabolism Is Dysregulated at Transcriptomic and Metabolic Levels in the Spinal Cord of an Animal Model of Amyotrophic Lateral Sclerosis. *Front Mol Neurosci* 10(January):1–14.
24. Yoshida Y, Kodai S, Takemura S, Minamiyama Y, Niki E (2008) Simultaneous measurement of F2-isoprostane, hydroxyoctadecadienoic acid, hydroxyeicosatetraenoic acid, and hydroxycholesterols from physiological samples. *Anal Biochem* 379(1):105–115.
25. Xia J, Wishart DS (2016) Using metaboanalyst 3.0 for comprehensive metabolomics data analysis. *Curr Protoc Bioinforma* 2016(September):14.10.1-14.10.91.
26. Aggarwal S, Yurlova L, Simons M (2011) Central nervous system myelin: Structure,

synthesis and assembly. *Trends Cell Biol* 21(10):585–593.

27. Yadav RS, Tiwari NK (2014) Lipid Integration in Neurodegeneration: An Overview of Alzheimer's Disease. *Mol Neurobiol* 50(1):168–176.
28. Chrast R, Saher G, Nave K-A, Verheijen MHG (2011) Lipid metabolism in myelinating glial cells: lessons from human inherited disorders and mouse models. *J Lipid Res* 52(3):419–434.
29. Uchida Y, Holleran WM (2008) Omega-O-acylceramide, a lipid essential for mammalian survival. *J Dermatol Sci* 51(2):77–87.
30. Meixner M, Jungnickel J, Grothe C, Gieselmann V, Eckhardt M (2011) Myelination in the absence of UDP-galactose:ceramide galactosyl-transferase and fatty acid 2 -hydroxylase. *BMC Neurosci* 12(1):22.
31. Grösch S, Schiffmann S, Geisslinger G (2012) Chain length-specific properties of ceramides. *Prog Lipid Res* 51(1):50–62.
32. Siddique MM, et al. (2013) Ablation of Dihydroceramide Desaturase 1, a Therapeutic Target for the Treatment of Metabolic Diseases, Simultaneously Stimulates Anabolic and Catabolic Signaling. *Mol Cell Biol* 33(11):2353–2369.
33. Kota V, Hama H (2014) 2'-Hydroxy ceramide in membrane homeostasis and cell signaling. *Adv Biol Regul* 54(1):223–230.
34. Lee JK, Shin JH, Lee JE, Choi EJ (2015) Role of autophagy in the pathogenesis of amyotrophic lateral sclerosis. *Biochim Biophys Acta - Mol Basis Dis* 1852(11):2517–2524.
35. Zhang J, Liu Q (2015) Cholesterol metabolism and homeostasis in the brain. *Protein Cell* 6(4):254–264.
36. Liu L, et al. (2015) Glial lipid droplets and ROS induced by mitochondrial defects promote neurodegeneration. *Cell* 160(1–2):177–190.
37. Liu L, MacKenzie KR, Putluri N, Maletić-Savatić M, Bellen HJ (2017) The Glia-Neuron Lactate Shuttle and Elevated ROS Promote Lipid Synthesis in Neurons and Lipid Droplet Accumulation in Glia via APOE/D. *Cell Metab* 26(5):719–737.e6.
38. Jiménez-Riani M, et al. (2017) Ultrastructural features of aberrant glial cells isolated from the spinal cord of paralytic rats expressing the amyotrophic lateral sclerosis-linked SOD1G93A mutation. *Cell Tissue Res* 370(3):391–401.
39. Cluskey S, Ramsden DB (2001) Mechanisms of neurodegeneration in amyotrophic lateral sclerosis. *Mol Pathol* 54(6):386–92.
40. Shi P, Gal J, Kwinter DM, Liu X, Zhu H (2010) Mitochondrial dysfunction in

amyotrophic lateral sclerosis. *Biochim Biophys Acta* 1802(1):45–51.

41. Bowling a C, Schulz JB, Brown RH, Beal MF (1993) Superoxide dismutase activity, oxidative damage, and mitochondrial energy metabolism in familial and sporadic amyotrophic lateral sclerosis. *J Neurochem* 61(6):2322–2325.
42. Sasaki S, Horie Y, Iwata M (2007) Mitochondrial alterations in dorsal root ganglion cells in sporadic amyotrophic lateral sclerosis. *Acta Neuropathol* 114(6):633–639.
43. Schlame M, Rua D, Greenberg ML (2000) The biosynthesis and functional role of cardiolipin. *Prog Lipid Res* 39(3):257–288.
44. Horvath SE, Daum G (2013) Lipids of mitochondria. *Prog Lipid Res* 52(4):590–614.
45. Ohtsuka T, Nishijima M, Suzuki K, Akamatsu Y (1993) Mitochondrial dysfunction of a cultured Chinese hamster ovary cell mutant deficient in cardiolipin. *J Biol Chem* 268(30):22914–9.
46. Yoshinaga MY, Kellermann MY, Valentine DL, Valentine RC (2016) Phospholipids and glycolipids mediate proton containment and circulation along the surface of energy-transducing membranes. *Prog Lipid Res* 64:1–15.
47. Jaarsma D, et al. (2000) Human Cu/Zn superoxide dismutase (SOD1) overexpression in mice causes mitochondrial vacuolization, axonal degeneration, and premature motoneuron death and accelerates motoneuron disease in mice expressing a familial amyotrophic lateral sclerosis mutant SO. *Neurobiol Dis* 7(6):623–643.
48. Kong J, Xu Z (1998) Massive mitochondrial degeneration in motor neurons triggers the. *J Neurosci* 18(9):3241–3250.
49. So E, et al. (2017) Mitochondrial abnormalities and disruption of the neuromuscular junction precede the clinical phenotype and motor neuron loss in hFUSWT transgenic mice. *Hum Mol Genet* 27(3):463–474.
50. Siklós L, et al. (1996) Ultrastructural evidence for altered calcium in motor nerve terminals in amyotrophc lateral sclerosis. *Ann Neurol* 39(2):203–216.
51. Xu Y-F, et al. (2010) Wild-Type Human TDP-43 Expression Causes TDP-43 Phosphorylation, Mitochondrial Aggregation, Motor Deficits, and Early Mortality in Transgenic Mice. *J Neurosci* 30(32):10851–10859.
52. Fünfschilling U, et al. (2012) Glycolytic oligodendrocytes maintain myelin and long-term axonal integrity. *Nature* 485(7399):517–521.
53. Pellerin L, Magistretti PJ (1994) Glutamate uptake into astrocytes stimulates aerobic glycolysis: a mechanism coupling neuronal activity to glucose utilization. *Proc Natl Acad Sci* 91(22):10625–10629.

54. Bailey AP, et al. (2015) Antioxidant Role for Lipid Droplets in a Stem Cell Niche of Drosophila. *Cell* 163(2):340–353.

55. Panov A, Orynbayeva Z, Vavilin V, Lyakhovich V (2014) Fatty acids in energy metabolism of the central nervous system. *Biomed Res Int* 2014. doi:10.1155/2014/472459.

56. Schönfeld P, Reiser G (2013) Why does brain metabolism not favor burning of fatty acids to provide energy-Reflections on disadvantages of the use of free fatty acids as fuel for brain. *J Cereb Blood Flow Metab* 33(10):1493–1499.

Supporting information

Altered lipid metabolism in CNS reflecting increased oxidative stress in amyotrophic lateral sclerosis

Adriano B. Chaves-Filho[1], Marcos Y. Yoshinaga[1], Isabella F.D. Pinto[1], Lucas S. Dantas[1], Alex Inague[1], Rodrigo L. de Faria[1], Ohara Augusto[1], Isaías Glezer[2], Sayuri Miyamoto[1,*]

1. Supplementary figures and tables

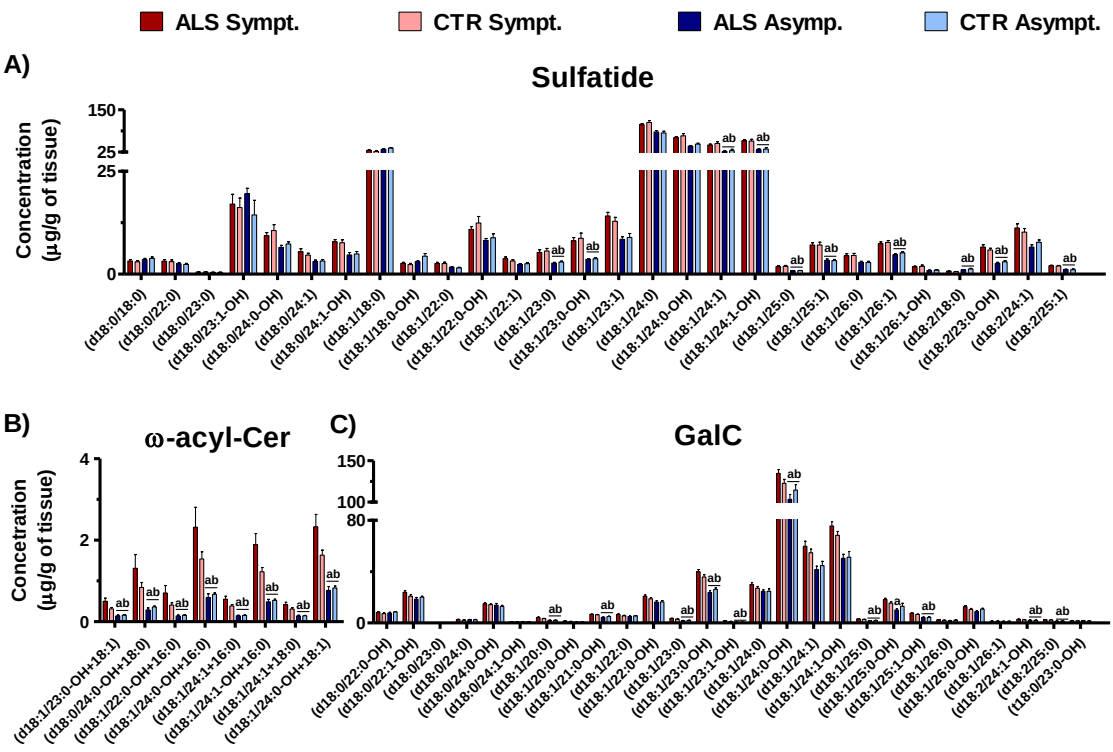

Figure S1. Lipid molecular species of sphingolipids altered in motor cortex of SOD1^{G93A} transgenic rat model. (A) Lipid molecular species of sulfatides. (B) Lipid molecular species of ω-acyl-ceramides. (C) Lipid molecular species of galactosylceramdide (GalC). Data are shown as the mean ± SEM. Statistical significance was evaluated by one way ANOVA fallowed by Turkey's post-test using Metaboanalyst ($p < 0.05$). a = different when compared to ALS symptomatic group; b = different when compared to CTR symptomatic group.

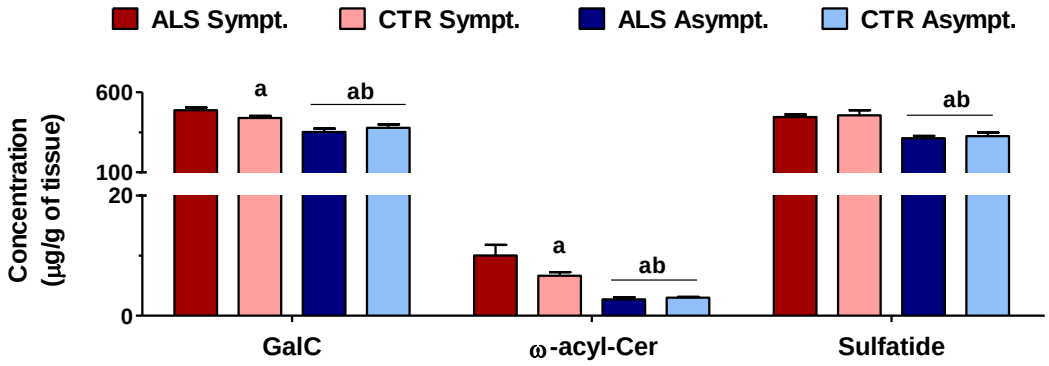

Figure S2. Total levels of the altered sphingolipids in motor cortex of SOD1^{G93A} transgenic rat model. Data are shown as the mean ± SEM. Statistical significance was evaluated by one way ANOVA fallowed by Turkey's post-test using Metaboanalyst ($p < 0.05$). a = different when compared to ALS symptomatic group; b = different when compared to CTR symptomatic group.

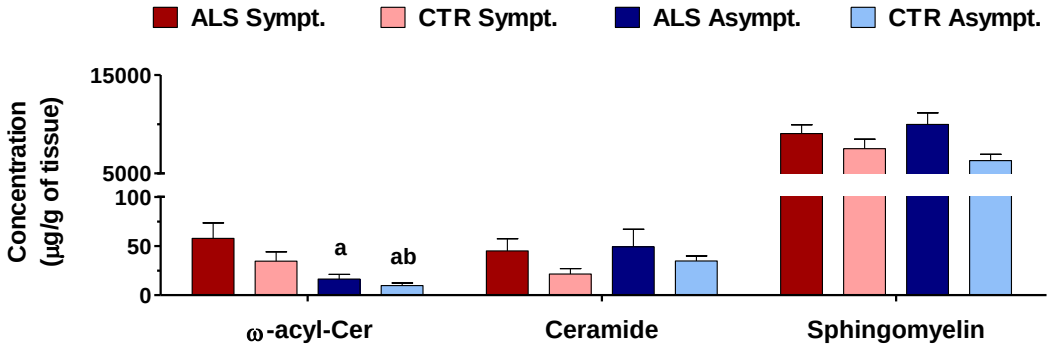

Figure S3. Total levels of the altered sphingolipids in spinal cord of SOD1^{G93A} transgenic rat model. Data are shown as the mean ± SEM. Statistical significance was evaluated by one way ANOVA fallowed by Turkey's post-test using Metaboanalyst ($p < 0.05$). a = different when compared to ALS symptomatic group; b = different when compared to CTR symptomatic group.

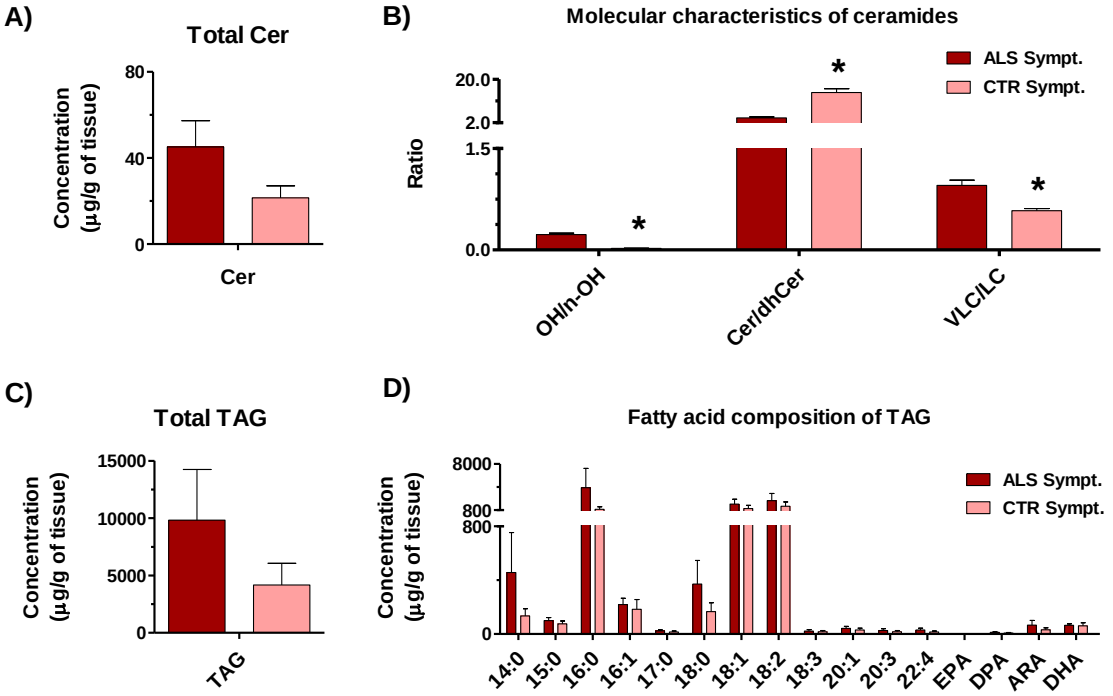

Figure S4. Profile of the altered ceramides and triacylglycerols in spinal cord of SOD1^{G93A} transgenic rat model. (A) Concentration of total ceramides. (B) Molecular characteristics of ceramides. (C) Concentration of total TAGs. (D) Fatty acid composition of TAGs. Data are shown as mean ± SEM. Statistical significance was evaluated by t-test ($p < 0.05$) using Metaboanalyst. (*) Different when compared to the ALS symptomatic group.

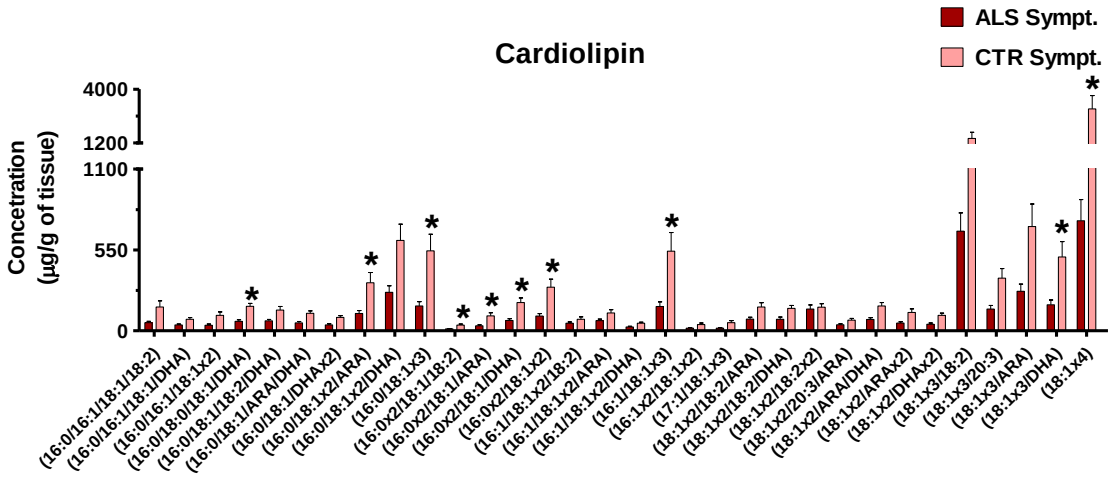

Figure S5. Lipid molecular species of cardiolipins in spinal cord of SOD1^{G93A} transgenic rat model. Data are shown as the mean ± SEM. Statistical significance was evaluated by one way ANOVA fallowed by Turkey's post-test using Metaboanalyst ($p < 0.05$). (*) Different when compared to ALS symptomatic group.

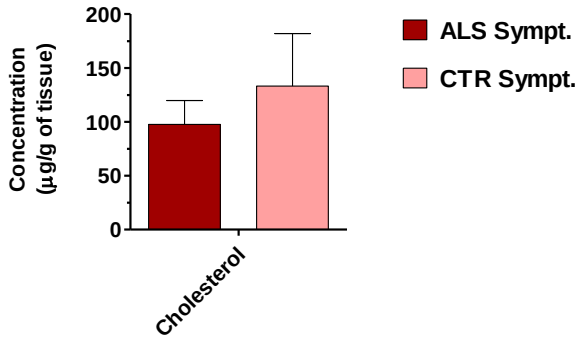

Figure S6. Levels of cholesterol in spinal cord of SOD1^{G93A} transgenic rat model. Data are shown as the mean ± SEM. Statistical significance was evaluated by t-test ($p < 0.05$) using Metaboanalyst. (*) Different when compared to ALS symptomatic group.

Supplementary Table 1. Internal Standard used for the semi quantification.

Internal Standard	Work concentration (ng/µL)	Quantified lipid classes
Cer (d18:1/10:0)	10	GalC, Cer, glycosylated ω-acyl-Cer
CL (14:0x4)	20	CL
LPC (17:0)	20	FFA, PC, pPC, oPC, PI, PE, Semino, 1G-AEG, Cholesterol, Cholesteryl ester, DAG, TAG, Coenzyme
Sulfatide (d18:1/17:0)	20	Sulfatide
PG (17:0/17:0)	20	PG
PS (17:0/17:0)	20	PS, pPS
SM (d18:1/17:0)	16	SM

FINAL REMARKS

Lipids encompass a wide range of biomolecules with putative cellular functions such as major components of membranes, energy reservoir and signaling pathways. Nonetheless, there is a staggering number of studies evidencing that lipid functions are as diverse as their huge structural variety (conservatively estimated at hundreds of thousand structures). In this context, mass spectrometry-based lipidomics analysis uncovering hundreds to thousands of individual molecular species of lipids has been deemed essential to allowing researchers to work at the boundaries of the "actual" lipid diversity. In this thesis, liquid chromatography coupled to mass spectrometry (UHPLC-MS/MS) was applied to investigate the mechanisms involved in thiol modification by autoxidation products derived from PUFAs (Chapter 1) and to study lipid metabolism alterations in the CNS of a rodent model of amyotrophic lateral sclerosis (ALS) (Chapter 2).

In Chapter 1, several glutathione (GSH) adducts covalently modified by hydroxy-endoperoxides derived from DHA and ARA, two of the most abundant PUFAs in mammals, were discovered. Detailed inspection of MS/MS spectra of GSH-adducts revealed that GSH and hydroxy-endoperoxides are bonded through a labile sulfur-oxygen chemical bond. We suggest that the reaction between GSH and hydroxy-endoperoxides involves a nucleophilic attack by the thiolate anion. In further experiments performed with SOD1 protein and n-acetyl cysteine (NAC), modification in the cysteine residue (SOD1-Cys111) by penta-oxygenated AA-(O5) and formation of NAC-adducts with DHA, respectively, support the idea that reactive thiols in proteins could be modified by the hydroxy-endoperoxides. Collectively, our findings bear evidence of chemical modifications of thiol groups induced by hydroxy-endoperoxides, which may modulate the formation of GSH conjugates, protein aggregation and cellular redox status.

Thus far, the great majority of studies has been focusing on enzymatically oxidized PUFAs rather than autoxidation, specially in inflammation. In a broader perspective, because DHA and ARA are highly enriched in the CNS and oxidative stress is constantly implicated in neurodegenerative diseases, cyclic products derived from PUFAs autoxidation may be important modulators of thiol-based signaling pathways involved in neurodegeneration. As reported for LTC4 (sulfide conjugate derived from ARA) (Liu and Yokomizo 1970) and MCTR1 (sulfide conjugate derived from DHA) (Dalli *et al*. 2014), modification of thiol groups by hydroxy-endoperoxides either derived from n-6 or n-3 PUFAs may represent a double edged sword for cellular homeostasis, triggering biological effects linked to cell survival or even death (e.g. inflammatory or anti-inflammatory mediators). In this respect, increasing the synthetic yield of hydroxy-endoperoxides and adducts is required for testing the biological activity of these molecules. For instance, cell cultures of macrophages and microglia could be used to assess the role of GSH-adducts in inflammatory processes. Moreover, as lipid peroxidation has been linked to aging and neurodegeneration, it would be interesting to probe the presence of GSH adducts in brain tissues of aged symptomatic subjects.

In chapter 2, untargeted analysis performed by UHPLC-MS/MS and manual lipid identification based on retention time and MS/MS profile of lipids, allowed us to characterize the lipidome of motor cortex and spinal cord of SOD1G93A rats, a model for ALS. Analysis of the motor cortex showed that the main lipid alterations were age-dependent and mostly linked to metabolism of sphingolipids. In contrast, lipidomics analysis performed in spinal cord tissues revealed major alterations in the levels of cholesteryl esters and cardiolipin in ALS symptomatic rats. According to these findings and data reported in the literature (Liu *et al*. 2015), a mechanism is proposed involving neuroprotection by accumulation of cholesteryl esters esterified to PUFAs in astrocytes as a response to elevated ROS in neurons during ALS.

In studies performed in models of Alzheimer's disease (AD), it was suggested that inhibiting the synthesis of cholesteryl esters via ACAT could be a target for treatment (Bryleva *et al*. 2010). The proposed mechanism evidenced in this thesis may put a new spin into this story, in that any perturbation of the lipid transport between neurons and glial cells for neuroprotection may rather result in augmented neurodegeneration. That is, accumulation of free fatty acids or cholesterol in neurons may stimulate beta-oxidation, which in turn may increase the generation of ROS.

It will be interesting to test whether neuroprotection via neuron-glia transport of cholesteryl ester. Currently under investigation by our lab, we have analyzed the pre-frontal cortex of 3-, 18- and 24-months old rats (data not shown). The unpublished results obtained so far revealed increased amounts of sphingolipids and cholesteryl esters in 18- and 24-months old animals, similar to the results reported in Chapter 2. Future investigations using cells such as neurons and astrocytes lineages and primary cultures may help deciphering the role of lipid metabolism in the CNS in response to elevated oxidative stress. Nonetheless, it is worth highlighting that a precise analysis of molecular species by lipidomics analysis, including peroxidation products of PUFAs, is strongly required to further knowledge in the mechanisms involved in lipidome alterations in aging and neurodegenerative diseases.

REFERENCES

Adibhatla RM, Hatcher JF (2007) Role of lipids in brain injury and diseases. Future Lipidol 2:403–422. doi: 10.2217/17460875.2.4.403

Aggarwal S, Yurlova L, Simons M (2011) Central nervous system myelin: Structure, synthesis and assembly. Trends Cell Biol 21:585–593. doi: 10.1016/j.tcb.2011.06.004

Almer G, Teismann P, Stevic Z, et al (2002) Increased levels of the pro-inflammatory prostaglandin PGE2 in CSF from ALS patients. Neurology 58:1277–1279

Andersen JK (2004) Oxidative stress in neurodegeneration: Cause or consequence? Nat Rev Neurosci 10:S18. doi: 10.1038/nrn1434

Appolinário PP, Medinas DB, Chaves-Filho AB, et al (2015) Oligomerization of Cu,Zn-superoxide dismutase (SOD1) by Docosahexaenoic acid and its hydroperoxides in vitro: Aggregation dependence on fatty acid unsaturation and thiols. PLoS One 10:1–15. doi: 10.1371/journal.pone.0125146

Arima H, Omura T, Hayasaka T, et al (2015) Reductions of docosahexaenoic acid-containing phosphatidylcholine levels in the anterior horn of an ALS mouse model. Neuroscience 297:127–136. doi: 10.1016/j.neuroscience.2015.03.060

Balsinde J, Balboa MA (2005) Cellular regulation and proposed biological functions of group VIA calcium-independent phospholipase A2in activated cells. Cell Signal 17:1052–1062. doi: 10.1016/j.cellsig.2005.03.002

Barber SC, Mead RJ, Shaw PJ (2006) Oxidative stress in ALS: A mechanism of neurodegeneration and a therapeutic target. Biochim Biophys Acta - Mol Basis Dis 1762:1051–1067. doi: 10.1016/j.bbadis.2006.03.008

Bazan NG, Calandria JM, Serhan CN (2010) Rescue and repair during photoreceptor cell renewal mediated by docosahexaenoic acid-derived neuroprotectin D1. J Lipid Res 51:2018–2031. doi: 10.1194/jlr.R001131

Bezzi P, Carmignoto G, Pasti L, et al (1998) Prostaglandins stimulate calcium-dependent glutamate release in astrocytes. Nature 391:281–285. doi: 10.1038/34651

Blasco H, Veyrat-Durebex C, Bocca C, et al (2017) Lipidomics Reveals Cerebrospinal-Fluid Signatures of ALS. Sci Rep 7:1–10. doi: 10.1038/s41598-017-17389-9

Bruijn LI, Miller TM, Cleveland W (2004) UNRAVELING THE MECHANISMS INVOLVED IN MOTOR NEURON DEGENERATION IN ALS. Annu Rev Neurosci 27:723–49. doi: 10.1146/annurev.neuro.27.070203.144244

Bryleva EY, Rogers MA, Chang CCY, et al (2010) ACAT1 gene ablation increases 24(S)-

hydroxycholesterol content in the brain and ameliorates amyloid pathology in mice with AD. Proc Natl Acad Sci 107:3081–3086. doi: 10.1073/pnas.0913828107

Carrasco-Pancorbo A, Navas-Iglesias N, Cuadros-Rodríguez L (2009) From lipid analysis towards lipidomics, a new challenge for the analytical chemistry of the 21st century. Part I: Modern lipid analysis. TrAC - Trends Anal Chem 28:263–278. doi: 10.1016/j.trac.2008.12.005

Catalá A (2009) Lipid peroxidation of membrane phospholipids generates hydroxy-alkenals and oxidized phospholipids active in physiological and/or pathological conditions. Chem Phys Lipids 157:1–11. doi: 10.1016/j.chemphyslip.2008.09.004

Chen WW, Zhang X, Huang WJ (2016) Role of neuroinflammation in neurodegenerative diseases (Review). Mol Med Rep 13:3391–3396. doi: 10.3892/mmr.2016.4948

Chrissobolis S, Faraci F (2008) The role of oxidative stress and NADPH oxidase in cerebrovascular disease. 14:495–502. doi: 10.1109/TMI.2012.2196707.Separate

Circu ML, Aw TY (2010) Reactive oxygen species, cellular redox systems, and apoptosis. Free Radic Biol Med 48:749–762. doi: 10.1016/j.freeradbiomed.2009.12.022

Cnop M, Hannaert JC, Hoorens A, et al (2001) Inverse relationship between cytotoxicity of free fatty acids in pancreatic islet cells and cellular triglyceride accumulation. Diabetes 50:1771–7. doi: 10.2337/diabetes.50.8.1771

Cutler RG, Pedersen WA, Camandola S, et al (2002) Evidence that accumulation of ceramides and cholesterol esters mediates oxidative stress - Induced death of motor neurons in amyotrophic lateral sclerosis. Ann Neurol 52:448–457. doi: 10.1002/ana.10312

Dalli J, Chiang N, Serhan CN (2014) Identification of 14-series sulfido-conjugated mediators that promote resolution of infection and organ protection. Proc Natl Acad Sci 111:E4753–E4761. doi: 10.1073/pnas.1415006111

Dalli J, Vlasakov I, Riley IR, et al (2016) Maresin conjugates in tissue regeneration biosynthesis enzymes in human macrophages. Proc Natl Acad Sci 113:12232–12237. doi: 10.1073/pnas.1607003113

Dodge JC, Treleaven CM, Pacheco J, et al (2015) Glycosphingolipids are modulators of disease pathogenesis in amyotrophic lateral sclerosis. Proc Natl Acad Sci 112:8100–8105. doi: 10.1073/pnas.1508767112

Drachman DB, Frank K, Dykes-Hoberg M, et al (2002) Cyclooxygenase 2 inhibition protects motor neurons and prolongs survival in a transgenic mouse model of ALS. Ann Neurol 52:771–778. doi: 10.1002/ana.10374

Dunbar BS, Bosire RV, Deckelbaum RJ (2014) Omega 3 and omega 6 fatty acids in human and animal health: An African perspective. Mol Cell Endocrinol 398:69–77. doi: 10.1016/j.mce.2014.10.009

Dupree JL, Pomicter AD (2010) Myelin, DIGs, and membrane rafts in the central nervous system. Prostaglandins Other Lipid Mediat 91:118–129. doi: 10.1016/j.prostaglandins.2009.04.005

Fahy E, Subramaniam S, Brown HA, et al (2005) A comprehensive classification system for lipids. J Lipid Res 46:839–862. doi: 10.1194/jlr.E400004-JLR200

Fahy E, Subramaniam S, Murphy RC, et al (2009) Update of the LIPID MAPS comprehensive classification system for lipids. J Lipid Res 50:S9–S14. doi: 10.1194/jlr.R800095-JLR200

Finkel T, Holbrook NJ (2000) Oxidants, oxidative stress and the biology of ageing. Nature 408:239–247. doi: 10.1038/35041687

Forman BM, Chen J, Evans RM (1997) Hypolipidemic drugs, polyunsaturated fatty acids, and eicosanoids are ligands for peroxisome proliferator-activated receptors and . Proc Natl Acad Sci 94:4312–4317. doi: 10.1073/pnas.94.9.4312

Fra A, Yoboue ED, Sitia R (2017) Cysteines as Redox Molecular Switches and Targets of Disease. Front Mol Neurosci 10:1–9. doi: 10.3389/fnmol.2017.00167

Fukai T, Ushio-Fukai M (2011) Superoxide Dismutases: Role in Redox Signaling, Vascular Function, and Diseases. Antioxid Redox Signal 15:1583–1606. doi: 10.1089/ars.2011.3999

Galano JM, Lee JCY, Gladine C, et al (2015) Non-enzymatic cyclic oxygenated metabolites of adrenic, docosahexaenoic, eicosapentaenoic and α-linolenic acids; Bioactivities and potential use as biomarkers. Biochim Biophys Acta - Mol Cell Biol Lipids 1851:446–455. doi: 10.1016/j.bbalip.2014.11.004

García-Ramírez M, Francisco G, García-Arumí E, et al (2008) Mitochondrial DNA oxidation and manganese superoxide dismutase activity in peripheral blood mononuclear cells from type 2 diabetic patients. Diabetes Metab 34:117–124. doi: 10.1016/j.diabet.2007.10.011

Garthwaite J, Boulton CL (1995) Nitric Oxide Signaling in the Central Nervous System. Annu Rev Physiol 57:683–706. doi: 10.1146/annurev.ph.57.030195.003343

Gaschler MM, Stockwell BR (2017) Lipid peroxidation in cell death. Biochem Biophys Res Commun 482:419–425. doi: 10.1016/j.bbrc.2016.10.086

Groeger AL, Cipollina C, Cole MP, et al (2010) Cyclooxygenase-2 generates anti-

inflammatory mediators from omega-3 fatty acids. Nat Chem Biol 6:433–441. doi: 10.1038/nchembio.367

Gros-Louis F, Gaspar C, Rouleau GA (2006) Genetics of familial and sporadic amyotrophic lateral sclerosis. Biochim Biophys Acta - Mol Basis Dis 1762:956–972. doi: 10.1016/j.bbadis.2006.01.004

Grösch S, Schiffmann S, Geisslinger G (2012) Chain length-specific properties of ceramides. Prog Lipid Res 51:50–62. doi: 10.1016/j.plipres.2011.11.001

Halliwell B (2006) Oxidative stress and neurodegeneration: Where are we now? J Neurochem 97:1634–1658. doi: 10.1111/j.1471-4159.2006.03907.x

Han X, Gross RW (2005) Shotgun lipidomics: Electrospray ionization mass spectrometric analysis and quantitation of cellular lipidomes directly from crude extracts of biological samples. Mass Spectrom Rev 24:367–412. doi: 10.1002/mas.20023

Hannun YA, Obeid LM (2008) Principles of bioactive lipid signalling: Lessons from sphingolipids. Nat Rev Mol Cell Biol 9:139–150. doi: 10.1038/nrm2329

Hansen RE, Winther JR (2009) An introduction to methods for analyzing thiols and disulfides: Reactions, reagents, and practical considerations. Anal Biochem 394:147–158. doi: 10.1016/j.ab.2009.07.051

Harayama T, Riezman H (2018) Understanding the diversity of membrane lipid composition. Nat Rev Mol Cell Biol. doi: 10.1038/nrm.2017.138

Hauck AK, Bernlohr DA (2016) Oxidative Stress and Lipotoxicity. J Lipid Res 1–37

Henriques A, Croixmarie V, Priestman DA, et al (2015) Amyotrophic lateral sclerosis and denervation alter sphingolipids and up-regulate glucosylceramide synthase. Hum Mol Genet 24:7390–7405. doi: 10.1093/hmg/ddv439

Hishikawa D, Hashidate T, Shimizu T, Shindou H (2014) Diversity and function of membrane glycerophospholipids generated by the remodeling pathway in mammalian cells. J Lipid Res 55:799–807. doi: 10.1194/jlr.R046094

Jaarsma D, Haasdijk ED, Grashorn JAC, et al (2000) Human Cu/Zn superoxide dismutase (SOD1) overexpression in mice causes mitochondrial vacuolization, axonal degeneration, and premature motoneuron death and accelerates motoneuron disease in mice expressing a familial amyotrophic lateral sclerosis mutant SO. Neurobiol Dis 7:623–643. doi: 10.1006/nbdi.2000.0299

Kim HY, Huang BX, Spector AA (2014) Phosphatidylserine in the brain: Metabolism and function. Prog Lipid Res 56:1–18. doi: 10.1016/j.plipres.2014.06.002

Lehner R, Kuksis A (1996) Biosynthesis of triacylglycerols. Prog Lipid Res 35:169–201. doi:

10.1016/0163-7827(96)00005-7

Leonard AE, Pereira SL, Sprecher H, Huang YS (2004) Elongation of long-chain fatty acids. Prog Lipid Res 43:36–54. doi: 10.1016/S0163-7827(03)00040-7

Leonarduzzi G, Arkan MC, Başağa H, et al (2000) Lipid oxidation products in cell signaling. Free Radic Biol Med 28:1370–1378. doi: 10.1016/S0891-5849(00)00216-1

Liu D, Wen J, Liu J, Li L (1999) The roles of free radicals in amyotrophic lateral sclerosis: reactive oxygen species and elevated oxidation of protein, DNA, and membrane phospholipids. FASEB J 13:2318–2328

Liu L, Komatsu H, Murray IVJ, Axelsen PH (2008) Promotion of Amyloid β Protein Misfolding and Fibrillogenesis by a Lipid Oxidation Product. J Mol Biol 377:1236–1250. doi: 10.1016/j.jmb.2008.01.057

Liu L, Zhang K, Sandoval H, et al (2015) Glial lipid droplets and ROS induced by mitochondrial defects promote neurodegeneration. Cell 160:177–190. doi: 10.1016/j.cell.2014.12.019

Liu M, Yokomizo T (1970) The role of leukotrienes in allergic diseases. Allergol Int 64:17–26. doi: 10.1016/j.alit.2014.09.001

Lutjohann D, von Bergmann K (2003) 24S-Hydroxycholesterol: a Marker of Brain Cholesterol Metabolism. Pharmacopsychiatry 36:102–106. doi: 10.1055/s-2003-43053

Maulucci G, Cohen O, Daniel B, et al (2016) Fatty acid-related modulations of membrane fluidity in cells: detection and implications. Free Radic Res 50:S40–S50. doi: 10.1080/10715762.2016.1231403

Mehta P, Kaye W, Bryan L, et al (2016) Prevalence of Amyotrophic Lateral Sclerosis — United States, 2012–2013. MMWR Surveill Summ 65:1–12. doi: 10.15585/mmwr.ss6508a1

Merrill AH (2008) Sphingolipids. Biochem Lipids, Lipoproteins Membr 6:282–283. doi: 10.1016/B978-0-444-53219-0.50015-5

Miller TA, LeBrasseur NK, Cote GM, et al (2005) Oleate prevents palmitate-induced cytotoxic stress in cardiac myocytes. Biochem Biophys Res Commun 336:309–315. doi: 10.1016/j.bbrc.2005.08.088

Murphy MP, Holmgren A, Larsson NG, et al (2011) Unraveling the biological roles of reactive oxygen species. Cell Metab 13:361–366. doi: 10.1016/j.cmet.2011.03.010

Naini A, Musumeci O, Hayes L, et al (2002) Identification of a novel mutation in Cu/Zn superoxide dismutase gene associated with familial amyotrophic lateral sclerosis. J Neurol Sci 198:17–19

Niki E (2009) Lipid peroxidation: Physiological levels and dual biological effects. Free Radic Biol Med 47:469–484. doi: 10.1016/j.freeradbiomed.2009.05.032

Paradies G, Paradies V, De Benedictis V, et al (2014) Functional role of cardiolipin in mitochondrial bioenergetics. Biochim Biophys Acta - Bioenerg 1837:408–417. doi: 10.1016/j.bbabio.2013.10.006

Payne AH, Hales DB (2004) Overview of steroidogenic enzymes in the pathway from cholesterol to active steroid hormones. Endocr Rev 25:947–970. doi: 10.1210/er.2003-0030

Pedersen W, Fu W, Keller J (1998) Protein modification by the lipid peroxidation product 4-hydroxynonenal in the spinal cords of amyotrophic lateral sclerosis patients. Ann 819–824. doi: 10.1002/ana.410440518

Perluigi M, Poon HF, Hensley K, et al (2005) Proteomic analysis of 4-hydroxy-2-nonenal-modified proteins in G93A-SOD1 transgenic mice - A model of familial amyotrophic lateral sclerosis. Free Radic Biol Med 38:960–968. doi: 10.1016/j.freeradbiomed.2004.12.021

Phillis JW, Horrocks LA, Farooqui AA (2006) Cyclooxygenases, lipoxygenases, and epoxygenases in CNS: Their role and involvement in neurological disorders. Brain Res Rev 52:201–243. doi: 10.1016/j.brainresrev.2006.02.002

Pierpaoli W (2005) Neurodegenerative diseases: A common etiology and a common therapy. Ann N Y Acad Sci 1057:319–326. doi: 10.1196/annals.1356.024

Poon HF, Calabrese V, Scapagnini G, Butterfield DA (2004) Free radicals and brain aging. Clin Geriatr Med 20:329–359. doi: 10.1016/j.cger.2004.02.005

Poudyal H, Panchal SK, Diwan V, Brown L (2011) Omega-3 fatty acids and metabolic syndrome: Effects and emerging mechanisms of action. Prog Lipid Res 50:372–387. doi: 10.1016/j.plipres.2011.06.003

Pruett ST, Bushnev A, Hagedorn K, et al (2008) *Thematic Review Series: Sphingolipids.* Biodiversity of sphingoid bases (“sphingosines”) and related amino alcohols. J Lipid Res 49:1621–1639. doi: 10.1194/jlr.R800012-JLR200

Pulfer M, Murphy RC (2003) Electrospray mass spectrometry of phospholipids. Mass Spectrom Rev 22:332–364. doi: 10.1002/mas.10061

Quehenberger O, Armando AM, Dennis EA (2011) High sensitivity quantitative lipidomics analysis of fatty acids in biological samples by gas chromatography-mass spectrometry. Biochim Biophys Acta - Mol Cell Biol Lipids 1811:648–656. doi: 10.1016/j.bbalip.2011.07.006

Ricciotti E, Fitzgerald GA (2011) Prostaglandins and inflammation. Arterioscler Thromb Vasc Biol 31:986–1000. doi: 10.1161/ATVBAHA.110.207449

Robertson RP, Harmon J, Tran POT, Poitout V (2004) Oxidative Stress in Type 2 Diabetes. Diabetes 2004 53:

Schink KO, Raiborg C, Stenmark H (2013) Phosphatidylinositol 3-phosphate, a lipid that regulates membrane dynamics, protein sorting and cell signalling. BioEssays 35:900–912. doi: 10.1002/bies.201300064

Schneider C, Pratt DA, Porter NA, Brash AR (2007) Control of Oxygenation in Lipoxygenase and Cyclooxygenase Catalysis. Chem Biol 14:473–488. doi: 10.1016/j.chembiol.2007.04.007

Schönfeld P, Reiser G (2013) Why does brain metabolism not favor burning of fatty acids to provide energy-Reflections on disadvantages of the use of free fatty acids as fuel for brain. J Cereb Blood Flow Metab 33:1493–1499. doi: 10.1038/jcbfm.2013.128

Schwartz CC, VandenBroek JM, Cooper PS (2004) Lipoprotein cholesteryl ester production, transfer, and output in vivo in humans. J Lipid Res 45:1594–1607. doi: 10.1194/jlr.M300511-JLR200

Serhan CN (2014) Pro-resolving lipid mediators are leads for resolution physiology. Nature 510:92–101. doi: 10.1038/nature13479

Serhan CN, Dalli J, Karamnov S, et al (2012) Macrophage proresolving mediator maresin 1 stimulates tissue regeneration and controls pain. FASEB J 26:1755–1765. doi: 10.1096/fj.11-201442

Siddiqui RA, Harvey K, Stillwell W (2008) Anticancer properties of oxidation products of docosahexaenoic acid. Chem Phys Lipids 153:47–56. doi: 10.1016/j.chemphyslip.2008.02.009

Spiteller G (2006) Peroxyl radicals: Inductors of neurodegenerative and other inflammatory diseases. Their origin and how they transform cholesterol, phospholipids, plasmalogens, polyunsaturated fatty acids, sugars, and proteins into deleterious products. Free Radic Biol Med 41:362–387. doi: 10.1016/j.freeradbiomed.2006.03.013

Stockwell BR, Friedmann Angeli JP, Bayir H, et al (2017) Ferroptosis: A Regulated Cell Death Nexus Linking Metabolism, Redox Biology, and Disease. Cell 171:273–285. doi: 10.1016/j.cell.2017.09.021

Ursini F, Maiorino M, Valente M, et al (1982) Purification from pig liver of a protein which protects liposomes and biomembranes from peroxidative degradation and exhibits glutathione peroxidase activity on phosphatidylcholine hydroperoxides. Biochim

Biophys Acta (BBA)/Lipids Lipid Metab 710:197–211. doi: 10.1016/0005-2760(82)90150-3

Valentine J, Doucette P, Potter S (2005) Copper-zinc superoxide dismutase and amyotrophic lateral sclerosis. Annu Rev Biochem 74:563–593. doi: 10.1146/annurev.biochem.72.121801.161647

Valko M, Leibfritz D, Moncol J, et al (2007) Free radicals and antioxidants in normal physiological functions and human disease. Int J Biochem Cell Biol 39:44–84. doi: 10.1016/j.biocel.2006.07.001

Valle C, Carrì MT (2017) Cysteine Modifications in the Pathogenesis of ALS. Front Mol Neurosci 10:1–8. doi: 10.3389/fnmol.2017.00005

Van Meer G, Voelker DR, Feigenson GW (2008) Membrane lipids: Where they are and how they behave. Nat Rev Mol Cell Biol 9:112–124. doi: 10.1038/nrm2330

Vandoorne T, De Bock K, Van Den Bosch L (2018) Energy metabolism in ALS: an underappreciated opportunity? Acta Neuropathol 135:489–509. doi: 10.1007/s00401-018-1835-x

Wang Y, Armando AM, Quehenberger O, et al (2014) Comprehensive ultra-performance liquid chromatographic separation and mass spectrometric analysis of eicosanoid metabolites in human samples. J Chromatogr A 1359:60–69. doi: 10.1016/j.chroma.2014.07.006

Warnick GR (1986) Enzymatic Methods for Quantification of Lipoprotein Lipids. Methods Enzymol 129:101–123. doi: 10.1016/0076-6879(86)29064-3

Wenk MR (2005) The emerging field of lipidomics. Nat Rev Drug Discov 4:594–610. doi: 10.1038/nrd1776

Wenk MR (2010) Lipidomics: New tools and applications. Cell 143:888–895. doi: 10.1016/j.cell.2010.11.033

Winterbourn CC, Hampton MB (2008) Thiol chemistry and specificity in redox signaling. Free Radic Biol Med 45:549–561. doi: 10.1016/j.freeradbiomed.2008.05.004

Wymann MP, Schneiter R (2008) Lipid signalling in disease. Nat Rev Mol Cell Biol 9:162–176. doi: 10.1038/nrm2335

Yamashita A, Hayashi Y, Nemoto-Sasaki Y, et al (2014) Acyltransferases and transacylases that determine the fatty acid composition of glycerolipids and the metabolism of bioactive lipid mediators in mammalian cells and model organisms. Prog Lipid Res 53:18–81. doi: 10.1016/j.plipres.2013.10.001

Yang WS, Stockwell BR (2016) Ferroptosis: Death by Lipid Peroxidation. Trends Cell Biol

26:165–176. doi: 10.1016/j.tcb.2015.10.014

Yin H, Xu L, Porter NA (2011) Free Radical Lipid Proxidation: Mechanisms and Analysis. Chem Rev 111:5944–5972. doi: 10.1021/cr200084z

Yuan L, Kaplowitz N (2009) Glutathione in liver diseases and hepatotoxicity. Mol Aspects Med 30:29–41. doi: 10.1016/j.mam.2008.08.003

CURRICULUM VITAE

Personal data

Name: Adriano de Britto Chaves Filho

Birth and place: September 17th 1990, in Aracaju (Brazil)

E-mail: adrianobcfilho@usp.br

Current occupation: PhD student – Biological Sciences (Biochemistry), Universidade de São Paulo (São Paulo, SP), with scholarship from Conselho Nacional de Desenvolvimento Científico e tecnológico (CNPq).

Education

2013 – present: PhD student – Biological Sciences (Biochemistry), Universidade de São Paulo (São Paulo, SP). Advisor: Dra. Sayuri Miyamoto

2008 – 2013: Bachelor in Pharmacy. Universidade Federal de Sergipe (Aracaju, SE).

Complementary education

2015 – 2015: Extensão universitária em Summer Research Program in Tsukuba. (Carga horária: 72h). University of Tsukuba, Japão.

2015 – 2015: 8º Curso de Interação clínico-laboratorial. (Carga horária: 14h). Instituto Israelita de Ensino e Pesquisa Albert Einstein, Brasil.

2015 – 2015: Controle de Qualidade em Química Especial. (Carga horária: 5h). Instituto Israelita de Ensino e Pesquisa Albert Einstein, Brasil.

2015 – 2015: Redox Chemistry and Biology of Thiols. (Carga horária: 72h). International Centre for Genetic Engineering and Biotechnology, Uruguai.

2015 – 2015: Treinamento do Sistema LC/MS/MS SCIEX TripleTOF® 6600. (Carga horária: 40h). Sciex, Brasil.

2014 – 2014: Processos Redox em Biomedicina. (Carga horária: 6h). Sociedade Brasileira de Bioquímica e Biologia Molecular, SBBQ, Brasil.

2012 – 2012: Extensão universitária em VII Curso de Verão em Bioquímica e Biologia Molecular. (Carga horária: 80h). Universidade de São Paulo, USP, Brasil.

2012 – 2012: Curso Básico sobre HPLC. (Carga horária: 9h). Universidade Federal de Sergipe, UFS, Brasil.

2009 – 2013: Iniciação científica. Universidade Federal de Sergipe, UFS, Brasil.

Awards

- University of Tsukuba (Japan) - Student Travel Award 2015 to attend the course "Summer Research program in Tsukuba 2015" for Master's program in Medical Sciences (2015).
- International Centre for Genetic Engineering and Biotechnology (Uruguay) - Student Travel Award 2015 to attend the course "Redox Chemistry and Biology thiols" and symposium "Thiol Metabolism and redox Regulation of Cellular Functions" (2015).

Publications

1. Mies, M.; **Chaves-Filho, A. B.**; Miyamoto, S; Güth, A; Tenório, A; Castro, C; Pires, D; Calderón, E; Sumida, P. **(2017)** Production of three symbiosis-related fatty acids by Symbiodinium types in clades A–F associated with marine invertebrate larvae. *Coral Reefs* 36(4): 1319-1328. (doi: 10.1007/s00338-017-1627-0).

2. Chimin, P; Andrade, M; Belchior, T; Paschoal, V; Magdalon, J; Yamashita, A; Castro, E; Castoldi, A; **Chaves-Filho, A**; Yoshinaga, M; Miyamoto, S; Camara, N; Festuccia, W. **(2017)** Adipocyte mTORC1 deficiency promotes adipose tissue inflammation and NLRP3 inflammasome activation via oxidative stress and de novo ceramide synthesis. *Journal of Lipid Research* 58: 1797-1807. (doi: 10.1194/jlr.M074518).

3. Bispo, V; Dantas, L ; **Chaves-Filho, A**; Pinto, I; Silva, R; Otsuka, F; Santos, R; Santos, A; Trindade, D; Matos, H. **(2017)** Reduction of the DNA damages, Hepatoprotective Effect and Antioxidant Potential of the Coconut Water, ascorbic and Caffeic Acids in Oxidative Stress Mediated by Ethanol. *Annals of the Brazilian Academy of Sciences* 89(2): 1095-1109 (doi: 10.1590/0001-3765201720160581).

4. Galvão, J; Trindade, G; Santos, A; Santos, R; **Chaves-Filho, A**; Lira, A; Miyamoto, S; Nunes, R. **(2016)** Effect of Ouratea sp. butter in the crystallinity of solid lipids used in nanostructured lipid carriers (NLCs). *Journal of Thermal Analysis and Calorimetry* 123: 941-948 (doi: 10.1007/s10973-015-4890-8).

5. Belchior, T; Paschoal, V; Magdalon, J; Chimin, P; Farias, T; **Chaves-Filho, A**; Gorjão, R; St.-pierre, P; Miyamoto, S; Kang, J; Deshaies, Y; Marette, A; Festuccia, W. **(2015)** Omega-3 fatty acids protect from diet-induced obesity, glucose intolerance, and adipose tissue inflammation through PPARγ-dependent and PPARγ-independent actions. *Molecular Nutrition & Food Research* 59: 957-967 (doi: 10.1002/mnfr.201400914).

6. Appolinário, P; Medinas, D; **Chaves-Filho, A**; Genaro-Mattos, T; Cussiol, J; Netto, L; Augusto, O; Miyamoto, S. **(2015)** Oligomerization of Cu,Zn-Superoxide Dismutase (SOD1)

by Docosahexaenoic Acid and Its Hydroperoxides In Vitro: Aggregation Dependence on Fatty Acid Unsaturation and Thiols. *Plos One* 10(4): e0125146 (doi: 10.1371/journal.pone.0125146).

7. Pinto, I; Silva, R; **Chaves-Filho, A**; Dantas, L; Bispo, V; Matos, I; Otsuka, F; Santos, A; Matos, H. **(2015)** Study of Antiglycation, Hypoglycemic, and Nephroprotective Activities of the Green Dwarf Variety Coconut Water (*Cocos nucifera* L.) in Alloxan-Induced Diabetic Rats. *Journal of Medicinal Food* 18(7): 802-809 (doi: 10.1007/s10973-015-4890-8).

8. Santos, J; Bispo, V; **Chaves-Filho, A**; Pinto, I; Dantas, L; Vasconcelos, D; Abreu, F; Melo, D; Matos, I; Freitas, F; Gomes, O; Medeiros, M; Matos, H. **(2013)** Evaluation of Chemical Constituents and Antioxidant Activity of Coconut Water (*Cocus nucifera* L.) and Caffeic Acid in Cell Culture. *Annals of the Brazilian Academy of Sciences* 85(4): 1235-1246 (doi: 10.1590/0001-37652013105312).

Participation in scientific events

2017 - 15th Euro Fed Lipid Congress and Expo (Suécia).

2016 - 23rd Annual Meeting of Society for Redox Biology and Medicine (Estados Unidos).

2015 - International Symposium on Dietary Antioxidants and Oxidative Stress in Health (Japão).

2015 - Thiol Metabolism and Redox Regulation of Cellular Functions (Uruguai).

2014 - 1st Workshop on Redox Processes in Biochemistry (Brasil).

2014 - 1ª Escola Brasileira de Espectrometria de Massas (Brasil).

2014 - IX Simpósio Lipídeos e Saúde (Brasil).

2014 - Mini-Symposium on Singlet Oxygen (Brasil).

2014 - XLIII Annual Meeting of the Brazilian Biochemistry and Molecular Biology Society (Brasil).

2013 - Antioxidants and Redox Process in Health (Brasil).

2013 - XLII Annual Meeting of the Brazilian Biochemistry and Molecular Biology Society (Brasil).

2012 - XLI Annual Meeting of the Brazilian Biochemistry and Molecular Biology Society (Brasil).

2011 - 1° Workshop Brasileiro de Tecnologia Farmacêutica e Inovação (Brasil).

2011 - V Simpósio Sergipano de Microbiologia e I Encontro de Controle de Qualidade Microbiológica (Brasil).

2011 - XL Annual Meeting of the Brazilian Biochemistry and Molecular Biology Society (Brasil).

2010 - I Simpósio Sergipano de Farmácia Clínica (Brasil).

2010 - X Reunião Regional Nordeste Sociedade Brasileira de Bioquímica e Biologia Molecular (Brasil).